

Systematic effects and a new determination of the primordial abundance of ${}^4\text{He}$ and dY/dZ from observations of blue compact galaxies

Yuri I. Izotov¹

Main Astronomical Observatory, Ukrainian National Academy of Sciences, 27 Zabolotnoho str., Kyiv 03680, Ukraine

`izotov@mao.kiev.ua`

and

Trinh X. Thuan¹

Astronomy Department, University of Virginia, Charlottesville, VA 22903

`txt@virginia.edu`

ABSTRACT

We use spectroscopic observations of a sample of 82 H II regions in 76 blue compact galaxies to determine the primordial helium abundance Y_p and the slope dY/dZ from the Y – O/H linear regression. To improve the accuracy of the dY/dZ measurement, we have included new spectrophotometric observations of 33 H II regions which span a large metallicity range, with oxygen abundance $12 + \log(\text{O/H})$ varying between 7.43 and 8.30 ($Z_\odot/30 \leq Z \leq Z_\odot/4$). Most of the new galaxies were selected from the First Byurakan, the Hamburg/SAO and the University of Michigan objective prism surveys. For a subsample of 7 H II regions, we derive the He mass fraction taking into account known systematic effects, including collisional and fluorescent enhancements of He I emission lines, collisional excitation of hydrogen emission, underlying stellar He I absorption and the difference between the temperatures $T_e(\text{He II})$ in the He^+ zone and $T_e(\text{O III})$ derived from the collisionally excited [O III] lines. We find that the net result of all the systematic effects combined is small, changing the He mass fraction by less than 0.6%. By extrapolating the Y vs. O/H linear regression to O/H = 0 for 7 H II regions of this subsample, we obtain $Y_p = 0.2421 \pm 0.0021$ and $dY/dO = 5.7 \pm 1.8$, which corresponds to $dY/dZ = 3.7 \pm 1.2$, assuming the oxygen mass fraction to be $O=0.66Z$. In the framework of the standard Big Bang nucleosynthesis theory, this Y_p corresponds to $\Omega_b h^2 = 0.012_{-0.002}^{+0.003}$, where h is the Hubble constant in units

of $100 \text{ km s}^{-1} \text{ Mpc}^{-1}$. This is smaller at the 2σ level than the value obtained from recent deuterium abundance and microwave background radiation measurements. The linear regression slope $dY/dO = 4.3 \pm 0.7$ (corresponding to $dY/dZ = 2.8 \pm 0.5$) for the whole sample of 82 H II regions is similar to that derived for the subsample of 7 H II regions, although it has a considerably smaller uncertainty.

Subject headings: galaxies: abundances — galaxies: irregular — galaxies: ISM — H II regions — ISM: abundances

1. INTRODUCTION

It is now well established that four light isotopes, D, ^3He , ^4He and ^7Li , were produced by nuclear reactions within the first few minutes after the birth of the Universe (Reeves 1994; Wilson & Rood 1994; Sarkar 1996; Tytler et al. 2000). In the standard theory of big bang nucleosynthesis (SBBN), given the number of light neutrino species $N_\nu = 3$, the abundances of these light elements depend on one cosmological parameter only, the baryon-to-photon number ratio η , which in turn is directly related to the density of ordinary baryonic matter $\Omega_b h^2$ (Walker et al. 1991), where h is the Hubble constant in units of $100 \text{ km s}^{-1} \text{ Mpc}^{-1}$. Thus precise abundance measurements of the four light elements can provide not only a strongest test of the consistency of SBBN, but also information about the mean density of ordinary matter in the Universe.

Deuterium is the best element for deriving the baryonic mass fraction because its abundance is strongly dependent on η . Much progress has been achieved during the last years in the precise measurement of the deuterium abundance in high-redshift low-metallicity Ly α absorption systems (Burles & Tytler 1998a,b; O'Meara et al. 2001; Pettini & Bowen 2001; Kirkman et al. 2003). These measurements appear to converge to the mean value $\text{D/H} \sim 3 \times 10^{-5}$ which corresponds to $\Omega_b h^2 \sim 0.020 \pm 0.002$. This value is in good agreement with the ones of $0.021 - 0.022$ from recent studies of the fluctuations of the cosmic microwave background (CMB) (Pryke et al. 2002; Netterfield et al. 2002; Spergel et al. 2003).

Determining the primordial abundance of ^3He is more difficult. Not only it is destroyed in stars, but it can also be produced by low-mass stars. Thus the derivation of its primordial

¹Visiting astronomer, Kitt Peak National Observatory, National Optical Astronomical Observatory, operated by the Association of Universities for Research in Astronomy, Inc., under contract with the National Science Foundation.

value is complicated by our lack of understanding of both the chemical evolution of the Galaxy and the production of ^3He in stars. However, recently Bania et al. (2002) determined an upper limit for the primordial abundance of ^3He relative to hydrogen $^3\text{He}/\text{H} = (1.1 \pm 0.2) \times 10^{-5}$ by arguing that most solar-mass stars do not produce enough ^3He to enrich the interstellar medium significantly. This corresponds to $\Omega_b h^2 \sim 0.020^{+0.007}_{-0.003}$, in excellent agreement with the value obtained from the deuterium and CMB measurements.

As for the primordial abundance of ^7Li , possible correlations of its value with temperature and metallicity in old hot population II stars may introduce systematic errors. The value for the ^7Li primordial abundance derived from the ^7Li abundance plateau of halo stars by Bonifacio & Molaro (1997) is $^7\text{Li}/\text{H} = (1.75 \pm 0.05_{1\sigma} \pm 0.20_{\text{sys}}) \times 10^{-10}$, corresponding to two possible values for the baryonic density $\Omega_b h^2 = 0.006$ and $\Omega_b h^2 = 0.015$, below the value derived from the D abundance and CMB measurements. Furthermore, Ryan et al. (1999) found a correlation of the ^7Li abundance with the metallicity of halo stars, and inferred $^7\text{Li}/\text{H} = 1.0 \times 10^{-10}$ corresponding to a single value of $\Omega_b h^2 = 0.009$, while Ryan et al. (2000) find $^7\text{Li}/\text{H} = 1.23^{+0.68}_{-0.32} \times 10^{-10}$, significantly below the value of $4.5^{+0.9}_{-0.8} \times 10^{-10}$, predicted by SBBN from the primordial D abundance (Kirkman et al. 2003). However, recently Ford et al. (2002) has shown that the ^7Li abundance derived in stars depends on the Li I line used. From the weak Li I $\lambda 6104$ subordinate line instead of the commonly used Li I $\lambda 6708$ resonance line, they derived a much higher ^7Li abundance of $\sim 3 \times 10^{-10}$, consistent with the SBBN predicted value.

The primordial mass fraction Y_p of ^4He can be derived with a much better precision compared to the primordial abundances of other light elements. Y_p is usually derived by extrapolating the $Y - \text{O}/\text{H}$ and $Y - \text{N}/\text{H}$ correlations to $\text{O}/\text{H} = \text{N}/\text{H} = 0$, as proposed originally by Peimbert & Torres-Peimbert (1974, 1976) and Pagel et al. (1986). Many attempts at determining Y_p have been made, constructing these correlations for various samples of dwarf irregular and blue compact galaxies (BCGs) (see references in Izotov & Thuan (1998b), hereafter IT98). These dwarf systems are the least chemically evolved galaxies known, so they contain very little helium manufactured by stars after the big bang, allowing us to bypass the chemical evolution problems which plague the determination of ^3He . However, because the big-bang production of ^4He is relatively insensitive to the density of baryonic matter, the primordial abundance of ^4He needs to be determined to a very high precision (to better than 1%) in order to put useful constraints on Ω_b and N_ν . Uncertainties in the determination of Y_p can be statistical or systematic. Statistical uncertainties can be decreased by obtaining very high signal-to-noise ratio spectra of BCGs. These BCGs are undergoing intense bursts of star formation, giving birth to high excitation supergiant H II regions and allowing an accurate determination of the helium abundance in the ionized gas through the BCG emission-line spectra. The theory of nebular emission is well-understood

enough not to introduce additional uncertainty.

Care should also be exercised to consider all possible systematic effects. We have considered several systematic effects in our previous primordial helium work. First, we have solved consistently for the electron density $N_e(\text{He II})$ in the He^+ zone rather than just setting it to $N_e(\text{S II})$ as was done by previous investigators. Second, we have corrected the He I emission lines for collisional and fluorescent enhancements. With those systematic effects taken into account, Izotov, Thuan & Lipovetsky (1997) (hereafter ITL97), by fitting linear regression lines to the $Y - \text{O/H}$ and $Y - \text{N/H}$ correlations for a sample of 23 BCGs, have derived $Y_p = 0.243 \pm 0.003$. IT98 by extending that sample to 45 H II regions in 41 BCGs have obtained 0.244 ± 0.002 . These values are significantly higher than those of $0.228 - 0.234$ obtained by Pagel et al. (1992) and Olive et al. (1997) with lower signal-to-noise ratio spectra, by setting $N_e(\text{He II}) = N_e(\text{S II})$ and not taking into account fluorescent enhancements of the He I lines.

We have also determined Y in individual very metal-deficient BCGs. Izotov et al. (1997), Izotov et al. (1999), Thuan et al. (1999), Guseva et al. (2001), Izotov et al. (2001a) have respectively derived the helium abundance in the BCGs I Zw 18 ($Z_\odot/50$), SBS 0335–052 ($Z_\odot/40$), SBS 0940+544 ($Z_\odot/29$), Tol 1214–277 ($Z_\odot/24$), Tol 65 ($Z_\odot/24$) and SBS 1415+437 ($Z_\odot/21$), using high signal-to-noise ratio spectra obtained with the MMT and the Keck telescope. Except for I Zw 18, these determinations have all resulted in a ${}^4\text{He}$ mass fraction in the narrow range $Y = 0.245 - 0.246$. The helium mass fraction for the SE component of I Zw 18, $Y = 0.243$, is lower because of the contribution of underlying stellar He I absorption (Izotov & Thuan 1998a; Izotov et al. 1999). Using the two most metal-deficient BCGs known, I Zw 18 and SBS 0335–052, Izotov et al. (1999) derived a primordial helium mass fraction $Y_p = 0.245 \pm 0.002$.

However, there are other systematic effects which may either increase or decrease Y_p , that were not taken into account in our previous work. First, there is the possible systematic effect of underlying He I stellar absorption (ITL97, IT98). Correction for this increases Y in the galaxy. In particular, He I stellar absorption is important in I Zw 18 (Izotov & Thuan 1998a; Izotov et al. 1999). Because it has the lowest metallicity known, I Zw 18 plays an important role in the determination of Y_p . The lower Y_p derived by other groups (Pagel et al. 1992; Olive et al. 1997) is largely the result of neglecting underlying He I stellar absorption in I Zw 18. A second possible systematic effect is the collisional excitation of hydrogen lines (Stasińska & Izotov 2001; Peimbert et al. 2002). Correction for this effect also increases Y . The third systematic effect concerns the temperature structure of the H II region. The electron temperature of the He^+ zone $T_e(\text{He II})$ is usually set equal to the temperature $T_e(\text{O III})$ derived from the collisionally excited $[\text{O III}]$ emission lines. Recent

work has shown that $T_e(\text{He II})$ may be smaller than $T_e(\text{O III})$ (Peimbert et al. 2000, 2002; Sauer & Jedamzik 2002). Correction for this effect decreases Y . A last systematic effect concerns the ionization structure of the H II region. The He^+ zone can be larger or smaller than the H^+ zone. Therefore, an ionization correction factor $ICF(\text{He})$ should be applied. In high excitation low-metallicity H II regions, the ionization correction factor $ICF(\text{He})$ may be slightly higher or lower than unity (Viegas et al. 2000; Izotov et al. 2001a; Gruenwald et al. 2002; Peimbert et al. 2002; Sauer & Jedamzik 2002). These different systematic effects work in opposite directions and it is a priori not clear whether combining all of them would increase or decrease Y_p . Preliminary estimates by Thuan & Izotov (2002) suggest that, after correction for all the systematic effects mentioned above, Y_p may increase by as much as $\sim 2\text{--}4\%$.

Besides the Y_p problem, there is also a need to improve the accuracy of the determination of the slope dY/dZ from the $Y - \text{O/H}$ linear regression. ITL97 and IT98 have derived $dY/dZ = 1.7 \pm 0.9$ and 2.4 ± 1.0 respectively. These values are in agreement, within the errors, with the slope $dY/dZ = 2.1 \pm 0.4$ derived by Jimenez et al. (2003) using K dwarf stars with accurate spectroscopic metallicities in the *Hipparcos* catalog, and with the slope $dY/dZ = 1.5 \pm 0.3$ derived by Peimbert (2003) from observations of two relatively metal-rich H II regions, 30 Dor and NGC 346. They are also in agreement with the values predicted by chemical evolution models of dwarf galaxies (Carigi et al. 1995, 1999), although the errors on dY/dZ are still large and do not allow to strongly constrain these models. The reason for this state of affair is that, for the Y_p problem, attention has been paid mainly to very low metallicity BCGs. For example, the sample of IT98 contains very few intermediate-metallicity BCGs.

We address the two problems of systematic effects on the determination of Y_p and of improving the accuracy of dY/dZ in this paper. To obtain a more accurate dY/dZ , we have added to our sample 31 new BCGs spanning a considerably wider range of oxygen abundance, resulting in a total sample of 76 BCGs with 82 H II regions. To take into account systematic effects on the determination of Y_p , we have studied them in detail in a subsample of 7 H II regions and then have applied the net correction to the total sample of 82 H II regions to derive the primordial helium abundance.

We describe the sample, observations and data reduction in §2. In §3 we determine the physical conditions and heavy element abundances for all 82 H II regions in the total sample. Helium abundances are derived in §4. In §5, we present our new best values for Y_p and for the linear regression slope dY/dZ which has considerably reduced errors. In §3, 4 and 5, to compare the Y_p derived from our new increased sample of 82 H II regions with our previous Y_p determinations from smaller samples (ITL97, IT98), we have proceeded in the same manner as in our previous work concerning systematic effects. We have determined

self-consistently $N_e(\text{He II})$ and corrected the He I line fluxes for collisional and fluorescent enhancements. To estimate the net change incurred by Y_p if all known systematic effects are taken into account, we have analyzed a restricted subsample of 7 H II regions. We apply the correction derived from the restricted sample to the whole sample and present our best value of Y_p and dY/dZ corrected for systematic effects in §6. The implications of our results on cosmology are discussed in §7. We summarize our conclusions in §8.

2. OBSERVATIONS AND DATA REDUCTION

We have obtained new high signal-to-noise ratio spectrophotometric observations for 33 H II regions in 31 BCGs with the Kitt Peak 4-meter telescope on the nights of 2002 December 30 – 31 and 2003 January 1. The majority of the galaxies were selected from the First Byurakan (Markarian) (Markarian 1967), the University of Michigan (Salzer & MacAlpine 1988) and Hamburg/SAO (Ugryumov et al. 1999) objective prism surveys. In choosing the candidates, we have used two main selection criteria. First, they need to have high equivalent widths (EW) of the H β emission line (in general, $\text{EW}(\text{H}\beta) > 200\text{\AA}$) to minimize the influence of underlying He absorption on the He abundance determination. Second, they are to span a wide range of metallicities, from $\sim Z_\odot/50$ to $\sim Z_\odot/3$, so as to allow an improved determination of dY/dZ . The observed galaxies are listed in Table 1 in order of increasing right ascension, along with some of their general properties such as coordinates, apparent magnitudes, redshifts and absolute magnitudes. Relevant references are also given.

All observations were made with the Ritchey-Chrétien spectrograph used in conjunction with the 2048 \times 2048 CCD detector. We use a 2'' \times 300'' slit with the grating KPC-10A in first order, and with a GG 375 order separation filter. This filter cuts off all second-order contamination for wavelengths blueward of 7400 \AA , which is the wavelength region of interest here. The above instrumental set-up gave a spatial scale along the slit of 0''.69 pixel $^{-1}$, a scale perpendicular to the slit of 2.7 \AA pixel $^{-1}$, a spectral range of 3500–7500 \AA and a spectral resolution of $\sim 7\text{\AA}$ (FWHM). These parameters permitted to cover simultaneously the blue and red spectral range with all the lines of interest in a single exposure and with enough spectral resolution to separate important emission lines as H γ λ 4340 and [O III] λ 4363, and H α λ 6563 and [N II] λ 6584. The seeing was in the range 1''–2''. Total exposure times varied between 20 and 60 minutes. Each exposure was broken up into 2–4 subexposures, not exceeding 20 minutes, to allow for removal of cosmic rays. Three Kitt Peak IRS spectroscopic standard stars Feige 110, Feige 34 and HZ 44 were observed at the beginning, middle and end of each night for flux calibration. Spectra of He–Ne–Ar comparison arcs were obtained

before or after each observation to calibrate the wavelength scale. The log of the observations is given in Table 2.

The two-dimensional spectra were bias subtracted and flat-field corrected using IRAF². We then use the IRAF software routines IDENTIFY, REIDENTIFY, FITCOORD, TRANSFORM to perform wavelength calibration and correct for distortion and tilt for each frame. One-dimensional spectra were then extracted from each frame using the APALL routine. Before extraction, distinct two-dimensional spectra of the same H II region were carefully aligned using the spatial locations of the brightest part in each spectrum, so that spectra were extracted at the same positions in all subexposures. For all objects we extracted the brightest part of the BCG, corresponding to a different spatial size for each object. In two BCGs, CGCG 007-025 and Mrk 450, spectra of two different H II regions in the same galaxy were extracted. The extraction apertures of the one-dimensional spectra used for abundance determinations are given in Table 2. These spectra have been corrected for the night sky absorption bands in the red part using spectra of the standard star Feige 34 which contains no absorption lines in that part of the spectrum. All extracted spectra from the same object were then co-added. To perform the co-adding and removal of the cosmic-ray hits, the IMCOMBINE routine is generally used. However, the use of the IMCOMBINE routine can introduce spurious changes in the line intensities of sharp narrow emission lines when small spatial shifts are still present. In those cases, we have simply summed the individual subexposures. Cosmic rays hits have been manually removed in each individual subexposure. Then spectra obtained from each individual subexposure were checked for cosmic rays hits at the location of strong emission lines. Fortunately, none of them were found.

Particular attention was paid to the derivation of the sensitivity curve. It is crucial that the latter be obtained with a very high accuracy for a precise primordial helium abundance determination. To derive the sensitivity curve, we have fitted with a high-order polynomial the observed spectral energy distribution of the bright hot white dwarf standard stars Feige 110, Feige 34 and HZ 44. Because the spectra of these stars have only a small number of a relatively weak absorption features, their spectral energy distributions are known with very good accuracy (Oke 1990). Moreover, the response function of the CCD detector is smooth, so we could derive a sensitivity curve with a precision better than 1% over the whole optical range, except for the region blueward of [O II] λ 3727 where the sensitivity drops precipitously. The resulting spectra for all 33 H II regions are shown in Figure 1. These spectra have been reduced to zero redshift and corrected for interstellar extinction.

²IRAF is distributed by National Optical Astronomical Observatory, which is operated by the Association of Universities for Research in Astronomy, Inc., under cooperative agreement with the National Science Foundation.

As a whole, the H II regions in our new BCG sample show high excitation spectra, except for Mrk 1063. Nineteen H II regions have a H β equivalent width greater than 200Å. The observed line fluxes $F(\lambda)$ normalized to $F(\text{H}\beta)$ and their errors for the 33 H II regions shown in Figure 1 are given in Table 3. They were measured using the IRAF SPLOT routine. The line flux errors listed include statistical errors derived with SPLOT from non-flux calibrated spectra, in addition to errors introduced in the standard star absolute flux calibration, which we set to 1% of the line fluxes. These errors will be later propagated into the calculation of abundance errors. The line fluxes were corrected for both reddening (Whitford 1958) and underlying hydrogen stellar absorption derived simultaneously by an iterative procedure as described in Izotov, Thuan & Lipovetsky (1994) (hereafter ITL94). The corrected line fluxes $I(\lambda)/I(\text{H}\beta)$, equivalent widths $\text{EW}(\lambda)$, extinction coefficients $C(\text{H}\beta)$, and equivalent widths $\text{EW}(\text{abs})$ of the hydrogen absorption stellar lines are also given in Table 3, along with the uncorrected H β fluxes.

3. PHYSICAL CONDITIONS AND DETERMINATION OF HEAVY ELEMENT ABUNDANCES

To determine element abundances, we follow the procedures of ITL94, ITL97 and Thuan et al. (1995). We adopt a two-zone photoionized H II region model: a high-ionization zone with temperature $T_e(\text{O III})$, where O III, Ne III and Ar IV lines originate, and a low-ionization zone with temperature $T_e(\text{O II})$, where O II, N II, S II and Fe III lines originate. As for the Ar III and S III lines they originate in the intermediate zone between the high and low-ionization regions (Garnett 1992). We have derived the chlorine abundance from Cl III emission lines in 22 H II regions. We assume that these lines also originate in the intermediate zone as the ionization potentials of the S⁺⁺, Ar⁺⁺ and Cl⁺⁺ ions are similar. The temperature $T_e(\text{O III})$ is calculated using the $[\text{O III}] \lambda 4363/(\lambda 4959 + \lambda 5007)$ ratio. To take into account the electron temperatures for different ions, we have used the H II photoionization models of Stasińska (1990), as fitted by the expressions in ITL94 and ITL97. The $[\text{S II}] \lambda 6717/\lambda 6731$ ratio is used to determine the electron density $N_e(\text{S II})$, the minimum value of which was set to be 10 cm^{-3} . Ionic and total heavy element abundances are derived for the 33 H II regions in the manner described in ITL94 and are given in Table 4 along with the adopted ionization correction factors (ICF).

As a result of our sample selection criteria, the oxygen abundances in the newly observed H II regions span a wide range of metallicities, going from $12 + \log (\text{O/H}) = 7.43$ ($Z_\odot/30$, J 0519+0007) to 8.30 ($Z_\odot/4$, Mrk 35) with a large fraction of high-metallicity galaxies. Five galaxies among those observed have $12 + \log (\text{O/H}) > 8.2$ ($Z_\odot/5$). This large metallicity

range is crucial for determining an accurate dY/dZ slope.

4. HELIUM ABUNDANCE

Because the $Y_p - \eta$ relation has a very shallow slope, Y_p has to be determined to better than 1% in order to put interesting constraints on the baryonic mass fraction of the universe. In principle, this high precision can be achieved if care is taken to: 1) obtain spectra of low-metallicity H II regions with the very highest signal-to-noise ratio; 2) take into account all physical processes which may make He I line intensities deviate from their recombination values such as collisional and fluorescence enhancements; 3) use the best possible atomic data; and 4) take into account systematic effects in the determination of the helium mass fraction, such as underlying stellar absorption, the ionization and temperature structures of the H II region.

In this section, to compare the results from the present enlarged sample with our previous work, we derive Y_p in the same way as ITL94, ITL97 and IT98. We solve self-consistently for $N_e(\text{He II})$ and the optical depth $\tau(\lambda 3889)$ in the He I $\lambda 3889$ emission line, but do not consider possible temperature and ionization structures in the H II regions. Thus, we set the temperature in the He^+ zone to be equal to that derived from the $[\text{O III}] \lambda 4363 / (\lambda 4959 + \lambda 5007)$ flux ratio, i.e. $T_e(\text{He II}) = T_e(\text{O III})$. The case where $T_e(\text{He II}) \leq T_e(\text{O III})$ will be discussed in §6 for a subsample of 7 H II regions. The He ionization correction factors are set to 1. We consider collisional and fluorescence enhancement effects but do not take into account other systematic effects such as the collisional excitation of hydrogen lines and underlying He I stellar absorption. These effects will be discussed in §6 as well.

Because observed He I fluxes deviate from their recombination values, corrections are necessary to take into account the physical mechanisms which modify line fluxes. In the range of high temperatures found in BCGs ($10^4 \text{ K} \lesssim T_e \lesssim 2 \times 10^4 \text{ K}$), the main such physical mechanism is collisional excitation from the metastable 2^3S level of He I. The second physical mechanism to consider is fluorescence enhancement where self-absorption in some optically thick emission lines populates the upper levels of He I. To correct line intensities for these effects we have evaluated the electron number density $N_e(\text{He II})$ and the optical depth $\tau(\lambda 3889)$ in the He I $\lambda 3889$ line in a self-consistent way by minimization of the expression

$$\chi^2 = \sum_i^n \frac{(y_i^+ - y_{\text{mean}}^+)^2}{\sigma^2(y_i^+)}, \quad (1)$$

where y_i^+ is the He^+ abundance derived from the flux of the He I emission line with label i .

The quantity y_{mean}^+ is the weighted mean of the He^+ abundance as derived from the equation

$$y_{\text{mean}}^+ = \frac{\sum_i^k y_i^+ / \sigma^2(y_i^+)}{\sum_i^k 1 / \sigma^2(y_i^+)}. \quad (2)$$

The numbers of lines n and k used for the minimization and determination of the weighted mean can be different, and in general $n \geq k$.

In this paper, following ITL94, ITL97 and IT98 we use the five strongest He I $\lambda 3889$, $\lambda 4471$, $\lambda 5876$, $\lambda 6678$ and $\lambda 7065$ emission lines to derive $N_e(\text{He II})$ and $\tau(\lambda 3889)$, i.e. $n = 5$. The He I $\lambda 3889$ and $\lambda 7065$ lines play an important role because they are particularly sensitive to both quantities. Since the He I $\lambda 3889$ line is blended with the H8 $\lambda 3889$ line, we have subtracted the latter, assuming its intensity to be equal to 0.107 $I(\text{H}\beta)$ (Aller 1984). However, the He^+ abundances derived from the He I $\lambda 3889$ and $\lambda 7065$ emission lines are more uncertain as compared to those derived from other He I emission lines because of their higher sensitivity to collisional and fluorescent enhancements and, in the case of $\lambda 3889$ line, also because of the uncertainties due to its blending with the H8 line. Therefore, we will consider two cases, one with $k = 5$ when all lines are used in the calculation of y_{mean}^+ , and the other with $k = 3$ when He I $\lambda 3889$ and $\lambda 7065$ are excluded.

In our spectra, other He I emission lines are seen, most often He I $\lambda 3820$, $\lambda 4387$, $\lambda 4026$, $\lambda 4921$, $\lambda 7281$. However, we do not attempt to use these lines for He abundance determination because they are much weaker as compared to the five brightest lines, and hence have larger uncertainties (Table 3).

Concerning the atomic data, we have used in our previous work (ITL97, IT98, Izotov et al. (1999), Guseva et al. (2001), Izotov et al. (2001a)) the He I emissivities of Smits (1996) along with He I collisional enhancement coefficients of Kingdon & Ferland (1995), and fits of the fluorescent enhancement factors of Robbins (1968) by ITL97. Recently, Benjamin et al. (2002) have computed new He I emission line strengths taking into account both collisional and fluorescent enhancements. Their calculations are also based on Smits (1996)' atomic data. They give simple and convenient fits for calculations of abundances for different He I emission lines. These authors also show that some of the correction factors used by ITL97 may be in error by a factor of ~ 2 , especially for He I $\lambda 7065$ emission line, which may lead to an overestimation of Y_p . Thus, in this paper we use the new Benjamin et al. (2002) fits to convert He I emission-line strengths to singly ionized helium $y^+ \equiv \text{He}^+/\text{H}^+$ abundances.

Additionally, in those cases when the nebular He II $\lambda 4686$ emission line was detected, we have added the abundance of doubly ionized helium $y^{++} \equiv \text{He}^{++}/\text{H}^+$ to y^+ . The value of y^{++} is small ($\leq 3\%$ of y^+) in all cases.

Finally the helium mass fraction is calculated as

$$Y = \frac{4y[1 - 20(\text{O/H})]}{1 + 4y}, \quad (3)$$

where $y = y^+ + y^{++}$ (Pagel et al. 1992).

In Table 4, we give for each galaxy $y^+(\lambda 4471)$, $y^+(\lambda 5876)$, $y^+(\lambda 6678)$, $y^{++}(\lambda 4686)$, the weighted mean helium abundance y and the weighted mean helium mass fraction Y . The weighted mean values are derived using only the three He I $\lambda 4471$, $\lambda 5876$ and $\lambda 6678$ emission lines.

5. THE dY/dZ SLOPE

To determine Y_p and dY/dZ , we fit the data points in the $Y - \text{O/H}$ and $Y - \text{N/H}$ planes by linear regression lines of the form (Peimbert & Torres-Peimbert 1974, 1976; Pagel et al. 1992)

$$Y = Y_p + \frac{dY}{d(\text{O/H})}(\text{O/H}), \quad (4)$$

$$Y = Y_p + \frac{dY}{d(\text{N/H})}(\text{N/H}). \quad (5)$$

The sample used to determine Y_p and dY/dZ is composed of 89 different observations of 82 H II regions in 76 BCGs. They are listed in Table 5 in order of increasing ionized gas metallicity. In addition to the new data for the 33 H II regions presented here (Table 1) we have also included the 45 H II regions from IT98, the 2 H II regions in Tol 1214–277 and Tol 65 from Izotov et al. (2001a), the H II region in HS 1442+4250 from Guseva et al. (2003a) and H II region No. 2 in SBS 1415+437 from Guseva et al. (2003b). The number of data points (89) is larger than the number of H II regions (82) because several H II regions have independent observations from different telescopes. We treat these independent observations as separate data points in our least-square fitting. Thus, I Zw 18 was observed with the 4m KPNO telescope and the MMT, SBS 0335–052 with the 2.1m KPNO telescope and with Keck (twice), SBS 0940+544 with the 4m KPNO telescope, the MMT and Keck, SBS 1415+437(#1) with the MMT and the 4m KPNO telescope (twice).

In order to have a homogeneous sample with all spectra reduced and analyzed in exactly the same way, we have recalculated the He abundances of all our previously published objects with the new Benjamin et al. (2002) corrections for collisional and fluorescent enhancements.

In Figure 2 we show by solid lines the $Y - \text{O/H}$ and $Y - \text{N/H}$ regression lines for the whole sample. The dashed lines are 1σ alternatives. The IT98 data are represented by open

circles, other data from Izotov et al. (1999) (I Zw 18 and SBS 0335–052), Thuan et al. (1999) (SBS 1415+437#1), Izotov et al. (2001a) (Tol 1214–277 and Tol 65), Guseva et al. (2001) (SBS 0940+544), Guseva et al. (2003a) (HS 1442+4250), Guseva et al. (2003b) (SBS 1415+437#1 and SBS 1415+437#2) by stars, and the new data presented in this paper by filled circles. Note that the sample includes now, in contrast to our previous work (ITL97, IT98), a significant number of the galaxies with relatively high oxygen abundances.

In Figs. 2a – 2b the He abundances have been obtained using all 5 lines for χ^2 minimization, but only 3 lines for abundance calculations ($n = 5, k = 3$ in Eqs. 1 and 2). In Figs. 2c – 2d all 5 lines are used for both χ^2 minimization and abundance calculations ($n = k = 5$ in Eqs. 1 and 2). It can be seen that there is no systematic difference between the old and new data in Figs. 2a – 2b, while the old data have systematically lower He abundances as compared to the new data in Figs. 2c – 2d. This is because the He abundances derived from the He I $\lambda 3889$ emission line, included in the second case but not in the first, are systematically lower. The He I $\lambda 3889$ line is subject to large uncertainties introduced by the corrections for hydrogen nebular emission and stellar absorption, as discussed by Olive & Skillman (2001) using the data of IT98. It is likely that the contribution of hydrogen absorption has been underestimated in our analysis. The effect is higher in objects with lower equivalent widths of emission lines since the relative contribution of underlying absorption is larger. This is the case for the IT98 galaxies. They generally have lower equivalent widths of the H β emission line as compared to the galaxies in the new sample, chosen to have large EW(H β). Hence the He I $\lambda 3889$ line in the new galaxies is less affected by stellar absorption and thus their derived Y s are systematically higher than those of the IT98 galaxies. The He abundance derived from the He I $\lambda 7065$ emission line is also uncertain because of its high sensitivity to collisional and fluorescent enhancements. Therefore, because they are less influenced by the aforementioned effects, the He abundances derived by using only the three He I $\lambda 4471$, $\lambda 5876$ and $\lambda 6678$ emission lines for the IT98 galaxies are much more consistent with those for the new galaxies.

The parameters of the linear regression fits for the old and (old+new) samples are given in Table 6. We also show the dispersions σ of Y about the regression lines. The first line of Table 6 gives the parameters for the IT98 sample of 45 H II regions, for which we have recalculated He abundances with the Benjamin et al. (2002) equations. The primordial He abundance derived from the Y – O/H relation is $Y_p = 0.245 \pm 0.002$, slightly larger than the value of 0.244 ± 0.002 obtained by IT98 for the same sample with the ITL97 and IT98 expressions for collisional and fluorescent enhancements of He I emission lines. The higher Y_p value is mainly the consequence of a slope which is ~ 2 times shallower ($dY/d(\text{O/H}) = 21 \pm 21$ in Table 6 as compared to 45 ± 19 in IT98). In the second line are given the regression parameters for the total sample. From the Y – O/H relation, we obtain $Y_p = 0.243 \pm 0.001$,

slightly lower than the value derived from the IT98 sample, because of the steeper slope ($dY/d(\text{O/H}) = 51 \pm 9$ as compared to 21 ± 21). The value derived from the $Y - \text{N/H}$ linear regression, is slightly higher, $Y_p = 0.244 \pm 0.001$. This is because the very highest metallicity BCGs in our sample have a slightly higher N/O ratio than the lower metallicity galaxies, thus making the $Y - \text{N/H}$ relation slightly non-linear. This higher N/O ratio is caused by the presence of secondary nitrogen in the higher-metallicity BCGs. The standard deviation of the data points is 0.004 for both $Y - \text{O/H}$ and $Y - \text{N/H}$ regressions, lower than for the IT98 sample. Lines 3 and 4 of Table 6 will be discussed in §6.

The slopes of the $Y - \text{O/H}$ and $Y - \text{N/H}$ linear regressions can be written as:

$$\frac{dY}{d(\text{O/H})} = 12 \frac{dY}{d\text{O}} = 18.2 \frac{dY}{dZ}, \quad (6)$$

$$\frac{dY}{d(\text{N/H})} = 10.5 \frac{dY}{d\text{N}} = 564 \frac{dY}{dZ}, \quad (7)$$

where O, N and Z are respectively the mass fractions of oxygen, nitrogen and heavy elements. We have assumed that $\text{O} = 0.66Z$ (Maeder 1992) for a metallicity $Z=0.001$, an IMF slope $x=1.35$ (where x is defined by $dN/d(\log M) \propto M^x$) and $\log(\text{N/H}) - \log(\text{O/H}) = -1.55$ (Thuan et al. 1995).

From Table 6 we derive $dY/d\text{O} = 4.3 \pm 0.7$ and $dY/dZ = 2.8 \pm 0.5$. Although the slope dY/dZ derived here is consistent within the errors with $dY/dZ = 2.6 \pm 1.4$ and 3.7 ± 1.5 derived respectively by ITL97 and IT98, we have decreased the errors on the slope by a factor of ~ 3 thanks to the larger number of high metallicity objects included in the sample. Our new value of dY/dZ is also consistent with that of 2.1 ± 0.4 derived by Jimenez et al. (2003) from nearby K dwarf stars. The extrapolation of the oxygen linear regression with $dY/d\text{O} = 4.3$ to solar metallicity gives $Y = 0.274$, in good agreement with $Y = 0.271$ derived for the Sun (Christensen-Dalsgaard 1998).

The increased accuracy of our $dY/d\text{O}$ and dY/dZ values allows us to constrain more stringently chemical evolution models. Our slope $dY/dZ = 2.8 \pm 0.5$ appears to be too steep as compared to the values $1.0 - 1.2$ obtained by Larsen et al. (2001) with their closed-box chemical evolution models for gas-rich dwarf galaxies and their adopted $\text{O}=0.6Z$. Open models with ordinary non-enriched winds, with or without gas inflow, predict also the same range of values $1.0 - 1.2$. The models of Larsen et al. (2001) with oxygen-enriched winds predict steeper slopes, more in agreement with our value, but would not fit gas mass fractions and N/O ratios simultaneously. On the other hand, analytical chemical evolution models with selective heavy element loss (Pilyugin 1994) predict $dY/d\text{O} > 5$ with $dY/d\text{O}$ increasing with increasing efficiency of the oxygen-enriched galactic wind. Hence, our derived

$dY/dO = 4.3 \pm 0.7$ excludes chemical evolution models with a high mass loss of the enriched gas. Our dY/dO is in agreement with the values predicted by chemical evolution closed-box models and models with non-selective galactic winds of Carigi et al. (1999) for dwarf irregular galaxies. However, those multi-parameter models do not consider the evolution of some elements, such as nitrogen, and it is not clear therefore, whether they can reproduce all the observational constraints for dwarf galaxies.

The above values were derived by neglecting other possible systematic effects, such as the difference between the electron temperatures in the He II and O III zones, underlying He I stellar absorption, the collisional excitation of hydrogen lines, and the ionization structure of the H II region. In the next section, we investigate, how these systematic effects may change our derived values of Y_p and dY/dZ , using a subsample of 7 H II regions.

6. SYSTEMATIC EFFECTS

We will consider successively the following four systematic effects: 1) the underlying stellar He I absorption; 2) the collisional excitation of hydrogen lines; 3) the temperature structure of the H II region, i.e. the temperature difference between $T_e(\text{He II})$ and $T_e(\text{O III})$; and 4) the ionization structure of the H II region.

6.1. Underlying stellar He I absorption

It has long been recognized (Rayo et al. 1982; Kunth & Sargent 1983; Dinerstein & Shields 1986; Pagel et al. 1992; Olofsson 1995) that absorption caused by hot stars in the He I lines can decrease the intensities of the nebular He I lines. In particular, Izotov & Thuan (1998a) have shown that the neglect of He I underlying stellar absorption has led to the derivation of a very low helium mass fraction in I Zw 18, the most metal-deficient BCG known (Pagel et al. 1992; Olive et al. 1997). This effect is most pronounced for the He I $\lambda 4471$ emission line. Recently, González Delgado et al. (1999) have produced synthetic spectra of H Balmer and He I absorption lines in starburst and poststarburst galaxies. They predict an equivalent width of the He I $\lambda 4471$ absorption line in the range $\sim 0.4 - 0.8 \text{ \AA}$, or $\sim 10 - 20\%$ of the He I $\lambda 4471$ emission line equivalent width for young starbursts with an age $\lesssim 7 \text{ Myr}$, which is the case for our H II regions. However, the equivalent width of the He I $\lambda 3889$ absorption line is not known. González Delgado et al. (1999) predict the total equivalent width of the H8 and He I $\lambda 3889$ absorption lines to be in the range of 0.85 – 0.95 that of the H β absorption line, but do not give the absorption equivalent width for the He

I $\lambda 3889$ line alone. Those authors did not calculate either absorption line equivalent widths for the other prominent He I lines, although the effect of underlying absorption appears to be smaller for the He I $\lambda 5876$, $\lambda 6678$ and $\lambda 7065$ emission lines. In any case, underlying stellar absorption must be taken into account for all He I lines if we are to achieve the desired high precision of $\lesssim 1\%$ in the primordial He abundance determination.

6.2. Collisional excitation of H lines

It was generally assumed in abundance studies that deviations of the observed $\text{H}\alpha/\text{H}\beta$ flux ratio from the theoretical recombination value are entirely due to interstellar extinction. Davidson & Kinman (1985) first noted that in the hot and dense H II regions of BCGs, collisional excitation of hydrogen emission lines can be important. This can affect the derived H abundances and hence the He abundances since the latter are always derived relative to H abundances. Stasińska & Izotov (2001) estimated that this effect can result in an upward correction in the He abundances of up to 5%, assuming that the excess of the $\text{H}\alpha/\text{H}\beta$ flux ratio above the theoretical recombination value is due only to collisional excitation. Realistically however, the $\text{H}\alpha/\text{H}\beta$ flux ratio excess is also partly caused by interstellar extinction, so that the effect of collisional excitation of the hydrogen lines is likely smaller, $\sim 2 - 3$ percent, similar to the estimate of Peimbert et al. (2002).

6.3. Temperature structure

To derive the He abundances, ITL94, ITL97 and IT98 have assumed that the temperatures $T_e(\text{He II})$ and $T_e(\text{O III})$ averaged over the whole H II region are equal. $T_e(\text{O III})$ is determined from the observed $[\text{O III}]\lambda 4363/(\lambda 4959 + \lambda 5007)$ emission line flux ratio. However, because of the high sensitivity of the flux of the auroral $[\text{O III}]\lambda 4363$ emission line to temperature, $T_e(\text{O III})$ tends to be characteristic of the hotter zones in the H II region, and it is generally higher than $T_e(\text{He II})$. To take into account the difference of the calculated electron temperature $T_e(\text{O III})$ as compared to the one in the H^+ and He^+ zones, Peimbert (1967) developed a formalism based on the average temperature T_0 and the mean square temperature variation t^2 in an H II region. Then the temperatures $T_e(\text{H II})$, $T_e(\text{He II})$ and $T_e(\text{O III})$ are expressed as different functions of T_0 and t^2 , and $T_e(\text{O III}) \geq T_e(\text{H II})$, $T_e(\text{He II})$. This approach has been applied by Peimbert et al. (2002) for the determination of the He abundance in some low-metallicity dwarf galaxies, including the two most-metal deficient BCGs known, I Zw 18 and SBS 0335–052. Using the observations of Izotov et al. (1999) they find that the difference between $T_e(\text{O III})$ and $T_e(\text{He II})$ results in a reduction of the He

mass fraction by 2 – 3 percent as compared to the case when $T_e(\text{O III}) = T_e(\text{He II})$.

6.4. Ionization structure

Another source of systematic uncertainties comes from the assumption that the H^+ and He^+ zones in the H II region are coincident. However, depending on the hardness of the ionizing radiation, the radius of the He^+ zone can be smaller than the radius of the H^+ zone in the case of soft ionizing radiation, or larger in the case of hard radiation. In the former case, a correction for unseen neutral helium should be made, resulting in an ionization correction factor $ICF(\text{He}) > 1$ and hence a higher helium abundance. In the latter case, the situation is opposite and $ICF(\text{He}) < 1$. The ionization correction factor problem has been discussed in several studies (Pagel et al. 1992; Steigman et al. 1997; Olive et al. 1997; Viegas et al. 2000; Peimbert et al. 2000; Ballantyne et al. 2000; Sauer & Jedamzik 2002). It was shown that the correction of the helium abundance can be as high as several percent in either downward or upward directions depending on the hardness of the radiation and the ionization parameter U . Sauer & Jedamzik (2002) have calculated an extensive grid of photoionized H II region models aiming to derive the correction factors as functions of hardness and U . Their conclusion was that a downward correction of Y by as much as 6% and 2% is required respectively for ionization parameters $\log U = -3.0$ and -2.5 . However, the downward correction is $\lesssim 1\%$ if $\log U \gtrsim -2.0$, which is the case for the majority of our H II regions. Therefore, we will not consider further this effect in the present paper and set $ICF(\text{He}) = 1$.

6.5. Analysis of a subsample of 7 H II regions

Although these systematic effects are still poorly studied and difficult to determine precisely, Izotov et al. (2001a) have concluded that when taken into account together, they largely offset each other. Thuan & Izotov (2002) have suggested that combining all systematic effects may push Y_p upward by at most $\sim 2 - 4\%$. Peimbert et al. (2002) have considered collisional and fluorescent enhancements, along with all systematic effects discussed in this section, in their analysis of the He abundance in five H II regions. They attack the problem in three steps. First, using the ionization code CLOUDY (Ferland 1996; Ferland et al. 1998) these authors estimate the parameter t^2 , the optical depth $\tau(\lambda 3889)$, the ionization correction factor $ICF(\text{He})$ and the contribution of collisional enhancement to the hydrogen lines. Second, they adopt the equivalent widths of the H I and He I absorption lines calculated by González Delgado et al. (1999) for a particular age of the star formation

burst in each H II region, except for NGC 346 where the equivalent widths of absorption lines were set to zero. No correction for underlying stellar absorption was applied to the strong He I $\lambda 5876$, $\lambda 6678$ and $\lambda 7065$ emission lines. These lines play an important role in the helium abundance determination, but their absorption equivalent widths were not calculated by González Delgado et al. (1999). Peimbert et al. (2002) then use a χ^2 minimization procedure with input parameters t^2 , $\tau(\lambda 3889)$, $T_e(\text{O III})$ and the equivalent widths of the He I absorption lines to find new values of t^2 , $\tau(\lambda 3889)$ and derive the electron temperature $T_e(\text{He II})$, the electron number density $N_e(\text{H II})$ and the He abundance. In the case of the two most metal-deficient BCGs known, I Zw 18 and SBS 0335–052, Peimbert et al. (2002) derive, after correction for all systematic effects, helium abundances very close to the values obtained when systematic effects other than collisional and fluorescent enhancements are not taken into account. However, for three other higher-metallicity H II regions in their sample, they derive also relatively low He mass fractions, similar to those of I Zw 18 and SBS 0335–052. This resulted in a very flat $Y - \text{O/H}$ linear regression, leading these authors to conclude that they have probably overestimated the collisional excitation of hydrogen lines in I Zw 18 and SBS 0335–052, resulting in artificially high He mass fractions.

To estimate the systematic effects in our derived Y_p value in §5, and to compare our results with those of Peimbert et al. (2002), we have analyzed the same objects as these authors: I Zw 18 and SBS 0335–052 (Izotov et al. 1999), Mrk 209 \equiv Haro 29 and Mrk 71 (ITL97) and NGC 346 (Peimbert et al. 2000). Because the range of oxygen abundance spanned by the five galaxies is relatively small, we have added two more metal-rich galaxies Mrk 450 (this paper) and UM 311 (IT98) to improve the metallicity range and obtain a more accurate determination of dY/dZ . However, our approach is somewhat different from that of Peimbert et al. (2002).

Instead of using CLOUDY to derive model parameters, we adopt the self-consistent approach which we have used in all of our previous studies and in §4 of this paper. Our method consists of using the five strongest He I lines $\lambda 3889$, $\lambda 4471$, $\lambda 5876$, $\lambda 6678$ and $\lambda 7065$ and correct for systematic effects in such a way so as to obtain after correction the best agreement between the He abundances derived from each He I line separately, i.e. we search for the minimum χ^2 as defined by Eq. 1. In our previous work, we have considered as free parameters the electron number density $N_e(\text{He II})$ and the optical depth $\tau(\lambda 3889)$. Here we add the electron temperature $T_e(\text{He II})$ and $\Delta I(\text{H}\alpha)/I(\text{H}\alpha)$, the fraction of the H α flux due to collisional excitation. These values should be well determined as we have only four unknowns for five constraints, i.e. the problem is overdetermined.

We proceed in the following manner. We first correct for collisional excitation of the hydrogen lines by varying $\Delta I(\text{H}\alpha)/I(\text{H}\alpha)$ in the range between 0 and 5%, and subtract-

ing $\Delta I(\text{H}\alpha)$ and $\Delta I(\text{H}\beta)$ respectively from the observed fluxes of $\text{H}\alpha$ and $\text{H}\beta$. We adopt $\Delta I(\text{H}\beta)/I(\text{H}\beta) = 0.33 \times \Delta I(\text{H}\alpha)/I(\text{H}\alpha)$ (Stasińska & Izotov 2001). Then the whole spectrum is corrected for extinction and underlying hydrogen absorption derived from the hydrogen emission line fluxes, including the new reduced $\text{H}\alpha$ and $\text{H}\beta$ fluxes.

Underlying He I absorption constitutes a major problem as each of the $\text{He I } \lambda 3889, \lambda 4471, \lambda 5876, \lambda 6678$ and $\lambda 7065$ lines has its own absorption equivalent width EW_a . Additionally, $\text{He I } \lambda 3889$ is blended with $\text{H}8$ and deblending it is subject to large uncertainties because of the imperfect correction for hydrogen emission and absorption.

Because the equivalent widths of He I absorption lines are dependent on the age of the star formation burst, we first need to determine the age of the burst using the equivalent width of the $\text{H}\beta$ emission line. The values of $\text{EW}(\text{H}\beta)$ for the H II regions considered in this section are in the range $100 - 250 \text{\AA}$, which corresponds to a burst age of ~ 4 Myr for the metallicity $Z \lesssim Z_\odot/5$ (Schaerer & Vacca 1998). The equivalent widths of the He I absorption lines have large variations in the age range $3 - 5$ Myr (González Delgado et al. 1999) and are not well constrained. In particular, $\text{EW}_a(\text{He I } \lambda 4471)$ at $Z = Z_\odot/20$ varies in the range $0.4 - 0.6 \text{\AA}$, or by factor of ~ 1.5 . As for the equivalent width of the blend $\text{H}8 + \text{He I } \lambda 3889$, it varies in the range $2.0 - 3.9 \text{\AA}$, or by factor of ~ 2 . The mean equivalent widths in the $3 - 5$ Myr age range are $\text{EW}_a(\text{He I } \lambda 4471) \approx 0.5 \text{\AA}$ and $\text{EW}_a(\text{H}8 + \text{He I } \lambda 3889) \approx 3.0 \text{\AA}$. These values can be smaller if the gaseous continuum emission is significant. In the H II regions considered in this section, the gaseous continuum emission contributes $\sim 10\% - 25\%$ of the total continuum flux at the wavelength of $\text{H}\beta$, reducing by the same amount the equivalent width of the $\text{H}\beta$ absorption line. However, at shorter wavelengths the effect of gaseous continuum is smaller. We thus adopt two sets of equivalent widths: 1) $\text{EW}_a(\text{H}8 + \text{He I } \lambda 3889) = 3.0 \text{\AA}$ and $\text{EW}_a(\text{He I } \lambda 4471) = 0.4 \text{\AA}$, which takes into account the dilution by the gaseous continuum, and 2) $\text{EW}_a(\text{H}8 + \text{He I } \lambda 3889) = 3.0 \text{\AA}$ and $\text{EW}_a(\text{He I } \lambda 4471) = 0.5 \text{\AA}$ where gaseous continuum emission is negligible. As for the other He I lines, their EW_a decrease progressively from the blue to the red (see for example the spectrum of I Zw 18 NW in Fig. 2 of Izotov et al. (1999) which is strongly affected by He I underlying absorption and where $\text{He I } \lambda 4471$ is barely seen while both $\text{He I } \lambda 6678$ and $\lambda 7065$ can be seen in emission). We adopt for them $\text{EW}(\text{He I } \lambda 5876) = 0.3 \text{ EW}(\text{He I } \lambda 4471)$, $\text{EW}(\text{He I } \lambda 6678) = \text{EW}(\text{He I } \lambda 7065) = 0.1 \text{ EW}(\text{He I } \lambda 4471)$ in both cases.

For each of these two sets of EW_a , we solve the problem self-consistently to find the four parameters $\Delta I(\text{H}\alpha)/I(\text{H}\alpha)$, $T_e(\text{He II})$, $N_e(\text{He II})$ and $\tau(\lambda 3889)$ using the five He I emission line fluxes. We calculate χ^2 , $T_e(\text{He II})$, $N_e(\text{He II})$, and $\tau(\lambda 3889)$ as a function of $\Delta I(\text{H}\alpha)/I(\text{H}\alpha)$ in the range $0 - 5\%$, in steps of 0.0005, for a total of 100 models. The best solution corresponds to the minimum χ^2 . It is the one in which the separate helium

abundances y derived from each individual He I line are in best agreement with the weighted mean abundance. To exclude unphysical solutions we consider only models with $0.9 \leq T_e(\text{He II})/T_e(\text{O III}) \leq 1.0$, $10 \text{ cm}^{-3} \leq N_e(\text{He II}) \leq 450 \text{ cm}^{-3}$ and $0 \leq \tau(\lambda 3889) \leq 5$. The values found by Peimbert et al. (2002) in the analysis of their H II region sample fall within those ranges.

The parameters of the best models for each set of EW_a s and for each of the 7 H II regions are shown in Table 7. The best solutions are also shown in the $Y - \text{O/H}$ and $Y - \text{N/H}$ planes in Fig. 3a – 3b (models with $\text{EW}_a(\text{H8} + \text{He I } \lambda 3889) = 3.0 \text{ \AA}$ and $\text{EW}_a(\text{He I } \lambda 4471) = 0.4 \text{ \AA}$) and Fig. 3c – 3d (models with $\text{EW}_a(\text{H8} + \text{He I } \lambda 3889) = 3.0 \text{ \AA}$ and $\text{EW}_a(\text{He I } \lambda 4471) = 0.5 \text{ \AA}$). The corresponding linear regression parameters are given in Table 6.

Our derived values of Y are in general higher than the ones obtained by Peimbert et al. (2002) for the same H II regions. The differences come from the different ways our and their Y values have been derived: instead of estimating the physical parameters of the H II regions by CLOUDY, we have adopted an approach that does not depend on any particular physical model, external estimates or assumptions, i.e. we simply search the multi-parameter space for the smallest χ^2 . Other differences are: 1) we have included H II regions with higher metallicities to derive a more accurate dY/dZ slope; 2) Peimbert et al. (2002) used expressions for collisional enhancement of He I emission lines from Benjamin et al. (1999) while we use the expressions by the same authors (Benjamin et al. 2002) but which include not only collisional but also fluorescent enhancement; 2) Peimbert et al. (2002) assumed no underlying He I absorption for NGC 346 while we find it to be significant; 3) Peimbert et al. (2002) calculate their χ^2 in a slightly different manner from us. They use the expression from Peimbert et al. (2000) weighting by errors of line fluxes, while we use Eq. 1 weighting by errors of He abundances. However, we have checked (for NGC 346) that the choice of a weighting scheme makes little difference in the derived He abundance. The largest differences between Peimbert et al. (2002) and our values of Y are for NGC 346 and Mrk 209, our values being $\sim 2\text{--}3\%$ higher.

For the set $\text{EW}(\lambda 3889) = 3.0 \text{ \AA}$ and $\text{EW}(\lambda 4471) = 0.4 \text{ \AA}$ we derive a primordial He mass fraction $Y_p = 0.2421 \pm 0.0021$ from the $Y - \text{O/H}$ linear regression and 0.2446 ± 0.0016 from the $Y - \text{N/H}$ linear regression. For the set $\text{EW}(\lambda 3889) = 3.0 \text{ \AA}$ and $\text{EW}(\lambda 4471) = 0.5 \text{ \AA}$, $Y_p = 0.2444 \pm 0.0020$ from the $Y - \text{O/H}$ linear regression and 0.2466 ± 0.0016 from the $Y - \text{N/H}$ linear regression. The Y_p s obtained from the $Y - \text{O/H}$ linear regressions considering known systematic effects are very similar to the value $Y_p = 0.243 \pm 0.001$ derived in §5 for the whole sample without correcting for the difference between $T_e(\text{He II})$ and $T_e(\text{O III})$, the collisional excitation of hydrogen lines and the underlying stellar absorption in the He I lines. Thus, the combined effect of the corrections for all known systematic effects turned out to

be very small. In the more realistic case where gaseous continuum is taken into account, the Y_p s differ by only 0.4%. In the case where it is not taken into account, they differ by 0.6%.

This means that, even if all known systematic effects are taken into account in our previous work on the statistical derivation of Y_p by linear regressions (ITL94, ITL97 and IT98), the result will not be changed. While each individual systematic effect can change Y upward or downward by as much as 4%, they work in opposite sense and nearly cancel each other out. By nearly doubling our sample (from 45 to 82 H II regions) and choosing the galaxies so that they span as large a metallicity range as possible, we have considerably reduced the uncertainties in the slopes $dY/dO = 4.3 \pm 0.7$ and $dY/dZ = 2.8 \pm 0.5$ for the whole sample, as compared to $dY/dO = 5.7 \pm 1.8$ and $dY/dZ = 3.7 \pm 1.2$ for the restricted sample with $EW_a(\lambda 4471) = 0.4\text{\AA}$ and $dY/dO = 5.1 \pm 1.8$ and $dY/dZ = 3.4 \pm 1.2$ with $EW_a(\lambda 4471) = 0.5\text{\AA}$. These values are consistent within the errors with our previous determinations. In a future paper we will apply the χ^2 minimization technique to correct our whole sample of 82 H II regions for known systematic effects and reduce further the uncertainties in Y_p and dY/dZ . We will study in detail another possible additional systematic effect, that of the ionization structure of H II regions, which we have not considered in this paper, simply setting the ionization correction factors of He I to 1.

7. COSMOLOGICAL IMPLICATIONS

With our value of $Y_p = 0.2421 \pm 0.0021$ for $EW_a(\lambda 4471) = 0.4\text{\AA}$ and with an equivalent number of light neutrino species equal to 3, the SBBN model gives $\eta_{10} = 10^{10}\eta = 3.4_{-0.6}^{+0.7}$, where η is the baryon-to-photon number ratio and the error bars denote 1σ errors. This corresponds to a baryonic mass fraction $\Omega_b h^2 = 0.012_{-0.002}^{+0.003}$. The respective values of the cosmological parameters with $Y_p = 0.2444 \pm 0.0020$ (obtained for $EW_a(\lambda 4471) = 0.5\text{\AA}$) are $\eta_{10} = 10^{10}\eta = 4.0_{-0.5}^{+1.1}$ and $\Omega_b h^2 = 0.015_{-0.002}^{+0.003}$. These values are lower at the 2σ level than $\Omega_b h^2 = 0.021 \pm 0.002$ from recent measurements of the deuterium abundance in damped Ly α systems (Kirkman et al. 2003). The latter would correspond to $Y_p = 0.2476_{-0.0010}^{+0.0009}$. Recent measurements of the fluctuations of the microwave background radiation by the Wilkinson Microwave Anisotropy Probe (WMAP) observations have improved considerably the precision of η (Spergel et al. 2003). The WMAP data give $\Omega_b h^2 = 0.0224 \pm 0.0009$, corresponding to $Y_p = 0.2483 \pm 0.0004$ in the SBBN model, significantly higher than our values of Y_p , and inconsistent at the 95% C.L.

If, with improved determinations, η as obtained from the deuterium abundance and microwave background fluctuation measurements, remains systematically higher than its value obtained from the He abundance, then this may suggest deviations from SBBN theory.

One possibility is that the equivalent number of the light neutrino species N_ν is less than 3. Combining $\Omega_b h^2 = 0.0224 \pm 0.0009$ obtained by WMAP (Spergel et al. 2003) with $Y_p = 0.2421 \pm 0.0021$, we obtain $N_\nu = 2.48$ with an upper limit $N_\nu < 2.83$ at the 95% confidence level (Walker et al. 1991). With $Y_p = 0.2444 \pm 0.0020$, we obtain $N_\nu = 2.67$ with an upper limit $N_\nu < 3.01$ at the 95% confidence level.

8. SUMMARY AND CONCLUSIONS

We present in this paper new high signal-to-noise spectrophotometric observations of 31 low-metallicity blue compact galaxies (BCGs), containing 33 H II regions and spanning a large range of heavy element mass fractions from $\sim Z_\odot/30$ to $Z_\odot/4$. We combine this new data with our previous data (Izotov & Thuan 1998b) to construct a sample of 82 H II regions and determine the primordial helium mass fraction Y_p by linear regressions to the sample. Our sample constitutes one of the largest and most homogeneous (obtained, reduced and analyzed in the same way) data set now available for the determination of Y_p .

We have considered known systematic effects on the He abundance determination. For the total sample of 82 H II regions we have calculated $N_e(\text{He II})$ self-consistently and taken into account the effects of collisional and fluorescent enhancements. For a restricted sample of 6 H II regions from our sample and an additional H II region, NGC 346 in the Small Magellanic Cloud, we have examined, in addition to the collisional and fluorescent enhancements of He I emission lines, also the effects of collisional excitation of hydrogen emission lines, of underlying stellar He I absorption and of the difference between the temperature $T_e(\text{He II})$ in the He⁺ zone and the temperature $T_e(\text{O III})$ derived from the $[\text{O III}]\lambda 4363/(\lambda 4959 + \lambda 5007)$ flux ratio. The restricted sample was chosen because the systematic effects on the Y_p determination of 5 of the galaxies in the sample have been discussed by Peimbert et al. (2002), and we can compare our results to theirs.

We have derived the following results:

1. Although each systematic effect may move the helium mass fraction Y up or down by as much as 4%, the combined result of the systematic effects on the restricted sample is relatively small ($\lesssim 0.6\%$), as they act in opposite sense and mostly cancel each other out. We derive for the restricted sample $Y_p = 0.2421 \pm 0.0021$ adopting $\text{EW}_a(\lambda 4471) = 0.4 \text{\AA}$. This corresponds to a baryonic mass fraction $\Omega_b h^2 = 0.012_{-0.002}^{+0.003}$. If $\text{EW}_a(\lambda 4471) = 0.5 \text{\AA}$ is adopted then $Y_p = 0.2444 \pm 0.0020$ corresponding to $\Omega_b h^2 = 0.015_{-0.002}^{+0.003}$. These values of $\Omega_b h^2$ are lower than the values derived from the deuterium abundance and microwave background radiation fluctuation measurements. This may indicate that the equivalent number of light

neutrino species N_ν is less than 3 and hence that there are deviations from the standard Big Bang nucleosynthesis model.

2. The slopes dY/dO and dY/dZ derived from the $Y - \text{O/H}$ linear regressions for the restricted sample with two adopted values of $\text{EW}_a(\lambda 4471) = 0.4\text{\AA}$ and 0.5\AA are respectively 5.7 ± 1.8 , 3.7 ± 1.2 , and 5.1 ± 1.8 , 3.4 ± 1.2 . They are consistent with previous determinations by Izotov, Thuan & Lipovetsky (1997) and Izotov & Thuan (1998b) using BCGs, and by Jimenez et al. (2003) from nearby K dwarf stars.

3. We have considerably reduced the errors in the dY/dO and dY/dZ slopes derived for the whole sample as it contains galaxies spanning a wide range of metallicities, which was not the case in our previous work. From the $Y - \text{O/H}$ linear regression of the whole sample, with only collisional and fluorescent enhancements taken into account, we derive slopes $dY/dO = 4.3 \pm 0.7$ and $dY/dZ = 2.8 \pm 0.5$, in good agreement with the slopes derived from the subsample of 7 H II regions where all known systematic effects, with the exception of ionization correction effects, are taken into account.

Y.I.I. is grateful to the staff of the Astronomy Department at the University of Virginia for warm hospitality. Y.I.I. and T.X.T. thank the support of National Science Foundation grant AST 02-05785.

REFERENCES

Aller, L. H. 1984, Physics of Thermal Gaseous Nebulae (Dordrecht: Reidel)

Ballantyne, D. R., Ferland, G. J., & Martin, P. G. 2000, ApJ, 536, 773

Bania, T. M., Rood, R. T., & Balser, D. S. 2002, Nature, 415, 54

Benjamin, R. A., Skillman, E. D., & Smits, D. P. 1999, ApJ, 514, 307

———. 2002, ApJ, 569, 288

Bonifacio, P., & Molaro, P. 1997, MNRAS, 285, 847

Burles, S., & Tytler, D. 1998a, ApJ, 499, 699

———. 1998b, ApJ, 507, 732

Carigi, L., Colín, P., Peimbert, M., & Sarmiento, A. 1995, ApJ, 445, 98

Carigi, L., Colín, P., & Peimbert, M. 1999, ApJ, 514, 787

Christensen-Dalsgaard, J. 1998, Space Sci. Rev., 85, 19

Davidson, K., & Kinman, T. D. 1985, ApJS, 58, 321

Dinerstein, H. L., & Shields, G. A. 1986, ApJ, 311, 45

Ferland, G. J. 1996, Hazy: A Brief Introduction to CLOUDY (Univ. Kentucky, Dept. Phys & Astron., internal rep.)

Ferland, G. J., Korista, K. T., Verner, D. A., Ferguson, J. W., Kingdon, J. B., & Verner, E. M. 1998, PASP, 110, 761

Ford, A., Jeffries, R. D., Smalley, B., Ryan, S. G., Aoki, W., Kawanomoto, S., James, D. J., & Barnes, J. R. 2002, A&A, 393, 617

French, H. B. 1980, ApJ, 240, 41

Garnett, D. R. 1992, AJ, 103, 1330

González Delgado, R. M., Leitherer, C., & Heckman, T. M. 1999, ApJS, 125, 489

Gruenwald, R., Steigman, G., & Viegas, S. M. 2002, ApJ, 567, 931

Guseva, N. G., Izotov, Y. I., & Thuan, T. X. 2000, ApJ, 531, 776

Guseva, N. G., Izotov, Y. I., Papaderos, P., et al. 2001, *A&A*, 378, 756

Guseva, N. G., Papaderos, P., Izotov, Y. I., Green, R. F., Fricke, K. J., Thuan, T. X., & Noeske, K. G. 2003a, *A&A*, 407, 91

———. 2003b, *A&A*, 407, 105

Hopp, U., Engels, D., Green, R. F., et al. 2000, *A&AS*, 142, 417

Izotov, Y. I., & Thuan, T. X. 1998a, *ApJ*, 497, 227

———. 1998b, *ApJ*, 500, 188 (IT98)

———. 1999, *ApJ*, 511, 639

Izotov, Y. I., Thuan, T. X., & Lipovetsky, V. A. 1994, *ApJ*, 435, 647 (ITL94)

———. 1997a, *ApJS*, 108, 1 (ITL97)

Izotov, Y. I., Lipovetsky, V. A., Chaffee, F. H., Foltz, C. B., Guseva, N. G., & Kniazev, A. Y. 1997, *ApJ*, 476, 698

Izotov, Y. I., Chaffee, F. H., Foltz, C. B., Green, R. F., Guseva, N. G., & Thuan, T. X. 1999, *ApJ*, 527, 757

Izotov, Y. I., Chaffee, F. H., & Green, R. F. 2001a, *ApJ*, 562, 727

Izotov, Y. I., Chaffee, F. H., & Schaerer, D. 2001b, *A&A*, 378, 45L

Jimenez, R., Flynn, C., MacDonald, J., & Gibson, B. K. 2003, *Science*, 299, 1552

Kingdon, J. & Ferland, G. J. 1995, *ApJ*, 442, 714

Kinman, T. D., & Davidson, K. 1981, *ApJ*, 243, 127

Kirkman, D., Tytler, D., Suzuki, N., O'Meara, J. M., & Lubin, D. 2003, *ApJS*, submitted; preprint (astro-ph/0302006)

Kniazev, A. Y., Pustilnik, S. A., Ugryumov, A. V., & Kniazeva, T. F. 2000, *Ast.Lett.*, 26, 129

Kniazev, A. Y., Engels, D., Pustilnik, S. A., et al. 2001a, *A&A*, 366, 771

Kniazev, A. Y., Pustilnik, S. A., Ugryumov, A. V., & Pramsky, A. G. 2001b, *A&A*, 371, 404

Kniazev, A. Y., Grebel, E. K., Hao, L., Strauss, M. A., Brinkmann, J., & Fukugita, M. 2003, *ApJ*, 593, L73

Kunth, D., & Sargent, W. L. W. 1983, *ApJ*, 273, 81

Kunth, D., & Schild, H. 1986, *A&A*, 169, 71

Kunth, D., Sargent, W. L. W., & Kowal, C. 1981, *A&AS*, 44, 229

Larsen, T. I., Sommer-Larsen, J., & Pagel, B. E. J. 2001, *MNRAS*, 323, 555

Maeder, A. 1992, *A&A*, 264, 105

Markarian, B. E. 1967, *Astrofizika*, 3, 55

Netterfield, C. B., Ade, P. A. R., Bock, J. J., et al. 2002, *ApJ*, 571, 604

Oke, J. B. 1990, *AJ*, 99, 1621

Olive, K. A., & Skillman, E. D. 2001, *New Astronomy*, 6, 119

Olive, K. A., Skillman, D. A., & Steigman, G. 1997, *ApJ*, 483, 788

Olofsson, K. 1995, *A&AS*, 111, 57

O'Meara, J. M., Tytler, D., Kirkman, D., Suzuki, N., Prochaska, J. X., Lubin, D., & Wolfe, A. M. 2001, *ApJ*, 552, 718

Pagel, B. E. J., Terlevich, R. J., & Melnick, J. 1986, *PASP*, 98, 1005

Pagel, B. E. J., Simonson, E. A., Terlevich, R. J., & Edmunds, M. G. 1992, *MNRAS*, 255, 325

Peimbert, A. 2003, *ApJ*, 584, 735

Peimbert, A., Peimbert, M., & Luridiana, V. 2002, *ApJ*, 565, 668

Peimbert, M. 1967, *ApJ*, 150, 825

Peimbert, M., & Torres-Peimbert, S. 1974, *ApJ*, 193, 327

———. 1976, *ApJ*, 203, 581

Peimbert, M., Peimbert, A., & Ruiz, M. T. 2000, *ApJ*, 541, 688

Pettini, M., & Bowen, D. W. 2001, *ApJ*, 560, 41

Pilyugin, L. S. 1994, A&A, 287, 387

Pryke, C., Halverson, N. W., Leitch, E. M., Kovac, J., Carlstrom, J. E., Holzapfel, W. L., & Dragovan, M. 2002, ApJ, 568, 46

Pustilnik, S. A., Engels, D., Ugryumov, A. V., et al. 1999, A&AS, 137, 299

Rayo, J. F., Peimbert, M., & Torres-Peimbert, S. 1982, ApJ, 255, 1

Reeves, H. 1994, Rev.Mod.Phys., 66, 193

Robbins, R. R. 1968, ApJ, 151, 511

Ryan, S. G., Norris, J. E., & Beers, T. C. 1999, ApJ, 523, 654

Ryan, S. G., Beers, T. M., Olive, K. A., Fields, B. D., & Norris, J. E. 2000, ApJ, 530, L57

Salzer, J. J., & MacAlpine, G. M. 1988, AJ, 96, 1192

Sarkar, S. 1996, Rep.Prog.Phys., 59, 1493

Sauer, D., & Jedamzik, K. 2002, A&A, 381, 361

Schaerer, D., & Vacca, W. 1998, ApJ, 497, 618

Smits, D. P. 1996, MNRAS, 278, 683

Spergel, D. N., Verde, L., Peiris, H. V., et al. 2003, ApJS, 148, 175

Stasińska, G. 1990, A&AS, 83, 501

Stasińska, G., & Izotov, Y. I. 2001, A&A, 378, 817

Steel, S. J., Smith, N., Metcalfe, L., Rabbette, M., & McBreen, B. 1996, A&A, 311, 721

Steigman, G., Viegas, S. M., & Gruenwald, R. 1997, ApJ, 490, 187

Terlevich, R., Melnick, J., Masegosa, J., Moles, M., & Copetti, V. F. 1991, A&AS, 91, 285

Thuan, T. X., & Izotov, Y. I. 2002, Space Sci. Reviews, 100, 263

Thuan, T. X., Izotov, Y. I., & Lipovetsky, V. A. 1995, ApJ, 445, 108

Thuan, T. X., Izotov, Y. I., & Foltz, C. B. 1999, ApJ, 525, 105

Tytler, D., O'Meara, J. M., Suzuki, N., & Lubin, D. 2000, Phys. Rep., 333-334, 409

Ugryumov, A. V., Engels, D., Lipovetsky, V. A., et al. 1999 *A&AS*, 135, 511

Ugryumov, A. V., Engels, D., Kniazev, A. Y., et al. 2001, *A&A*, 374, 907

Ugryumov, A. V., Engels, D., Pustilnik, S. A., Kniazev, A. Y., Pramskij, A. G., & Hagen, H.-J. 2003, *A&A*, 397, 463

van Zee, L. 2000, *AJ*, 119, 2757

Viegas, S. M., Gruenwald, R., & Steigman, G. 2000, *ApJ*, 531, 813

Walker, T. P., Steigman, G., Kang, H. S., Schramm, D. M., & Olive, K. A. 1991, *ApJ*, 376, 51

Whitford, A. E. 1958, *AJ*, 63, 201

Wilson, T. L., & Rood, R. T. 1994, *ARA&A*, 32, 191

Table 1. General Parameters of Galaxies

Name	Coordinates (2000.0)			m_{pg}	z^a	M_{pg}^b	Other names	Ref.
	α	δ						
HS 2359 + 1659	00 ^h 02 ^m 09 ^s 9	+17°15'59"	16.6	0.02076 ± 0.00012	-18.0			1
UM 238	00 24 41.9	+01 44 03	16.5	0.01423 ± 0.00017	-17.3			2
HS 0029 + 1748	00 32 03.2	+18 04 44	17.6	0.00705 ± 0.00011	-14.7			1
HS 0111 + 2115	01 14 37.6	+21 31 16	16.1	0.03227 ± 0.00010	-19.5			1
HS 0122 + 0743	01 25 34.2	+07 59 22	15.7	0.00986 ± 0.00006	-17.3	UGC 993		1
HS 0128 + 2832	01 31 21.3	+28 48 12	17.6	0.01613 ± 0.00010	-16.4			1
HS 0134 + 3415	01 37 13.8	+34 31 12	18.0	0.01949 ± 0.00007	-16.5			1
UM 133	01 44 41.4	+04 53 27	15.7	0.00532 ± 0.00004	-15.9			3
UM 396	02 07 26.5	+02 56 55	...	0.02093 ± 0.00011	...			2
Mrk 1063	02 54 33.6	-10 01 40	13.6	0.00503 ± 0.00007	-17.9	NGC 1140, VV 482		7
J 0519 + 0007	05 19 02.7	+00 07 29	18.2	0.04476 ± 0.00006	-18.1			16
HS 0735 + 3512	07 38 58.4	+35 05 36	17.6	0.03020 ± 0.00003	-17.8			4
HS 0811 + 4913	08 14 47.0	+49 04 10	18.6	0.00177 ± 0.00009	-10.7			4
HS 0837 + 4717	08 40 29.9	+47 07 09	18.2	0.04195 ± 0.00004	-17.9			4,5
HS 0924 + 3821	09 28 06.3	+38 07 55	18.5	0.06088 ± 0.00006	-18.4			4
CGCG 007–025	09 44 01.9	-00 38 32	17.5	0.00483 ± 0.00004	-13.9			6
Mrk 1236	09 49 54.1	+00 36 59	13.5	0.00625 ± 0.00010	-18.5	VV 620		7
HS 1028 + 3843	10 31 51.8	+38 28 07	19.4	0.02945 ± 0.00005	-16.0			8
Mrk 724	10 41 09.6	+21 21 43	16.5	0.00402 ± 0.00005	-14.5			9
Mrk 35	10 45 22.4	+55 57 37	13.3	0.00323 ± 0.00008	-17.3	NGC 3353, Haro 3		15
UM 422	11 20 14.6	+02 31 51	...	0.00536 ± 0.00002	...			2
UM 439	11 36 36.8	+00 48 58	15.1	0.00359 ± 0.00004	-15.7	UGC 6578		2
POX 36	11 58 58.3	-19 01 41	14.3	0.00355 ± 0.00007	-16.5	I SZ 63		10
Mrk 1315	12 15 18.7	+20 38 28	16.5	0.00261 ± 0.00005	-13.6			2
HS 1213 + 3636A	12 15 34.4	+36 20 16	17.5	0.00092 ± 0.00004	-10.3			11
HS 1214 + 3801	12 17 09.7	+37 44 52	16.5	0.00110 ± 0.00004	-11.7			12
Mrk 1329	12 37 03.0	+06 55 36	14.6	0.00519 ± 0.00012	-17.0			7
HS 1311 + 3628	13 13 18.5	+36 12 09	18.0	0.00293 ± 0.00006	-12.3			11
Mrk 450	13 14 47.2	+34 53 01	16.0	0.00279 ± 0.00005	-14.2	UGC 8323, VV 616		13
Mrk 67	13 41 55.9	+30 30 29	...	0.00311 ± 0.00002	...	UGCA 372		14
HS 2236 + 1344	22 38 31.1	+14 00 29	18.2	0.02115 ± 0.00034	-16.4			1

^aderived from spectra in this paper.

^ball objects are assumed to be at their redshift distances with $H_0=75 \text{ km s}^{-1}\text{Mpc}^{-1}$.

References. — (1) Uglyumov et al. (2003); (2) Terlevich et al. (1991); (3) Kniazev et al. (2001b);(4) Pustilnik et al. (1999); (5) Kniazev et al. (2000); (6) van Zee (2000); (7) Guseva et al. (2000); (8) Kniazev et al. (2001a); (9) Kunth & Schild (1986); (10) Kunth et al. (1981); (11) Uglyumov et al. (2001); (12) Hopp et al. (2000); (13) Kinman & Davidson (1981); (14) French (1980); (15) Steel et al. (1996); (16) Kniazev et al. (2003).

Table 2. Journal of Observations

Galaxy	Date	Number of Exposures	Exposure time (minutes)	Airmass	Position angle (degrees)	Aperture ^a (arcsec)
HS 2359 + 1659	December 31, 2002	3	45	1.1	158	2.0 × 6.9
UM 238	December 31	3	45	1.3	100	2.0 × 4.5
HS 0029 + 1748	January 1, 2003	3	45	1.2	180	2.0 × 6.9
HS 0111 + 2115	December 30	2	30	1.1	0	2.0 × 4.1
HS 0122 + 0743	December 31	3	45	1.2	0	2.0 × 4.8
HS 0128 + 2832	December 31	3	45	1.3	0	2.0 × 4.1
HS 0134 + 3415	January 1	3	45	1.4	100	2.0 × 6.9
UM 133	December 30	4	60	1.2	22	2.0 × 6.9
UM 396	December 31	2	30	1.3	0	2.0 × 6.9
Mrk 1063	January 1	3	30	1.5	180	2.0 × 11.0
J 0519 + 0007	December 30	3	60	1.2	22	2.0 × 6.9
HS 0735 + 3512	January 1	3	45	1.1	100	2.0 × 5.5
HS 0811 + 4913	December 31	3	60	1.2	0	2.0 × 6.9
HS 0837 + 4717	January 1	4	60	1.1	100	2.0 × 6.9
HS 0924 + 3821	January 1	3	45	1.0	100	2.0 × 6.9
CGCG 007 – 025 ^b	December 30	3	60	1.4	155	2.0 × 3.5
Mrk 1236	December 31	3	45	1.2	80	2.0 × 4.1
HS 1028 + 3843	December 31	3	60	1.3	0	2.0 × 4.1
Mrk 724	December 30	3	45	1.1	155	2.0 × 6.9
Mrk 35	December 30	3	30	1.5	45	2.0 × 6.9
UM 422	December 31	3	45	1.2	170	2.0 × 5.5
UM 439	December 31	2	30	1.2	170	2.0 × 5.5
POX 36	December 30	3	30	1.7	155	2.0 × 5.5
Mrk 1315	December 30	3	45	1.2	155	2.0 × 6.9
HS 1213 + 3636A	January 1	3	45	1.3	45	2.0 × 6.9
HS 1214 + 3801	December 31	3	45	1.2	135	2.0 × 6.9
Mrk 1329	December 30	3	45	1.1	60	2.0 × 4.1
HS 1311 + 3628	January 1	3	45	1.2	45	2.0 × 6.9
Mrk 450 ^b	January 1	2	30	1.1	45	2.0 × 5.5
Mrk 67	January 1	2	20	1.1	45	2.0 × 6.9
HS 2236 + 1344	December 30	2	40	1.3	0	2.0 × 9.7

^aAperture used for extraction of one-dimensional spectra.

^bGalaxies in which two H II regions are used for abundance determination. The two spectra are extracted within equal apertures.

TABLE 3
EMISSION LINE INTENSITIES AND EQUIVALENT WIDTHS

Ion	GALAXY											
	HS 2359+1659			UM 238			HS 0029+1748			HS 0111+2115		
	$F(\lambda)/F(H\beta)$	$I(\lambda)/I(H\beta)$	EW ^a									
3727 [O II]	103.40 ± 1.66	127.71 ± 2.19	171.8	82.93 ± 1.41	96.69 ± 1.79	230.0	71.99 ± 1.21	91.40 ± 1.67	106.3	240.88 ± 4.46	320.70 ± 6.56	117.8
3750 H12	2.19 ± 0.32	2.71 ± 0.55	3.7	1.36 ± 0.35	3.59 ± 1.39	3.9	1.45 ± 0.29	4.42 ± 1.26	2.1
3771 H11	2.57 ± 0.36	3.16 ± 0.58	4.3	1.91 ± 0.32	4.24 ± 1.03	5.4	1.62 ± 0.30	4.62 ± 1.15	2.3
3798 H10	3.43 ± 0.27	4.19 ± 0.50	5.8	2.73 ± 0.31	5.19 ± 0.90	7.7	2.97 ± 0.26	6.37 ± 0.80	4.1
3820 He I	1.14 ± 0.25	1.38 ± 0.30	2.0
3835 H9	5.70 ± 0.28	6.89 ± 0.50	9.7	4.56 ± 0.30	7.25 ± 0.81	12.8	3.91 ± 0.24	7.51 ± 0.72	5.3
3868 [Ne III]	38.10 ± 0.65	45.69 ± 0.82	62.7	40.31 ± 0.71	45.88 ± 0.86	111.0	34.73 ± 0.59	42.53 ± 0.78	46.8	29.32 ± 1.13	37.35 ± 1.50	13.0
3889 He I + H8	15.69 ± 0.37	18.75 ± 0.60	24.1	13.00 ± 0.32	16.76 ± 0.76	36.6	12.38 ± 0.28	17.53 ± 0.62	18.3	10.97 ± 0.85	18.86 ± 1.87	5.1
3968 [Ne III] + H7	24.21 ± 0.47	28.46 ± 0.67	41.2	25.12 ± 0.50	30.17 ± 0.90	68.9	21.39 ± 0.39	28.33 ± 0.76	27.4	14.73 ± 0.86	23.03 ± 1.75	6.9
4026 He I	1.79 ± 0.24	2.08 ± 0.28	3.1	1.30 ± 0.24	1.44 ± 0.27	3.4	1.57 ± 0.19	1.85 ± 0.23	2.0
4068 [S II]	2.19 ± 0.25	2.53 ± 0.29	3.9	1.08 ± 0.22	1.19 ± 0.25	2.8	0.86 ± 0.21	1.01 ± 0.25	1.1	1.92 ± 0.78	2.31 ± 0.97	0.9
4101 H δ	21.93 ± 0.42	25.12 ± 0.59	39.3	19.15 ± 0.40	23.15 ± 0.84	48.5	18.75 ± 0.35	24.34 ± 0.69	24.3	18.09 ± 0.81	25.97 ± 1.54	8.8
4340 H γ	43.37 ± 0.69	47.47 ± 0.83	81.5	39.98 ± 0.65	44.32 ± 0.99	101.4	41.21 ± 0.64	47.57 ± 0.90	54.5	38.57 ± 0.96	46.52 ± 1.44	21.4
4363 [O III]	6.17 ± 0.22	6.72 ± 0.24	11.7	8.66 ± 0.25	9.12 ± 0.27	22.1	7.05 ± 0.20	7.68 ± 0.22	9.3	3.52 ± 0.59	3.89 ± 0.67	1.8
4387 He I	0.42 ± 0.15	0.45 ± 0.16	0.8
4471 He I	3.70 ± 0.20	3.95 ± 0.22	7.1	3.84 ± 0.18	3.98 ± 0.19	9.8	3.34 ± 0.16	3.56 ± 0.17	4.4	3.66 ± 0.69	3.93 ± 0.77	2.0
4658 [Fe III]	0.48 ± 0.13	0.48 ± 0.14	1.2
4686 He II	0.87 ± 0.14	0.90 ± 0.15	1.8	0.76 ± 0.14	0.77 ± 0.14	1.0
4711 [Ar IV] + He I	1.12 ± 0.14	1.14 ± 0.14	2.3	1.84 ± 0.16	1.85 ± 0.16	4.8	1.09 ± 0.12	1.10 ± 0.12	1.5
4740 [Ar IV]	1.12 ± 0.16	1.11 ± 0.17	3.0	0.57 ± 0.14	0.58 ± 0.15	0.8
4861 H β	100.00 ± 1.50	100.00 ± 1.52	218.5	100.00 ± 1.50	100.00 ± 1.63	274.3	100.00 ± 1.47	100.00 ± 1.56	149.4	100.00 ± 1.81	100.00 ± 1.96	63.0
4921 He I	0.97 ± 0.13	0.96 ± 0.13	2.2	1.15 ± 0.16	1.12 ± 0.16	3.1	1.10 ± 0.14	1.07 ± 0.14	1.6
4959 [O III]	210.56 ± 3.10	207.27 ± 3.07	469.0	250.99 ± 3.70	243.38 ± 3.67	692.4	200.30 ± 2.92	192.67 ± 2.89	298.6	153.34 ± 2.66	145.59 ± 2.62	98.3
5007 [O III]	642.64 ± 9.40	627.82 ± 9.23	1450.0	767.77 ± 11.2	739.93 ± 11.1	2109.0	609.64 ± 8.83	581.01 ± 8.64	912.1	476.39 ± 7.83	447.24 ± 7.63	307.0
5199 [N I]	0.51 ± 0.14	0.48 ± 0.14	1.5	1.75 ± 0.59	1.57 ± 0.55	1.2
5271 [Fe III]	0.42 ± 0.14	0.39 ± 0.13	1.0
5518 [Cl III]	0.51 ± 0.11	0.46 ± 0.10	1.4	0.61 ± 0.14	0.55 ± 0.13	1.9	0.38 ± 0.09	0.33 ± 0.08	0.6
5538 [Cl III]	0.59 ± 0.14	0.53 ± 0.12	1.6	0.65 ± 0.10	0.56 ± 0.08	1.1
5755 [N II]	0.51 ± 0.13	0.45 ± 0.12	1.4
5876 He I	12.76 ± 0.27	11.02 ± 0.24	36.3	13.56 ± 0.27	11.82 ± 0.25	44.7	12.98 ± 0.24	10.64 ± 0.21	22.8	15.13 ± 0.57	11.82 ± 0.47	11.4
6300 [O I]	3.24 ± 0.14	2.66 ± 0.11	10.1	3.29 ± 0.16	2.75 ± 0.13	11.9	2.18 ± 0.13	1.68 ± 0.10	4.4	5.43 ± 0.45	3.93 ± 0.34	4.6
6312 [S III]	1.99 ± 0.12	1.63 ± 0.10	6.2	1.88 ± 0.13	1.57 ± 0.11	6.8	3.00 ± 0.13	2.30 ± 0.10	6.1	1.00 ± 0.35	0.72 ± 0.26	0.9
6363 [O I]	1.24 ± 0.14	1.01 ± 0.11	4.0	1.04 ± 0.14	0.86 ± 0.12	3.8	0.83 ± 0.12	0.63 ± 0.09	1.7	2.18 ± 0.48	1.56 ± 0.36	1.9
6548 [N II]	3.17 ± 0.15	2.53 ± 0.12	10.6	3.15 ± 0.16	2.57 ± 0.14	12.5	2.64 ± 0.15	1.96 ± 0.11	5.4	10.03 ± 0.55	6.96 ± 0.40	8.6
6563 H α	358.71 ± 5.26	285.60 ± 4.57	1202.0	347.03 ± 5.10	284.27 ± 4.65	1380.0	381.76 ± 5.54	284.34 ± 4.60	793.9	413.52 ± 6.92	287.66 ± 5.42	357.9
6583 [N II]	8.62 ± 0.22	6.85 ± 0.18	28.9	9.66 ± 0.25	7.87 ± 0.21	38.6	7.41 ± 0.19	5.48 ± 0.15	15.5	27.50 ± 0.76	18.97 ± 0.56	23.9
6678 He I	3.91 ± 0.20	3.07 ± 0.16	13.1	3.82 ± 0.18	3.09 ± 0.15	15.1	4.10 ± 0.15	3.00 ± 0.11	8.8	4.47 ± 0.54	3.04 ± 0.38	4.0
6717 [S II]	15.99 ± 0.31	12.52 ± 0.26	57.4	13.45 ± 0.30	10.83 ± 0.26	52.9	13.80 ± 0.27	10.04 ± 0.21	29.5	36.09 ± 0.94	24.38 ± 0.69	32.4
6731 [S II]	10.58 ± 0.25	8.27 ± 0.20	38.1	11.45 ± 0.27	9.21 ± 0.23	45.2	10.29 ± 0.22	7.47 ± 0.17	22.0	24.69 ± 0.80	16.64 ± 0.57	22.1
7065 He I	3.49 ± 0.22	2.64 ± 0.17	13.2	4.92 ± 0.23	3.85 ± 0.19	22.1	3.52 ± 0.18	2.45 ± 0.13	8.4	4.37 ± 0.72	2.80 ± 0.48	4.2
7136 [Ar III]	11.47 ± 0.33	8.61 ± 0.26	44.2	10.18 ± 0.30	7.93 ± 0.25	46.3	11.62 ± 0.24	8.03 ± 0.18	27.4	11.94 ± 0.81	7.58 ± 0.54	11.4
7320 [O II]	1.99 ± 0.22	1.47 ± 0.17	7.8	2.03 ± 0.30	1.56 ± 0.24	9.8	2.03 ± 0.17	1.37 ± 0.12	5.1
7330 [O II]	1.92 ± 0.23	1.42 ± 0.17	7.6	1.78 ± 0.26	1.36 ± 0.21	8.4	1.35 ± 0.16	0.92 ± 0.11	3.4
$C(H\beta)$	0.298			0.242			0.365			0.444		
$F(H\beta)$ ^b	2.00			2.74			2.30			0.63		
EW(abs) Å	0.02			5.00			2.97			1.82		

TABLE 3—Continued

Ion	GALAXY											
	HS 0122+0743			HS 0128+2832			HS 0134+3415			UM 133		
	$F(\lambda)/F(H\beta)$	$I(\lambda)/I(H\beta)$	EW ^a									
3727 [O II]	66.68 ± 1.13	71.89 ± 1.31	103.1	61.10 ± 0.90	78.90 ± 1.29	134.0	60.91 ± 1.02	65.24 ± 1.16	108.8	150.02 ± 2.39	180.61 ± 3.08	73.3
3750 H I 2	2.00 ± 0.27	3.86 ± 0.64	3.1	0.95 ± 0.21	4.16 ± 1.03	2.1	2.49 ± 0.27	2.67 ± 0.42	4.4
3771 H I 1	2.80 ± 0.27	4.72 ± 0.57	4.3	1.49 ± 0.18	4.90 ± 0.69	3.2	3.19 ± 0.26	3.41 ± 0.41	5.7	2.32 ± 0.42	2.77 ± 0.68	1.1
3798 H I 0	3.61 ± 0.27	5.60 ± 0.53	5.5	2.10 ± 0.17	5.74 ± 0.57	4.3	4.87 ± 0.26	5.19 ± 0.41	8.7	2.74 ± 0.47	3.25 ± 0.73	1.3
3820 He I	1.06 ± 0.25	1.14 ± 0.27	1.6	1.06 ± 0.15	1.34 ± 0.19	2.2	0.93 ± 0.19	0.99 ± 0.20	1.7
3835 H I 9	6.01 ± 0.26	8.15 ± 0.47	9.1	3.00 ± 0.14	6.86 ± 0.41	6.1	6.47 ± 0.27	6.88 ± 0.42	11.7	4.57 ± 0.36	5.39 ± 0.62	2.3
3868 [Ne III]	33.76 ± 0.57	35.97 ± 0.64	51.5	32.59 ± 0.48	40.48 ± 0.65	65.2	59.93 ± 0.93	63.58 ± 1.04	109.1	34.31 ± 0.68	40.25 ± 0.83	16.9
3889 He I + H 8	16.55 ± 0.34	19.39 ± 0.52	24.2	11.17 ± 0.20	16.75 ± 0.37	23.4	18.92 ± 0.37	20.04 ± 0.50	34.3	17.08 ± 0.47	19.96 ± 0.71	8.6
3968 [Ne III] + H 7	23.85 ± 0.42	26.87 ± 0.57	37.2	19.58 ± 0.30	26.70 ± 0.48	39.2	33.16 ± 0.56	34.95 ± 0.67	62.9	22.73 ± 0.47	26.20 ± 0.69	12.3
4026 He I	0.95 ± 0.13	0.99 ± 0.14	1.5	1.08 ± 0.11	1.28 ± 0.13	2.1	1.59 ± 0.19	1.67 ± 0.20	3.0
4068 [S II]	0.84 ± 0.16	0.88 ± 0.17	1.4	1.09 ± 0.12	1.28 ± 0.14	2.1	0.67 ± 0.16	0.70 ± 0.17	1.3
4101 H δ	23.08 ± 0.41	25.66 ± 0.53	38.7	17.20 ± 0.27	23.10 ± 0.42	33.3	26.55 ± 0.45	27.74 ± 0.55	52.6	24.33 ± 0.46	27.40 ± 0.64	15.1
4340 H γ	45.11 ± 0.70	47.67 ± 0.80	83.6	38.47 ± 0.55	45.05 ± 0.70	78.7	46.52 ± 0.71	47.90 ± 0.78	104.8	44.89 ± 0.72	48.59 ± 0.84	32.0
4363 [O III]	11.90 ± 0.24	12.20 ± 0.26	22.3	8.18 ± 0.15	8.96 ± 0.17	16.9	16.76 ± 0.30	17.23 ± 0.32	38.0	8.43 ± 0.29	9.09 ± 0.31	6.0
4387 He I	0.36 ± 0.12	0.37 ± 0.13	0.7
4471 He I	3.53 ± 0.15	3.59 ± 0.16	7.0	3.60 ± 0.10	3.84 ± 0.11	7.4	3.78 ± 0.16	3.86 ± 0.17	8.8	3.15 ± 0.20	3.34 ± 0.21	2.4
4658 [Fe III]	0.31 ± 0.08	0.31 ± 0.08	0.7	0.60 ± 0.08	0.61 ± 0.08	1.2	0.57 ± 0.12	0.59 ± 0.12	0.5
4686 He II	0.76 ± 0.10	0.76 ± 0.10	1.7	0.58 ± 0.18	0.59 ± 0.19	1.5	1.57 ± 0.14	1.61 ± 0.15	1.4
4711 [Ar IV] + He I	1.57 ± 0.11	1.57 ± 0.11	3.5	1.25 ± 0.08	1.27 ± 0.08	2.6	3.52 ± 0.15	3.55 ± 0.15	9.2	0.70 ± 0.14	0.72 ± 0.14	0.6
4740 [Ar IV]	0.78 ± 0.11	0.78 ± 0.11	1.8	1.13 ± 0.08	1.13 ± 0.08	2.4	2.32 ± 0.13	2.33 ± 0.13	6.2
4861 H β	100.00 ± 1.48	100.00 ± 1.51	232.5	100.00 ± 1.42	100.00 ± 1.47	223.0	100.00 ± 1.47	100.00 ± 1.48	275.0	100.00 ± 1.49	100.00 ± 1.50	97.2
4921 He I	0.90 ± 0.12	0.89 ± 0.12	2.2	0.91 ± 0.08	0.88 ± 0.08	2.0	1.08 ± 0.14	1.07 ± 0.14	2.9	0.80 ± 0.13	0.80 ± 0.13	0.8
4959 [O III]	151.46 ± 2.22	148.93 ± 2.21	369.1	248.66 ± 3.52	238.25 ± 3.47	556.2	244.82 ± 3.55	243.57 ± 3.54	691.7	127.29 ± 1.88	125.55 ± 1.86	126.3
5007 [O III]	457.45 ± 6.65	448.41 ± 6.61	1151.0	753.28 ± 10.7	714.58 ± 10.4	1686.0	746.60 ± 10.8	740.97 ± 10.7	2115.0	382.89 ± 5.58	375.15 ± 5.49	387.0
5199 [N I]	0.60 ± 0.09	0.58 ± 0.09	1.6	0.62 ± 0.09	0.59 ± 0.09	0.7
5271 [Fe III]	0.40 ± 0.11	0.38 ± 0.10	0.5
5518 [Cl III]	0.40 ± 0.07	0.34 ± 0.06	1.0
5538 [Cl III]	0.44 ± 0.07	0.37 ± 0.06	1.1
5876 He I	10.82 ± 0.21	10.09 ± 0.20	35.1	14.47 ± 0.22	11.67 ± 0.19	37.1	10.79 ± 0.21	10.29 ± 0.20	41.6	10.97 ± 0.23	9.64 ± 0.21	16.2
6300 [O I]	2.28 ± 0.10	2.08 ± 0.09	9.0	2.62 ± 0.08	1.97 ± 0.06	7.8	2.01 ± 0.11	1.88 ± 0.10	8.9	3.04 ± 0.15	2.55 ± 0.13	5.1
6312 [S III]	1.37 ± 0.09	1.25 ± 0.08	5.4	2.21 ± 0.08	1.66 ± 0.06	6.6	1.50 ± 0.12	1.40 ± 0.11	6.6	1.55 ± 0.12	1.30 ± 0.10	2.6
6363 [O I]	0.71 ± 0.08	0.65 ± 0.07	2.8	1.02 ± 0.08	0.76 ± 0.06	3.1	0.66 ± 0.09	0.61 ± 0.09	2.9	1.06 ± 0.12	0.88 ± 0.10	1.8
6548 [N II]	3.62 ± 0.10	2.63 ± 0.07	11.4
6563 H α	305.85 ± 4.46	276.45 ± 4.43	1263.0	391.50 ± 5.54	284.87 ± 4.51	1271.4	299.36 ± 4.34	277.96 ± 4.38	1344.0	340.17 ± 4.96	278.47 ± 4.43	592.5
6583 [N II]	2.54 ± 0.11	2.29 ± 0.10	10.5	9.87 ± 0.16	7.13 ± 0.13	31.0	2.96 ± 0.13	2.75 ± 0.12	11.7	5.06 ± 0.17	4.13 ± 0.15	9.1
6678 He I	3.08 ± 0.11	2.77 ± 0.10	15.2	4.26 ± 0.10	3.04 ± 0.08	13.8	3.04 ± 0.14	2.81 ± 0.13	14.2	3.23 ± 0.16	2.61 ± 0.13	6.0
6717 [S II]	7.24 ± 0.16	6.49 ± 0.15	32.3	12.82 ± 0.20	9.09 ± 0.16	42.5	7.93 ± 0.19	7.33 ± 0.18	38.8	14.18 ± 0.27	11.44 ± 0.23	26.8
6731 [S II]	5.35 ± 0.13	4.79 ± 0.12	24.0	9.78 ± 0.16	6.92 ± 0.13	32.5	6.40 ± 0.17	5.91 ± 0.17	31.6	10.02 ± 0.22	8.08 ± 0.19	18.9
7065 He I	2.94 ± 0.13	2.60 ± 0.12	13.9	4.90 ± 0.13	3.32 ± 0.09	18.0	3.20 ± 0.16	2.92 ± 0.14	16.7	2.74 ± 0.18	2.14 ± 0.14	5.8
7136 [Ar III]	3.03 ± 0.13	2.67 ± 0.12	15.8	12.32 ± 0.21	8.27 ± 0.16	47.3	5.74 ± 0.20	5.23 ± 0.18	31.3	6.40 ± 0.27	4.98 ± 0.21	13.6
7281 He I	0.70 ± 0.16	0.54 ± 0.12	1.6
7320 [O II]	1.23 ± 0.11	1.08 ± 0.09	6.7	2.09 ± 0.15	1.37 ± 0.10	8.2	2.11 ± 0.19	1.61 ± 0.15	4.7
7330 [O II]	0.83 ± 0.11	0.72 ± 0.09	4.5	1.94 ± 0.03	1.27 ± 0.02	7.6	1.86 ± 0.18	1.42 ± 0.14	4.1
$C(H\beta)$	0.121	0.392					0.097			0.262		
$F(H\beta)$ ^b	2.22	2.06					2.36			2.08		
EW(abs) Å	2.46	5.00					0.00			0.00		

TABLE 3—Continued

Ion	GALAXY											
	UM 396			Mrk 1063			J 0519+0007			HS 0735+3512		
	$F(\lambda)/F(H\beta)$	$I(\lambda)/I(H\beta)$	EW ^a									
3727 [O II]	98.24 ± 1.48	111.66 ± 1.88	132.4	219.33 ± 3.54	232.26 ± 4.33	47.9	34.18 ± 0.76	42.35 ± 0.98	41.3	180.34 ± 2.66	210.96 ± 3.37	166.7
3750 H I 2	2.33 ± 0.58	6.84 ± 1.84	3.1	2.31 ± 0.36	2.84 ± 0.60	2.8	2.78 ± 0.30	3.25 ± 0.44	2.6
3771 H I 1	2.92 ± 0.62	7.50 ± 1.71	3.9	3.32 ± 0.35	4.07 ± 0.58	4.2	3.60 ± 0.26	4.19 ± 0.40	3.4
3798 H I 0	3.28 ± 0.44	7.93 ± 1.18	4.3	5.23 ± 0.35	6.38 ± 0.56	6.8	4.07 ± 0.29	4.72 ± 0.43	3.8
3820 He I	0.96 ± 0.22	1.17 ± 0.26	1.3
3835 H 9	4.17 ± 0.36	8.86 ± 0.88	5.5	6.34 ± 0.31	7.67 ± 0.51	8.7	5.35 ± 0.27	6.16 ± 0.41	4.9
3868 [Ne III]	41.97 ± 0.66	46.62 ± 0.80	50.1	21.61 ± 0.66	22.45 ± 0.75	3.7	37.17 ± 0.66	44.70 ± 0.84	51.0	44.87 ± 0.71	51.35 ± 0.85	41.4
3889 He I + H 8	13.10 ± 0.32	19.06 ± 0.57	15.9	8.02 ± 0.53	19.73 ± 1.70	1.5	17.29 ± 0.42	20.70 ± 0.63	22.9	16.82 ± 0.34	19.19 ± 0.48	15.1
3968 [Ne III] + H 7	22.58 ± 0.42	29.30 ± 0.65	26.7	7.96 ± 0.46	19.29 ± 1.51	1.6	27.59 ± 0.54	32.51 ± 0.72	40.3	26.42 ± 0.45	29.79 ± 0.58	25.6
4026 He I	1.95 ± 0.24	2.11 ± 0.27	2.2	1.23 ± 0.22	1.43 ± 0.26	1.9	1.66 ± 0.22	1.85 ± 0.25	1.5
4068 [S II]	1.91 ± 0.22	2.05 ± 0.25	2.2	1.47 ± 0.47	1.49 ± 0.52	0.3	0.70 ± 0.23	0.81 ± 0.27	1.1	1.96 ± 0.21	2.17 ± 0.23	1.8
4101 H δ	19.58 ± 0.36	25.53 ± 0.58	23.0	14.48 ± 0.51	25.04 ± 1.16	3.0	25.92 ± 0.50	29.73 ± 0.65	41.4	23.11 ± 0.40	25.55 ± 0.52	22.8
4340 H γ	39.64 ± 0.60	45.25 ± 0.77	47.9	38.15 ± 0.69	47.01 ± 1.06	8.2	46.85 ± 0.75	51.34 ± 0.87	86.8	45.73 ± 0.69	48.90 ± 0.78	50.5
4363 [O III]	5.71 ± 0.20	5.88 ± 0.22	6.9	2.05 ± 0.35	2.00 ± 0.37	0.4	14.16 ± 0.33	15.45 ± 0.36	26.7	5.92 ± 0.18	6.31 ± 0.19	6.5
4471 He I	3.90 ± 0.19	3.96 ± 0.20	4.8	3.60 ± 0.36	3.47 ± 0.38	0.8	3.68 ± 0.22	3.94 ± 0.23	7.6	3.70 ± 0.15	3.89 ± 0.16	4.3
4658 [Fe III]	0.67 ± 0.14	0.67 ± 0.14	0.8	1.85 ± 0.43	1.75 ± 0.44	0.4	1.22 ± 0.18	1.26 ± 0.19	1.5
4686 He II	2.01 ± 0.17	1.98 ± 0.18	2.5	2.45 ± 0.20	2.52 ± 0.20	5.8	0.79 ± 0.17	0.81 ± 0.18	1.0
4711 [Ar IV] + He I	1.33 ± 0.16	1.30 ± 0.17	1.7	2.22 ± 0.18	2.28 ± 0.19	5.3	0.83 ± 0.17	0.84 ± 0.17	1.0
4740 [Ar IV]	1.44 ± 0.17	1.47 ± 0.17	3.4
4861 H β	100.00 ± 1.43	100.00 ± 1.51	132.7	100.00 ± 1.49	100.00 ± 1.66	26.1	100.00 ± 1.50	100.00 ± 1.52	242.5	100.00 ± 1.46	100.00 ± 1.48	134.5
4921 He I	0.92 ± 0.19	0.91 ± 0.18	2.2	1.14 ± 0.17	1.13 ± 0.17	1.5
4959 [O III]	215.88 ± 3.08	205.53 ± 3.05	283.3	105.64 ± 1.57	96.69 ± 1.56	26.0	145.09 ± 2.16	142.80 ± 2.13	375.0	189.74 ± 2.75	187.54 ± 2.72	262.5
5007 [O III]	658.79 ± 9.38	623.51 ± 9.25	868.4	319.39 ± 4.66	290.90 ± 4.61	79.8	443.82 ± 6.51	433.47 ± 6.39	1154.0	577.40 ± 8.32	567.50 ± 8.22	805.0
5199 N I	1.71 ± 0.32	1.53 ± 0.31	0.5	0.85 ± 0.11	0.82 ± 0.11	1.3
5271 [Fe III]	0.37 ± 0.10	0.35 ± 0.10	0.6
5518 [Cl III]	0.76 ± 0.25	0.66 ± 0.24	0.2	0.61 ± 0.16	0.57 ± 0.15	1.0
5538 [Cl III]	0.51 ± 0.15	0.47 ± 0.14	0.8
5876 He I	13.33 ± 0.24	11.46 ± 0.22	20.7	13.69 ± 0.32	11.52 ± 0.29	4.4	12.14 ± 0.26	10.47 ± 0.23	43.6	12.86 ± 0.23	11.53 ± 0.21	22.7
6300 [O I]	2.91 ± 0.16	2.40 ± 0.13	5.0	4.49 ± 0.27	3.66 ± 0.24	1.6	0.98 ± 0.12	0.80 ± 0.10	3.9	4.87 ± 0.15	4.20 ± 0.13	9.7
6312 [S III]	1.59 ± 0.15	1.32 ± 0.12	2.8	0.87 ± 0.11	0.71 ± 0.09	3.7	1.88 ± 0.11	1.62 ± 0.10	3.7
6363 [O I]	0.95 ± 0.16	0.78 ± 0.14	1.7	1.20 ± 0.27	0.97 ± 0.24	0.4	1.74 ± 0.13	1.50 ± 0.11	3.5
6548 [N II]	3.24 ± 0.19	2.62 ± 0.16	5.8	10.52 ± 0.31	8.41 ± 0.28	4.0	4.47 ± 0.15	3.77 ± 0.13	9.6
6563 H α	352.01 ± 5.01	286.18 ± 4.61	635.3	355.26 ± 5.18	288.14 ± 4.95	136.2	345.75 ± 5.08	274.35 ± 4.40	1450.0	337.53 ± 4.88	284.99 ± 4.48	726.2
6583 [N II]	10.13 ± 0.23	8.16 ± 0.20	18.3	32.06 ± 0.54	25.56 ± 0.50	12.4	2.11 ± 0.20	1.67 ± 0.16	5.5	13.24 ± 0.24	11.16 ± 0.22	28.7
6678 He I	3.93 ± 0.21	3.14 ± 0.17	7.1	3.72 ± 0.31	2.95 ± 0.26	1.5	3.41 ± 0.20	2.67 ± 0.16	15.1	3.82 ± 0.17	3.20 ± 0.14	8.5
6717 [S II]	14.62 ± 0.28	11.65 ± 0.25	26.6	29.25 ± 0.53	23.11 ± 0.48	11.7	2.71 ± 0.19	2.12 ± 0.15	11.6	20.41 ± 0.35	17.02 ± 0.32	45.4
6731 [S II]	10.59 ± 0.25	8.43 ± 0.21	19.1	22.11 ± 0.44	17.46 ± 0.40	8.9	2.36 ± 0.18	1.84 ± 0.14	10.0	15.23 ± 0.27	12.69 ± 0.24	33.8
7065 He I	3.81 ± 0.25	2.95 ± 0.20	7.1	2.51 ± 0.37	1.94 ± 0.31	1.1	5.76 ± 0.31	4.34 ± 0.24	25.6	3.77 ± 0.20	3.06 ± 0.17	9.3
7136 [Ar III]	11.56 ± 0.30	8.91 ± 0.25	21.3	8.51 ± 0.46	6.55 ± 0.39	3.8	2.59 ± 0.31	1.94 ± 0.23	12.9	9.45 ± 0.26	7.64 ± 0.22	24.3
7281 He I	0.46 ± 0.37	0.35 ± 0.30	0.2
7320 [O II]	2.76 ± 0.50	2.10 ± 0.41	1.3
7330 [O II]	1.98 ± 0.42	1.51 ± 0.35	0.9
$C(H\beta)$	0.233			0.192			0.303			0.221		
$F(H\beta)^b$	1.42			18.62			1.50			3.26		
EW(abs) Å	4.99			2.13			0.00			0.01		

TABLE 3—Continued

Ion	GALAXY											
	HS 0811+4913			HS 0837+4717			HS 0924+3821			CGCG 007-025 (#1)		
	$F(\lambda)/F(H\beta)$	$I(\lambda)/I(H\beta)$	EW ^a									
3727 [O II]	109.13 ± 1.78	117.20 ± 2.06	265.0	50.18 ± 0.78	61.59 ± 1.03	65.9	172.36 ± 2.58	184.70 ± 3.05	133.4	88.70 ± 1.33	109.44 ± 1.77	127.8
3750 H I 2	3.13 ± 0.49	4.87 ± 0.94	7.6	3.10 ± 0.21	3.79 ± 0.34	4.1	2.11 ± 0.34	6.22 ± 1.23	1.6	2.83 ± 0.19	3.48 ± 0.34	4.1
3771 H I 1	2.80 ± 0.38	4.53 ± 0.82	6.7	3.48 ± 0.18	4.23 ± 0.31	4.6	2.01 ± 0.28	6.23 ± 1.10	1.5	3.49 ± 0.19	4.27 ± 0.33	5.1
3798 H I 0	4.42 ± 0.34	6.26 ± 0.71	10.4	4.77 ± 0.19	5.77 ± 0.32	6.2	2.80 ± 0.29	7.10 ± 0.94	2.1	4.34 ± 0.18	5.27 ± 0.32	6.4
3820 He I	0.76 ± 0.23	0.81 ± 0.24	1.8	0.84 ± 0.14	1.01 ± 0.17	1.1	0.78 ± 0.14	0.94 ± 0.17	1.1
3835 H I 9	5.46 ± 0.27	7.36 ± 0.63	12.8	6.59 ± 0.20	7.91 ± 0.32	8.8	4.27 ± 0.30	8.55 ± 0.75	3.2	6.15 ± 0.17	7.42 ± 0.31	9.1
3868 [Ne III]	49.39 ± 0.79	52.44 ± 0.89	118.8	47.16 ± 0.72	56.24 ± 0.91	65.3	37.37 ± 0.65	39.52 ± 0.73	27.9	43.26 ± 0.65	51.83 ± 0.83	65.3
3889 He I + H 8	16.82 ± 0.35	19.31 ± 0.64	41.2	16.24 ± 0.30	19.29 ± 0.42	21.9	14.28 ± 0.36	19.05 ± 0.61	10.9	17.65 ± 0.30	21.06 ± 0.44	26.3
3968 [Ne III] + H 7	30.20 ± 0.50	33.30 ± 0.75	73.5	28.61 ± 0.46	33.46 ± 0.60	43.3	23.16 ± 0.44	28.25 ± 0.66	17.5	27.75 ± 0.43	32.59 ± 0.56	46.3
4026 He I	1.39 ± 0.15	1.46 ± 0.15	3.7	1.72 ± 0.14	1.99 ± 0.16	2.6	1.25 ± 0.24	1.30 ± 0.26	0.9	1.51 ± 0.10	1.76 ± 0.11	2.6
4068 [S II]	1.68 ± 0.18	1.76 ± 0.19	4.4	1.61 ± 0.17	1.85 ± 0.19	2.5	1.41 ± 0.17	1.46 ± 0.19	1.1	1.15 ± 0.10	1.32 ± 0.11	2.0
4101 H δ	22.81 ± 0.40	25.15 ± 0.63	59.8	25.71 ± 0.41	29.31 ± 0.51	41.3	22.00 ± 0.41	26.42 ± 0.60	18.0	23.69 ± 0.36	27.10 ± 0.47	42.8
4340 H γ	45.19 ± 0.69	47.57 ± 0.84	128.1	45.50 ± 0.68	49.65 ± 0.77	84.5	42.74 ± 0.69	46.57 ± 0.83	39.2	47.01 ± 0.69	51.41 ± 0.78	100.4
4363 [O III]	11.30 ± 0.23	11.63 ± 0.24	32.7	16.65 ± 0.28	18.09 ± 0.31	31.3	6.27 ± 0.25	6.36 ± 0.26	5.8	11.91 ± 0.20	12.98 ± 0.22	25.7
4387 He I	0.59 ± 0.13	0.61 ± 0.13	1.8	0.50 ± 0.13	0.54 ± 0.14	0.9	0.41 ± 0.08	0.44 ± 0.09	0.9
4471 He I	3.79 ± 0.16	3.85 ± 0.17	11.8	3.89 ± 0.13	4.15 ± 0.14	8.1	3.56 ± 0.20	3.58 ± 0.21	3.4	3.54 ± 0.09	3.78 ± 0.10	8.1
4658 [Fe III]	0.25 ± 0.12	0.25 ± 0.13	0.9	1.08 ± 0.16	1.07 ± 0.16	1.1	0.49 ± 0.05	0.51 ± 0.06	1.2
4686 He II	0.40 ± 0.13	0.40 ± 0.13	1.4	2.25 ± 0.11	2.31 ± 0.12	5.1	1.34 ± 0.06	1.38 ± 0.06	3.4
4711 [Ar IV] + He I	1.80 ± 0.13	1.80 ± 0.13	6.3	2.28 ± 0.12	2.33 ± 0.12	5.3	0.77 ± 0.16	0.76 ± 0.16	0.8	1.53 ± 0.06	1.57 ± 0.06	3.8
4740 [Ar IV]	0.96 ± 0.12	0.96 ± 0.12	3.5	1.62 ± 0.11	1.65 ± 0.11	3.8	0.85 ± 0.06	0.87 ± 0.06	2.2
4861 H β	100.00 ± 1.46	100.00 ± 1.51	371.9	100.00 ± 1.45	100.00 ± 1.46	241.8	100.00 ± 1.50	100.00 ± 1.55	114.2	100.00 ± 1.43	100.00 ± 1.45	270.2
4921 He I	1.05 ± 0.13	1.04 ± 0.13	3.9	1.04 ± 0.09	1.03 ± 0.09	2.6	0.75 ± 0.19	0.73 ± 0.19	0.9	0.97 ± 0.07	0.96 ± 0.07	2.7
4959 [O II]	222.15 ± 3.22	218.83 ± 3.20	846.5	188.19 ± 2.71	185.35 ± 2.68	472.6	173.17 ± 2.55	167.76 ± 2.54	203.2	185.76 ± 2.66	182.89 ± 2.63	535.6
5007 [O III]	666.67 ± 9.61	654.80 ± 9.55	2572.0	573.80 ± 8.22	561.01 ± 8.08	1427.0	528.40 ± 7.72	510.17 ± 7.66	626.3	564.20 ± 8.05	551.30 ± 7.91	1633.0
5199 [N I]	0.50 ± 0.11	0.49 ± 0.11	2.2	1.03 ± 0.15	0.98 ± 0.15	1.3	0.62 ± 0.06	0.59 ± 0.06	2.0
5271 [Fe III]	0.38 ± 0.07	0.36 ± 0.07	1.1	0.33 ± 0.06	0.31 ± 0.05	1.1
5518 [Cl III]	0.39 ± 0.10	0.37 ± 0.10	1.8	0.28 ± 0.09	0.25 ± 0.08	0.9	0.96 ± 0.16	0.89 ± 0.15	1.3	0.45 ± 0.06	0.41 ± 0.05	1.6
5538 [Cl III]	0.35 ± 0.08	0.34 ± 0.08	1.7	0.38 ± 0.12	0.36 ± 0.11	0.5	0.25 ± 0.04	0.22 ± 0.03	0.9
5755 [N II]	0.58 ± 0.09	0.51 ± 0.08	2.2	0.47 ± 0.14	0.44 ± 0.13	0.7
5876 He I	11.09 ± 0.20	10.39 ± 0.19	57.9	12.82 ± 0.21	11.12 ± 0.19	51.2	12.02 ± 0.25	10.99 ± 0.24	18.9	12.22 ± 0.19	10.56 ± 0.17	47.4
6300 [O I]	2.66 ± 0.11	2.44 ± 0.10	15.7	1.85 ± 0.09	1.53 ± 0.07	8.3	5.55 ± 0.21	4.96 ± 0.19	10.1	2.71 ± 0.06	2.23 ± 0.05	11.6
6312 [S III]	1.73 ± 0.10	1.59 ± 0.09	10.1	1.10 ± 0.08	0.90 ± 0.07	4.9	1.58 ± 0.17	1.41 ± 0.16	2.9	1.79 ± 0.05	1.46 ± 0.04	7.8
6363 [O I]	0.91 ± 0.10	0.83 ± 0.09	5.4	0.48 ± 0.08	0.39 ± 0.07	2.2	1.85 ± 0.18	1.64 ± 0.16	3.4	0.92 ± 0.05	0.75 ± 0.04	3.9
6548 [N II]	2.44 ± 0.11	2.22 ± 0.10	14.8
6563 H α	308.35 ± 4.46	280.66 ± 4.46	1872.0	343.65 ± 4.94	275.52 ± 4.31	1546.0	320.33 ± 4.71	283.69 ± 4.65	622.2	349.92 ± 4.99	278.94 ± 4.34	1544.0
6583 [N II]	6.08 ± 0.16	5.52 ± 0.15	37.1	4.94 ± 0.16	3.95 ± 0.13	7.1	16.05 ± 0.35	14.13 ± 0.33	31.4	4.06 ± 0.08	3.23 ± 0.06	15.7
6678 He I	3.10 ± 0.12	2.81 ± 0.11	20.4	3.36 ± 0.12	2.66 ± 0.10	16.6	3.41 ± 0.20	2.99 ± 0.18	6.8	3.60 ± 0.08	2.83 ± 0.07	15.8
6717 [S II]	10.94 ± 0.21	9.88 ± 0.21	72.0	4.49 ± 0.14	3.54 ± 0.11	22.5	21.53 ± 0.43	18.84 ± 0.41	43.0	9.02 ± 0.15	7.07 ± 0.13	40.4
6731 [S II]	8.04 ± 0.19	7.25 ± 0.18	52.5	3.92 ± 0.13	3.08 ± 0.10	19.4	15.41 ± 0.33	13.47 ± 0.31	30.9	6.94 ± 0.12	5.44 ± 0.10	31.3
7065 He I	2.81 ± 0.14	2.50 ± 0.13	19.6	7.01 ± 0.20	5.35 ± 0.16	38.4	2.55 ± 0.29	2.20 ± 0.26	5.8	3.97 ± 0.10	3.01 ± 0.08	20.4
7136 [Ar III]	7.34 ± 0.20	6.52 ± 0.18	53.4	3.54 ± 0.17	2.68 ± 0.13	20.0	6.15 ± 0.13	4.63 ± 0.10	33.5
7281 He I	0.52 ± 0.14	0.46 ± 0.12	4.2	0.70 ± 0.05	0.52 ± 0.04	4.0
7320 [O II]	1.59 ± 0.18	1.40 ± 0.16	11.5	1.56 ± 0.06	1.15 ± 0.05	9.1
7330 [O II]	1.57 ± 0.20	1.39 ± 0.18	11.3	1.30 ± 0.07	0.96 ± 0.05	7.6
$C(H\beta)$	0.114			0.289			0.133			0.297		
$F(H\beta)^b$	1.91			2.71			2.10			5.93		
EW(abs) Å	3.41			0.00			2.87			0.00		

TABLE 3—Continued

Ion	GALAXY											
	CGCG 007-025 (#2)			Mrk 1236			HS 1028+3843			Mrk 724		
	$F(\lambda)/F(H\beta)$	$I(\lambda)/I(H\beta)$	EW ^a									
3727 [O II]	135.20 ± 2.28	156.40 ± 2.81	131.0	115.87 ± 1.75	145.82 ± 2.38	223.2	54.47 ± 0.86	54.16 ± 0.92	113.0	137.50 ± 2.05	150.03 ± 2.41	65.8
3750 H12	2.34 ± 0.43	2.70 ± 0.81	2.4	1.81 ± 0.26	2.28 ± 0.46	3.5	2.59 ± 0.19	3.78 ± 0.36	5.6	2.47 ± 0.30	2.69 ± 0.44	1.2
3771 H11	3.43 ± 0.58	3.94 ± 0.92	3.6	2.12 ± 0.20	2.66 ± 0.40	4.0	4.14 ± 0.18	5.32 ± 0.31	8.9	3.24 ± 0.27	3.52 ± 0.41	1.6
3798 H10	4.95 ± 0.55	5.66 ± 0.88	5.2	3.60 ± 0.21	4.47 ± 0.40	6.8	5.02 ± 0.19	6.19 ± 0.31	10.9	3.63 ± 0.25	3.94 ± 0.40	1.7
3820 He I	0.48 ± 0.28	0.60 ± 0.35	1.0	1.06 ± 0.14	1.05 ± 0.14	2.3
3835 H9	6.79 ± 0.45	7.73 ± 0.78	7.4	5.04 ± 0.20	6.21 ± 0.40	9.5	7.58 ± 0.19	8.73 ± 0.30	16.4	5.41 ± 0.26	5.84 ± 0.40	2.6
3868 [Ne III]	40.52 ± 0.83	45.93 ± 0.97	46.2	39.98 ± 0.61	48.72 ± 0.79	74.4	62.04 ± 0.95	61.69 ± 1.00	136.2	45.00 ± 0.70	48.50 ± 0.80	22.2
3889 He I + H8	16.67 ± 0.48	18.84 ± 0.74	21.7	15.01 ± 0.29	18.23 ± 0.47	28.8	18.12 ± 0.35	19.29 ± 0.44	36.7	18.94 ± 0.36	20.38 ± 0.49	9.3
3968 [Ne III] + H7	27.32 ± 0.57	30.54 ± 0.85	31.7	25.18 ± 0.40	30.04 ± 0.58	47.5	34.66 ± 0.56	35.59 ± 0.63	80.0	28.33 ± 0.47	30.29 ± 0.58	15.3
4026 He I	1.52 ± 0.23	1.69 ± 0.26	1.9	1.56 ± 0.13	1.84 ± 0.15	3.0	2.17 ± 0.15	2.16 ± 0.15	5.2	1.38 ± 0.12	1.46 ± 0.13	0.8
4068 [S II]	0.77 ± 0.22	0.85 ± 0.24	1.0	1.51 ± 0.15	1.76 ± 0.18	2.9	1.13 ± 0.14	1.13 ± 0.14	3.0	1.07 ± 0.09	1.13 ± 0.09	0.6
4101 H δ	24.88 ± 0.48	27.31 ± 0.72	32.8	22.08 ± 0.36	25.60 ± 0.51	43.6	25.78 ± 0.42	26.55 ± 0.47	72.8	25.11 ± 0.41	26.55 ± 0.50	14.8
4340 H γ	45.71 ± 0.75	48.63 ± 0.90	72.3	43.38 ± 0.65	47.86 ± 0.77	90.3	45.90 ± 0.69	46.39 ± 0.72	157.6	46.49 ± 0.69	48.25 ± 0.76	32.6
4363 [O III]	10.20 ± 0.29	10.82 ± 0.31	16.5	6.50 ± 0.15	7.14 ± 0.16	13.7	16.28 ± 0.28	16.19 ± 0.28	56.8	7.03 ± 0.18	7.28 ± 0.18	5.0
4387 He I	0.47 ± 0.10	0.52 ± 0.11	1.0	0.47 ± 0.08	0.46 ± 0.08	1.6	0.38 ± 0.09	0.40 ± 0.09	0.3
4471 He I	3.39 ± 0.19	3.55 ± 0.19	5.9	3.51 ± 0.10	3.78 ± 0.11	7.7	4.37 ± 0.13	4.34 ± 0.13	16.1	3.80 ± 0.13	3.90 ± 0.14	2.9
4658 [Fe III]	0.69 ± 0.09	0.72 ± 0.09	1.6	0.87 ± 0.12	0.87 ± 0.12	3.6	0.65 ± 0.08	0.66 ± 0.08	0.5
4686 He II	0.85 ± 0.13	0.87 ± 0.14	1.6	0.38 ± 0.08	0.39 ± 0.08	0.9	1.37 ± 0.12	1.36 ± 0.12	5.8
4711 [Ar IV] + He I	0.88 ± 0.14	0.89 ± 0.15	1.7	1.04 ± 0.09	1.07 ± 0.09	2.5	3.25 ± 0.12	3.23 ± 0.12	14.0	0.77 ± 0.09	0.77 ± 0.09	0.6
4740 [Ar IV]	0.69 ± 0.18	0.69 ± 0.19	1.4	0.61 ± 0.08	0.63 ± 0.09	1.5	2.15 ± 0.12	2.13 ± 0.12	9.4
4861 H β	100.00 ± 1.52	100.00 ± 1.55	204.3	100.00 ± 1.45	100.00 ± 1.47	251.3	100.00 ± 1.46	100.00 ± 1.48	451.0	100.00 ± 1.44	100.00 ± 1.45	95.1
4921 He I	0.78 ± 0.17	0.78 ± 0.17	1.6	1.02 ± 0.09	1.01 ± 0.09	2.6	1.08 ± 0.10	1.07 ± 0.10	4.9	0.97 ± 0.07	0.97 ± 0.07	1.0
4959 [O III]	151.22 ± 2.26	149.59 ± 2.24	308.8	211.42 ± 3.04	207.82 ± 3.01	556.1	247.30 ± 3.58	245.88 ± 3.58	1184.0	178.69 ± 2.57	177.53 ± 2.56	178.0
5007 [O III]	463.42 ± 6.84	456.05 ± 6.76	952.1	625.48 ± 8.96	609.77 ± 8.79	1644.0	752.05 ± 10.8	747.74 ± 10.9	3670.0	541.51 ± 7.75	536.34 ± 7.70	551.4
5199 [N I]	0.78 ± 0.09	0.73 ± 0.08	2.2	0.45 ± 0.07	0.44 ± 0.07	0.5
5271 [Fe III]	0.36 ± 0.09	0.35 ± 0.09	0.4
5518 [Cl III]	0.71 ± 0.09	0.64 ± 0.08	2.2	0.45 ± 0.08	0.43 ± 0.08	0.6
5538 [Cl III]	0.35 ± 0.08	0.34 ± 0.08	0.5
5755 [N II]	0.31 ± 0.09	0.27 ± 0.08	1.0
5876 He I	11.07 ± 0.25	10.01 ± 0.23	34.0	13.56 ± 0.23	11.56 ± 0.20	44.8	12.29 ± 0.21	12.22 ± 0.21	85.8	11.34 ± 0.19	10.68 ± 0.19	16.8
6300 [O I]	3.09 ± 0.15	2.70 ± 0.13	10.7	4.19 ± 0.10	3.37 ± 0.08	16.0	1.39 ± 0.08	1.38 ± 0.09	12.2	1.93 ± 0.07	1.78 ± 0.07	3.3
6312 [S III]	1.32 ± 0.12	1.15 ± 0.10	4.6	2.11 ± 0.08	1.70 ± 0.07	8.1	1.16 ± 0.08	1.16 ± 0.08	10.2	2.14 ± 0.08	1.97 ± 0.08	3.7
6363 [O I]	0.98 ± 0.14	0.85 ± 0.12	3.5	1.45 ± 0.08	1.16 ± 0.07	5.6	0.51 ± 0.09	0.50 ± 0.09	4.4	0.65 ± 0.06	0.60 ± 0.06	1.1
6548 [N II]	2.21 ± 0.17	1.89 ± 0.15	7.7	4.70 ± 0.11	3.67 ± 0.09	18.3
6563 H α	325.72 ± 4.83	278.36 ± 4.50	1152.0	365.46 ± 5.25	285.13 ± 4.47	1427.0	279.46 ± 4.05	278.13 ± 4.40	2686.0	310.90 ± 4.46	282.99 ± 4.41	566.1
6583 [N II]	5.30 ± 0.19	4.52 ± 0.17	18.9	13.07 ± 0.22	10.17 ± 0.18	51.3	4.08 ± 0.12	4.06 ± 0.12	24.3	6.47 ± 0.13	5.88 ± 0.13	11.8
6678 He I	3.30 ± 0.17	2.79 ± 0.14	12.1	4.03 ± 0.10	3.10 ± 0.08	16.2	3.02 ± 0.11	3.01 ± 0.12	29.5	3.36 ± 0.10	3.04 ± 0.09	6.2
6717 [S II]	13.33 ± 0.29	11.26 ± 0.26	47.2	18.76 ± 0.30	14.38 ± 0.25	76.3	3.53 ± 0.12	3.51 ± 0.12	34.1	12.18 ± 0.20	11.01 ± 0.20	22.6
6731 [S II]	9.20 ± 0.25	7.77 ± 0.22	34.2	13.74 ± 0.23	10.51 ± 0.19	54.9	3.26 ± 0.12	3.24 ± 0.12	32.0	8.74 ± 0.16	7.90 ± 0.15	16.3
7065 He I	3.02 ± 0.19	2.49 ± 0.16	12.5	3.58 ± 0.11	2.64 ± 0.08	16.2	5.79 ± 0.17	5.76 ± 0.18	54.0	2.51 ± 0.12	2.23 ± 0.11	5.3
7136 [Ar III]	5.85 ± 0.23	4.80 ± 0.19	25.1	10.58 ± 0.20	7.74 ± 0.16	47.1	4.03 ± 0.16	4.01 ± 0.16	47.5	10.27 ± 0.20	9.12 ± 0.19	22.3
$C(H\beta)$	0.206			0.325			0.000			0.123		
$F(H\beta)$ ^b	0.88			3.64			1.83			6.24		
EW(abs) Å	0.00			0.03			2.60			0.00		

TABLE 3—Continued

Ion	GALAXY											
	Mrk 35			UM 422			UM 439			POX 36		
	$F(\lambda)/F(H\beta)$	$I(\lambda)/I(H\beta)$	EW ^a									
3727 [O II]	211.04 ± 3.03	250.94 ± 3.90	162.9	95.19 ± 1.55	103.17 ± 1.80	138.3	91.06 ± 1.50	105.80 ± 1.86	121.1	246.84 ± 3.83	277.07 ± 4.62	115.6
3750 H I 2	2.40 ± 0.19	2.84 ± 0.30	1.9	2.67 ± 0.33	2.89 ± 0.53	3.9	2.30 ± 0.33	3.18 ± 0.68	3.0	2.06 ± 0.48	2.30 ± 0.80	1.0
3771 H I 1	2.91 ± 0.16	3.43 ± 0.28	2.3	3.16 ± 0.33	3.41 ± 0.52	4.7	3.28 ± 0.33	4.33 ± 0.68	4.1	2.89 ± 0.55	3.22 ± 0.85	1.4
3798 H I 0	3.94 ± 0.16	4.62 ± 0.27	3.1	4.84 ± 0.35	5.21 ± 0.54	7.0	3.58 ± 0.29	4.68 ± 0.66	4.2	3.86 ± 0.56	4.30 ± 0.85	1.9
3820 He I	1.09 ± 0.12	1.28 ± 0.14	0.9	1.32 ± 0.35	1.42 ± 0.37	1.9	1.46 ± 0.32	1.67 ± 0.36	1.7
3835 H I 9	5.75 ± 0.15	6.71 ± 0.26	4.5	6.27 ± 0.29	6.74 ± 0.51	8.9	4.84 ± 0.25	6.11 ± 0.63	5.6	4.94 ± 0.41	5.48 ± 0.73	2.4
3868 [Ne III]	26.98 ± 0.41	31.31 ± 0.51	21.6	54.23 ± 0.87	58.11 ± 0.98	77.5	59.51 ± 0.94	67.67 ± 1.13	67.0	34.90 ± 0.76	38.55 ± 0.86	17.2
3889 He I + H 8	16.73 ± 0.28	19.35 ± 0.39	13.2	18.99 ± 0.39	20.32 ± 0.56	29.2	15.81 ± 0.34	18.50 ± 0.68	18.3	18.36 ± 0.53	20.23 ± 0.81	9.1
3968 [Ne III] + H 7	21.46 ± 0.33	24.49 ± 0.43	18.4	32.54 ± 0.54	34.60 ± 0.70	49.6	31.35 ± 0.52	35.70 ± 0.82	35.9	24.02 ± 0.53	26.24 ± 0.78	13.0
4026 He I	1.87 ± 0.10	2.12 ± 0.12	1.6	1.71 ± 0.18	1.81 ± 0.19	2.7	1.78 ± 0.17	1.97 ± 0.19	2.0	1.05 ± 0.30	1.14 ± 0.33	0.6
4068 [S II]	1.90 ± 0.08	2.13 ± 0.09	1.7	0.90 ± 0.23	0.95 ± 0.25	1.5	1.25 ± 0.20	1.38 ± 0.23	1.4	1.34 ± 0.24	1.44 ± 0.26	0.7
4101 H δ	24.37 ± 0.36	27.23 ± 0.45	23.0	24.53 ± 0.43	25.83 ± 0.58	40.1	22.62 ± 0.40	25.40 ± 0.68	27.8	25.45 ± 0.50	27.40 ± 0.70	15.8
4340 H γ	45.31 ± 0.65	48.78 ± 0.73	50.8	47.15 ± 0.73	48.79 ± 0.82	88.2	44.16 ± 0.68	47.46 ± 0.87	57.5	46.78 ± 0.76	49.15 ± 0.89	33.8
4363 [O III]	2.54 ± 0.09	2.73 ± 0.10	2.9	9.36 ± 0.22	9.67 ± 0.23	18.0	12.66 ± 0.24	13.43 ± 0.26	16.5	4.76 ± 0.28	4.98 ± 0.30	3.4
4387 He I	0.44 ± 0.07	0.47 ± 0.08	0.5	0.44 ± 0.11	0.46 ± 0.12	0.9	0.51 ± 0.13	0.54 ± 0.14	0.7
4471 He I	3.95 ± 0.09	4.17 ± 0.09	4.8	3.64 ± 0.15	3.74 ± 0.16	7.3	3.83 ± 0.16	4.01 ± 0.17	5.1	3.33 ± 0.24	3.45 ± 0.25	2.5
4658 [Fe III]	0.88 ± 0.05	0.91 ± 0.05	1.1	0.40 ± 0.13	0.41 ± 0.14	0.6	0.67 ± 0.15	0.68 ± 0.16	0.6
4686 He II	0.54 ± 0.13	0.55 ± 0.13	1.2
4711 [Ar IV] + He I	1.55 ± 0.14	1.57 ± 0.14	3.5	2.09 ± 0.14	2.12 ± 0.14	3.0	0.49 ± 0.17	0.50 ± 0.17	0.4
4740 [Ar IV]	0.82 ± 0.15	0.83 ± 0.15	2.0	1.23 ± 0.12	1.24 ± 0.13	1.8
4861 H β	100.00 ± 1.43	100.00 ± 1.43	153.0	100.00 ± 1.48	100.00 ± 1.50	244.9	100.00 ± 1.46	100.00 ± 1.52	158.5	100.00 ± 1.50	100.00 ± 1.53	95.6
4921 He I	1.05 ± 0.05	1.05 ± 0.05	1.7	1.22 ± 0.13	1.21 ± 0.13	3.0	1.04 ± 0.12	1.03 ± 0.12	1.6	0.49 ± 0.13	0.49 ± 0.12	0.5
4959 [O II]	134.11 ± 1.91	132.40 ± 1.89	215.9	233.55 ± 3.41	232.16 ± 3.40	601.8	273.45 ± 3.96	269.35 ± 3.92	438.9	131.30 ± 1.95	130.18 ± 1.94	128.6
5007 [O III]	413.39 ± 5.87	405.59 ± 5.79	681.9	721.31 ± 10.5	714.95 ± 10.4	1880.0	821.36 ± 11.8	804.60 ± 11.7	1335.0	405.40 ± 5.94	400.28 ± 5.88	404.9
5199 [N I]	0.76 ± 0.05	0.72 ± 0.05	1.4	0.86 ± 0.17	0.84 ± 0.16	1.0
5271 [Fe III]	0.50 ± 0.05	0.47 ± 0.05	0.9
5518 [Cl III]	0.64 ± 0.05	0.59 ± 0.04	1.3	0.47 ± 0.11	0.45 ± 0.10	1.5	0.28 ± 0.10	0.26 ± 0.10	0.5	0.82 ± 0.14	0.77 ± 0.13	1.0
5538 [Cl III]	0.46 ± 0.05	0.42 ± 0.04	0.9	0.35 ± 0.12	0.32 ± 0.11	0.7	0.61 ± 0.13	0.58 ± 0.13	0.8
5755 [N II]	0.41 ± 0.04	0.37 ± 0.04	0.9	0.41 ± 0.14	0.38 ± 0.13	0.6
5876 He I	13.04 ± 0.19	11.56 ± 0.18	30.3	11.85 ± 0.22	11.20 ± 0.21	43.3	12.12 ± 0.22	10.85 ± 0.20	25.9	11.57 ± 0.24	10.68 ± 0.23	16.7
6300 [O I]	3.17 ± 0.06	2.70 ± 0.05	8.3	2.15 ± 0.11	1.99 ± 0.11	9.1	2.64 ± 0.11	2.27 ± 0.10	6.4	3.03 ± 0.13	2.72 ± 0.12	4.5
6312 [S III]	1.43 ± 0.04	1.21 ± 0.04	3.7	1.60 ± 0.10	1.48 ± 0.09	6.8	1.71 ± 0.09	1.47 ± 0.08	4.2	1.27 ± 0.12	1.14 ± 0.11	1.9
6363 [O I]	1.09 ± 0.04	0.92 ± 0.04	2.9	0.46 ± 0.09	0.42 ± 0.09	2.0	0.96 ± 0.10	0.82 ± 0.09	2.4	0.82 ± 0.12	0.73 ± 0.11	1.2
6548 [N II]	8.26 ± 0.13	6.87 ± 0.11	21.7	1.50 ± 0.11	1.38 ± 0.10	6.7	1.83 ± 0.13	1.54 ± 0.11	4.7	3.97 ± 0.15	3.51 ± 0.13	6.2
6563 H α	347.73 ± 4.94	288.49 ± 4.47	919.1	308.58 ± 4.50	282.93 ± 4.49	1389.0	333.59 ± 4.82	281.74 ± 4.46	860.1	321.51 ± 4.72	283.84 ± 4.53	500.8
6583 [N II]	23.72 ± 0.34	19.64 ± 0.31	62.4	4.24 ± 0.13	3.88 ± 0.13	19.2	5.16 ± 0.15	4.35 ± 0.13	13.5	12.03 ± 0.25	10.61 ± 0.23	18.5
6678 He I	4.11 ± 0.08	3.38 ± 0.07	11.6	3.36 ± 0.13	3.06 ± 0.12	15.8	3.49 ± 0.12	2.92 ± 0.11	9.4	3.37 ± 0.17	2.95 ± 0.15	5.4
6717 [S II]	18.74 ± 0.27	15.34 ± 0.25	51.6	8.54 ± 0.20	7.78 ± 0.19	40.9	9.34 ± 0.19	7.79 ± 0.17	25.6	21.47 ± 0.37	18.79 ± 0.35	35.1
6731 [S II]	15.13 ± 0.22	12.37 ± 0.20	41.7	6.07 ± 0.16	5.53 ± 0.15	29.2	7.45 ± 0.17	6.21 ± 0.15	20.4	15.84 ± 0.30	13.85 ± 0.27	26.2
7065 He I	3.52 ± 0.08	2.80 ± 0.06	10.6	2.69 ± 0.15	2.42 ± 0.14	14.0	4.53 ± 0.15	3.68 ± 0.13	13.6	2.21 ± 0.18	1.90 ± 0.16	4.0
7136 [Ar III]	11.43 ± 0.18	9.04 ± 0.16	35.1	8.12 ± 0.21	7.28 ± 0.20	43.4	8.89 ± 0.20	7.19 ± 0.17	26.9	9.26 ± 0.26	7.92 ± 0.23	17.8
7281 He I	0.71 ± 0.05	0.56 ± 0.04	2.3
7320 [O II]	3.23 ± 0.08	2.52 ± 0.06	10.2	1.91 ± 0.16	1.52 ± 0.13	6.1	2.39 ± 0.17	2.02 ± 0.14	4.7
7330 [O II]	2.78 ± 0.08	2.16 ± 0.06	8.8	1.57 ± 0.16	1.25 ± 0.13	5.0	2.51 ± 0.18	2.13 ± 0.16	4.9
$C(H\beta)$	0.244			0.114			0.217			0.163		
$F(H\beta)^b$	26.44			1.83			3.92			3.78		
EW(abs) Å	0.00			0.00			0.59			0.00		

TABLE 3—Continued

Ion	GALAXY											
	Mrk 1315			HS 1213+3636A			HS 1214+3801			Mrk 1329		
	$F(\lambda)/F(\text{H}\beta)$	$I(\lambda)/I(\text{H}\beta)$	EW ^a									
3727 [O II]	96.89 ± 1.42	108.47 ± 1.72	211.5	308.19 ± 4.61	311.76 ± 5.01	360.6	114.36 ± 1.72	140.66 ± 2.31	198.9	110.67 ± 1.61	124.20 ± 1.95	171.6
3750 H I 2	3.01 ± 0.16	3.36 ± 0.24	6.6	3.03 ± 0.59	3.07 ± 0.85	3.5	1.75 ± 0.20	3.97 ± 0.60	3.0	2.45 ± 0.13	2.75 ± 0.22	3.8
3771 H I 11	3.84 ± 0.14	4.28 ± 0.22	8.4	3.56 ± 0.48	3.60 ± 0.77	4.2	2.62 ± 0.21	5.02 ± 0.52	4.5	3.07 ± 0.13	3.43 ± 0.21	4.8
3798 H I 0	5.24 ± 0.15	5.82 ± 0.22	11.6	5.28 ± 0.42	5.34 ± 0.73	6.3	3.57 ± 0.18	6.13 ± 0.43	6.2	4.31 ± 0.13	4.80 ± 0.22	6.8
3820 He I	1.23 ± 0.10	1.36 ± 0.11	2.8	1.63 ± 0.54	1.64 ± 0.55	2.0	0.69 ± 0.16	0.83 ± 0.20	1.2	1.28 ± 0.11	1.42 ± 0.12	2.0
3835 H I 9	7.16 ± 0.16	7.91 ± 0.23	16.0	7.48 ± 0.35	7.56 ± 0.67	9.2	5.08 ± 0.17	7.90 ± 0.39	8.8	6.40 ± 0.15	7.10 ± 0.23	10.2
3868 [Ne III]	44.01 ± 0.65	48.49 ± 0.76	100.1	23.19 ± 0.45	23.42 ± 0.47	28.4	36.55 ± 0.57	43.61 ± 0.72	63.7	36.33 ± 0.54	40.11 ± 0.63	58.7
3889 He I + H 8	18.71 ± 0.30	20.57 ± 0.37	40.1	20.36 ± 0.43	20.55 ± 0.75	23.7	15.37 ± 0.26	19.97 ± 0.45	27.7	17.71 ± 0.28	19.52 ± 0.35	31.9
3968 [Ne III] + H 7	29.36 ± 0.44	32.00 ± 0.52	73.3	23.41 ± 0.43	23.62 ± 0.70	30.3	24.16 ± 0.38	29.93 ± 0.56	43.3	26.08 ± 0.39	28.49 ± 0.47	45.0
4026 He I	1.80 ± 0.07	1.95 ± 0.08	4.7	1.97 ± 0.23	1.98 ± 0.23	2.6	1.30 ± 0.09	1.50 ± 0.11	2.4	1.73 ± 0.08	1.88 ± 0.08	2.9
4068 [S II]	0.94 ± 0.07	1.02 ± 0.07	2.5	2.85 ± 0.36	2.88 ± 0.37	4.2	1.06 ± 0.12	1.21 ± 0.14	2.0	1.01 ± 0.06	1.09 ± 0.07	1.8
4101 H δ	24.95 ± 0.37	26.82 ± 0.43	67.7	25.96 ± 0.46	26.16 ± 0.67	38.9	20.63 ± 0.33	25.00 ± 0.48	39.8	23.55 ± 0.35	25.36 ± 0.41	41.3
4340 H γ	46.40 ± 0.67	48.69 ± 0.72	149.6	46.85 ± 0.72	47.08 ± 0.84	80.9	42.40 ± 0.63	47.36 ± 0.75	91.5	45.22 ± 0.65	47.50 ± 0.71	94.8
4363 [O III]	4.99 ± 0.10	5.22 ± 0.10	16.1	2.55 ± 0.19	2.56 ± 0.19	4.4	7.87 ± 0.15	8.52 ± 0.17	17.1	4.22 ± 0.09	4.43 ± 0.10	8.9
4387 He I	0.45 ± 0.06	0.47 ± 0.06	1.5	0.47 ± 0.17	0.47 ± 0.18	0.8	0.47 ± 0.08	0.50 ± 0.09	1.0	0.36 ± 0.06	0.38 ± 0.07	0.8
4471 He I	4.01 ± 0.08	4.15 ± 0.09	14.2	3.85 ± 0.17	3.87 ± 0.17	6.8	3.74 ± 0.10	3.97 ± 0.11	8.6	3.97 ± 0.08	4.11 ± 0.09	8.9
4658 [Fe III]	0.23 ± 0.04	0.24 ± 0.05	0.9	0.27 ± 0.04	0.27 ± 0.05	0.6
4711 [Ar IV] + He I	0.90 ± 0.04	0.91 ± 0.04	3.3	0.52 ± 0.16	0.52 ± 0.16	1.0	1.03 ± 0.07	1.04 ± 0.07	2.6	0.85 ± 0.05	0.86 ± 0.05	2.1
4740 [Ar IV]	0.46 ± 0.04	0.46 ± 0.04	1.9	0.41 ± 0.18	0.41 ± 0.18	0.8	0.61 ± 0.07	0.61 ± 0.07	1.6	0.34 ± 0.04	0.34 ± 0.04	0.9
4861 H β	100.00 ± 1.43	100.00 ± 1.44	420.7	100.00 ± 1.47	100.00 ± 1.51	203.0	100.00 ± 1.44	100.00 ± 1.47	270.6	100.00 ± 1.43	100.00 ± 1.44	273.9
4921 He I	1.20 ± 0.05	1.20 ± 0.05	5.2	1.10 ± 0.13	1.10 ± 0.13	2.2	1.06 ± 0.06	1.04 ± 0.06	2.9	1.02 ± 0.05	1.02 ± 0.05	2.8
4959 [O III]	201.30 ± 2.87	199.62 ± 2.85	887.7	104.31 ± 1.53	104.22 ± 1.53	212.7	197.38 ± 2.83	192.39 ± 2.80	539.1	182.59 ± 2.60	181.03 ± 2.59	521.6
5007 [O III]	611.84 ± 8.71	604.29 ± 8.63	2764.0	319.58 ± 4.63	319.17 ± 4.63	656.8	599.07 ± 8.57	579.41 ± 8.41	1666.0	556.91 ± 7.93	549.87 ± 7.85	1610.0
5159 [N I]	0.45 ± 0.05	0.44 ± 0.04	2.3	0.41 ± 0.14	0.40 ± 0.14	0.9	0.69 ± 0.07	0.64 ± 0.07	2.1	0.24 ± 0.03	0.24 ± 0.03	0.8
5271 [Fe III]	0.18 ± 0.04	0.18 ± 0.04	0.9	0.19 ± 0.04	0.19 ± 0.03	0.6
5518 [Cl III]	0.50 ± 0.04	0.47 ± 0.04	2.8	0.47 ± 0.10	0.47 ± 0.10	1.1	0.54 ± 0.07	0.49 ± 0.06	1.9	0.42 ± 0.04	0.40 ± 0.03	1.5
5538 [Cl III]	0.38 ± 0.04	0.36 ± 0.03	2.1	0.33 ± 0.05	0.29 ± 0.05	1.1	0.29 ± 0.03	0.27 ± 0.03	1.0
5755 [N II]	0.14 ± 0.04	0.13 ± 0.04	0.8	0.46 ± 0.15	0.45 ± 0.15	1.1	0.14 ± 0.03	0.13 ± 0.03	0.5
5876 He I	12.41 ± 0.19	11.47 ± 0.18	77.7	11.72 ± 0.22	11.62 ± 0.22	27.6	12.82 ± 0.20	10.93 ± 0.18	47.5	13.12 ± 0.20	12.11 ± 0.19	51.6
6300 [O I]	1.20 ± 0.04	1.08 ± 0.04	8.4	1.90 ± 0.14	1.88 ± 0.14	4.9	2.62 ± 0.07	2.12 ± 0.06	11.0	1.49 ± 0.04	1.34 ± 0.04	6.7
6312 [S III]	1.78 ± 0.04	1.60 ± 0.04	12.5	1.66 ± 0.12	1.64 ± 0.12	4.3	2.27 ± 0.07	1.83 ± 0.06	9.5	1.85 ± 0.04	1.66 ± 0.04	8.3
6363 [O I]	0.50 ± 0.03	0.45 ± 0.03	3.5	0.87 ± 0.06	0.70 ± 0.05	3.7	0.49 ± 0.04	0.44 ± 0.03	2.2
6548 [N II]	2.46 ± 0.05	2.18 ± 0.05	16.0	6.27 ± 0.17	6.19 ± 0.17	16.9	2.67 ± 0.07	2.09 ± 0.06	11.9	2.84 ± 0.06	2.51 ± 0.05	12.6
6563 H α	323.60 ± 4.61	286.50 ± 4.44	2083.0	289.92 ± 4.21	286.34 ± 4.52	782.6	360.59 ± 5.16	283.22 ± 4.47	1619.0	325.02 ± 4.63	286.98 ± 4.45	1439.0
6583 [N II]	6.44 ± 0.11	5.70 ± 0.10	41.9	17.71 ± 0.31	17.49 ± 0.32	48.0	7.44 ± 0.14	5.82 ± 0.11	33.4	7.78 ± 0.12	6.86 ± 0.12	34.8
6678 He I	3.73 ± 0.07	3.28 ± 0.07	25.5	3.15 ± 0.14	3.11 ± 0.14	8.8	3.78 ± 0.09	2.93 ± 0.07	17.1	3.71 ± 0.07	3.25 ± 0.07	18.1
6717 [S II]	8.27 ± 0.13	7.26 ± 0.12	57.0	18.09 ± 0.32	17.86 ± 0.33	52.0	12.51 ± 0.20	9.64 ± 0.17	57.7	9.74 ± 0.15	8.52 ± 0.14	48.5
6731 [S II]	5.87 ± 0.10	5.14 ± 0.09	40.8	13.05 ± 0.24	12.88 ± 0.25	37.6	9.00 ± 0.16	6.93 ± 0.13	41.5	6.93 ± 0.11	6.06 ± 0.11	34.6
7065 He I	2.72 ± 0.07	2.34 ± 0.06	20.3	1.93 ± 0.16	1.90 ± 0.16	6.1	3.30 ± 0.09	2.45 ± 0.07	16.7	2.98 ± 0.07	2.56 ± 0.06	16.9
7136 [Ar III]	11.78 ± 0.19	10.11 ± 0.18	86.5	7.35 ± 0.20	7.24 ± 0.21	22.9	10.19 ± 0.18	7.52 ± 0.15	51.2	9.72 ± 0.16	8.31 ± 0.15	54.5
7281 He I	0.74 ± 0.08	0.54 ± 0.06	4.3	0.63 ± 0.04	0.54 ± 0.04	4.2
7320 [O II]	3.04 ± 0.19	2.99 ± 0.19	9.8	2.35 ± 0.09	1.71 ± 0.07	12.7	1.33 ± 0.05	1.13 ± 0.05	8.5
7330 [O II]	1.90 ± 0.17	1.87 ± 0.17	6.2	2.25 ± 0.10	1.63 ± 0.08	12.1	1.12 ± 0.05	0.95 ± 0.04	7.2
$C(\text{H}\beta)$	0.159			0.016			0.306			0.163		
$F(\text{H}\beta)^b$	9.56			3.22			4.51			9.86		
EW(abs) Å	0.00			0.00			2.60			0.01		

TABLE 3—Continued

Ion	GALAXY											
	HS 1311+3628			Mrk 450 (#1)			Mrk 450 (#2)			Mrk 67		
	$F(\lambda)/F(H\beta)$	$I(\lambda)/I(H\beta)$	EW ^a									
3727 [O II]	171.82 ± 2.64	180.27 ± 2.97	320.9	160.52 ± 2.41	176.95 ± 2.86	257.6	162.48 ± 3.05	172.77 ± 3.43	176.9	158.37 ± 2.59	181.67 ± 3.19	111.6
3750 H I 2	2.51 ± 0.36	2.63 ± 0.55	4.7	2.03 ± 0.27	2.60 ± 0.45	3.3	0.90 ± 0.78	1.57 ± 1.79	0.6
3771 H I 1	3.26 ± 0.29	3.41 ± 0.49	6.2	2.42 ± 0.21	3.02 ± 0.38	4.0	2.98 ± 0.87	3.17 ± 1.34	3.5	1.31 ± 0.60	2.06 ± 1.45	0.9
3798 H I 0	4.42 ± 0.26	4.62 ± 0.47	8.5	3.70 ± 0.19	4.41 ± 0.36	6.2	4.47 ± 1.00	4.74 ± 1.45	5.2	2.30 ± 0.67	3.19 ± 1.45	1.5
3820 He I	1.35 ± 0.37	1.41 ± 0.39	2.6	0.97 ± 0.16	1.06 ± 0.18	1.6
3835 H 9	6.42 ± 0.26	6.70 ± 0.47	12.5	6.09 ± 0.20	7.00 ± 0.36	10.2	6.45 ± 0.76	6.82 ± 1.26	7.5	4.76 ± 0.49	5.95 ± 1.25	3.1
3868 [Ne III]	37.42 ± 0.63	39.00 ± 0.68	70.7	36.29 ± 0.57	39.45 ± 0.65	60.9	41.55 ± 1.01	43.80 ± 1.10	45.6	43.89 ± 0.80	49.37 ± 0.94	26.5
3889 He I + H 8	18.44 ± 0.36	19.20 ± 0.56	34.1	15.85 ± 0.29	17.54 ± 0.42	27.7	17.55 ± 0.64	18.49 ± 1.23	19.4	15.25 ± 0.47	17.62 ± 1.14	10.8
3968 [Ne III] + H 7	26.70 ± 0.45	27.70 ± 0.62	51.5	25.42 ± 0.42	27.71 ± 0.54	43.5	25.93 ± 0.68	27.18 ± 1.26	28.5	23.04 ± 0.50	26.16 ± 1.28	14.1
4026 He I	1.72 ± 0.16	1.78 ± 0.16	3.3	1.57 ± 0.12	1.68 ± 0.13	2.7	1.48 ± 0.62	1.54 ± 0.65	1.6	1.46 ± 0.29	1.60 ± 0.32	0.8
4068 [S II]	1.54 ± 0.16	1.59 ± 0.16	3.0	1.75 ± 0.14	1.86 ± 0.15	3.1	1.67 ± 0.44	1.74 ± 0.46	1.9	1.43 ± 0.32	1.57 ± 0.35	0.9
4101 H δ	24.39 ± 0.41	25.15 ± 0.56	51.4	22.94 ± 0.38	24.71 ± 0.49	42.0	21.89 ± 0.61	22.77 ± 1.14	25.9	21.24 ± 0.50	23.70 ± 1.17	14.2
4340 H γ	47.55 ± 0.72	48.54 ± 0.81	113.2	45.42 ± 0.68	47.56 ± 0.75	94.7	47.80 ± 0.90	49.07 ± 1.22	66.2	45.24 ± 0.76	48.35 ± 1.25	32.0
4363 [O III]	4.79 ± 0.15	4.88 ± 0.15	11.7	5.04 ± 0.14	5.24 ± 0.15	10.6	6.31 ± 0.37	6.47 ± 0.38	8.8	7.60 ± 0.32	8.02 ± 0.34	5.1
4387 He I	0.63 ± 0.13	0.64 ± 0.13	1.6	0.49 ± 0.10	0.51 ± 0.10	1.0
4471 He I	3.82 ± 0.14	3.88 ± 0.15	10.2	3.73 ± 0.11	3.84 ± 0.11	8.4	3.63 ± 0.33	3.70 ± 0.33	5.3	3.63 ± 0.23	3.78 ± 0.25	2.5
4658 [Fe III]	0.54 ± 0.08	0.54 ± 0.08	1.2
4686 He II	0.31 ± 0.07	0.31 ± 0.07	0.7
4711 [Ar IV] + He I	0.67 ± 0.08	0.67 ± 0.08	1.6
4740 [Ar IV]	0.45 ± 0.09	0.45 ± 0.09	1.2
4861 H β	100.00 ± 1.46	100.00 ± 1.48	323.1	100.00 ± 1.45	100.00 ± 1.47	273.6	100.00 ± 1.61	100.00 ± 1.72	174.5	100.00 ± 1.52	100.00 ± 1.71	82.6
4921 He I	0.95 ± 0.13	0.95 ± 0.13	3.0	1.13 ± 0.09	1.12 ± 0.09	3.1	0.70 ± 0.22	0.70 ± 0.22	0.6
4959 [O II]	169.25 ± 2.46	168.65 ± 2.46	561.0	171.41 ± 2.48	169.82 ± 2.47	487.0	175.05 ± 2.72	174.24 ± 2.71	311.6	189.81 ± 2.83	187.09 ± 2.81	155.5
5007 [O III]	512.64 ± 7.40	509.94 ± 7.37	1699.0	514.89 ± 7.39	508.28 ± 7.34	1484.0	526.05 ± 8.03	522.48 ± 7.99	942.8	575.75 ± 8.49	564.63 ± 8.40	475.9
5199 [N I]	0.54 ± 0.12	0.54 ± 0.12	2.1	0.79 ± 0.09	0.77 ± 0.09	2.6
5271 [Fe III]	0.42 ± 0.09	0.41 ± 0.09	1.4
5518 [Cl III]	0.72 ± 0.10	0.70 ± 0.09	3.2	0.46 ± 0.07	0.44 ± 0.07	1.6
5538 [Cl III]	0.46 ± 0.09	0.45 ± 0.09	2.0	0.67 ± 0.07	0.64 ± 0.07	2.4
5755 [N II]	0.22 ± 0.06	0.21 ± 0.05	0.8
5876 He I	11.99 ± 0.22	11.60 ± 0.21	54.1	12.22 ± 0.20	11.38 ± 0.19	47.9	11.73 ± 0.34	11.24 ± 0.33	27.1	12.76 ± 0.30	11.52 ± 0.28	12.9
6300 [O I]	3.59 ± 0.12	3.43 ± 0.11	21.7	3.32 ± 0.10	3.02 ± 0.09	15.6	4.11 ± 0.27	3.88 ± 0.26	11.6	3.86 ± 0.19	3.37 ± 0.17	4.5
6312 [S III]	2.06 ± 0.10	1.97 ± 0.10	12.4	2.16 ± 0.08	1.96 ± 0.07	10.1	2.04 ± 0.24	1.93 ± 0.22	5.8	2.03 ± 0.18	1.77 ± 0.16	2.4
6363 [O I]	1.21 ± 0.10	1.15 ± 0.10	7.4	1.03 ± 0.08	0.93 ± 0.07	4.8	1.20 ± 0.23	1.13 ± 0.22	3.4	1.37 ± 0.20	1.19 ± 0.17	1.6
6548 [N II]	4.27 ± 0.11	4.05 ± 0.11	24.0	4.84 ± 0.11	4.34 ± 0.10	24.5	4.31 ± 0.31	4.03 ± 0.29	13.0	3.14 ± 0.18	2.69 ± 0.16	3.9
6563 H α	300.53 ± 4.36	285.36 ± 4.50	1700.0	317.99 ± 4.57	285.18 ± 4.47	1623.0	303.01 ± 4.70	283.55 ± 4.79	919.4	330.59 ± 4.90	282.98 ± 4.60	408.6
6583 [N II]	12.24 ± 0.23	11.62 ± 0.23	70.2	12.57 ± 0.21	11.26 ± 0.20	64.8	10.97 ± 0.37	10.26 ± 0.35	33.3	8.04 ± 0.27	6.87 ± 0.23	10.0
6678 He I	3.30 ± 0.11	3.13 ± 0.11	20.3	3.54 ± 0.10	3.15 ± 0.09	17.6	3.30 ± 0.34	3.07 ± 0.31	10.2	3.49 ± 0.21	2.96 ± 0.18	4.4
6717 [S II]	15.87 ± 0.27	15.01 ± 0.28	96.0	16.77 ± 0.28	14.92 ± 0.26	83.1	19.56 ± 0.50	18.22 ± 0.48	59.3	17.90 ± 0.37	15.15 ± 0.33	22.6
6731 [S II]	11.99 ± 0.21	11.34 ± 0.21	73.5	13.01 ± 0.22	11.57 ± 0.21	64.9	13.45 ± 0.43	12.52 ± 0.41	40.6	12.12 ± 0.29	10.24 ± 0.26	15.2
7065 He I	2.73 ± 0.12	2.56 ± 0.11	18.5	3.56 ± 0.11	3.11 ± 0.10	20.2	3.09 ± 0.43	2.85 ± 0.40	11.1	3.45 ± 0.25	2.85 ± 0.21	4.8
7136 [Ar III]	10.24 ± 0.23	9.60 ± 0.22	69.6	11.03 ± 0.20	9.62 ± 0.19	62.2	9.57 ± 0.44	8.81 ± 0.41	33.8	9.55 ± 0.28	7.85 ± 0.24	13.3
7281 He I	0.65 ± 0.10	0.56 ± 0.08	4.1	0.59 ± 0.24	0.48 ± 0.20	0.9
7320 [O II]	2.82 ± 0.11	2.44 ± 0.10	17.3	2.55 ± 0.26	2.07 ± 0.21	3.8
7330 [O II]	2.55 ± 0.13	2.20 ± 0.12	15.6	2.36 ± 0.35	1.92 ± 0.29	3.5
$C(H\beta)$	0.068			0.140			0.087			0.199		
$F(H\beta)^b$	2.45			5.17			1.10			3.41		
EW(abs) Å	0.00			0.54			0.01			0.33		

TABLE 3—Continued

Ion	GALAXY		
	HS 2236+1344		
	$F(\lambda)/F(H\beta)$	$I(\lambda)/I(H\beta)$	EW ^a
3727 [O II]	54.67 ± 0.95	60.87 ± 1.12	92.5
3750 H12	2.94 ± 0.37	3.86 ± 0.67	5.1
3771 H11	3.96 ± 0.33	4.97 ± 0.61	6.9
3798 H10	5.42 ± 0.33	6.56 ± 0.60	9.4
3820 He I	1.42 ± 0.35	1.57 ± 0.38	2.6
3835 H9	6.12 ± 0.27	7.29 ± 0.53	11.1
3868 [Ne III]	35.43 ± 0.62	38.84 ± 0.72	64.9
3889 He I + H8	15.84 ± 0.36	17.82 ± 0.57	31.5
3968 [Ne III] + H7	24.61 ± 0.45	27.23 ± 0.66	44.8
4026 He I	1.81 ± 0.19	1.96 ± 0.20	3.3
4101 H δ	22.42 ± 0.41	24.52 ± 0.62	41.1
4340 H γ	46.01 ± 0.72	48.54 ± 0.85	94.7
4363 [O III]	16.96 ± 0.31	17.68 ± 0.32	35.0
4387 He I	0.44 ± 0.15	0.46 ± 0.16	0.9
4471 He I	3.55 ± 0.16	3.66 ± 0.17	7.4
4686 He II	1.05 ± 0.12	1.07 ± 0.13	2.6
4711 [Ar IV] + He I	3.25 ± 0.14	3.28 ± 0.14	8.1
4740 [Ar IV]	2.31 ± 0.12	2.32 ± 0.13	5.8
4861 H β	100.00 ± 1.48	100.00 ± 1.51	261.5
4921 He I	0.81 ± 0.10	0.80 ± 0.10	2.1
4959 [O III]	163.62 ± 2.40	161.72 ± 2.39	439.2
5007 [O III]	487.34 ± 7.08	479.77 ± 7.02	1350.0
5876 He I	11.05 ± 0.20	10.20 ± 0.19	44.1
6300 [O I]	1.23 ± 0.11	1.10 ± 0.10	5.3
6312 [S III]	0.96 ± 0.09	0.86 ± 0.08	4.2
6363 [O I]	0.42 ± 0.11	0.38 ± 0.10	1.8
6563 H α	308.65 ± 4.50	273.08 ± 4.34	1338.0
6583 [N II]	1.89 ± 0.12	1.67 ± 0.11	8.1
6678 He I	3.00 ± 0.13	2.63 ± 0.12	13.6
6717 [S II]	3.90 ± 0.15	3.42 ± 0.13	18.1
6731 [S II]	2.97 ± 0.15	2.60 ± 0.13	13.6
7065 He I	5.26 ± 0.20	4.53 ± 0.18	25.7
7136 [Ar III]	2.72 ± 0.19	2.33 ± 0.16	14.1
$C(H\beta)$		0.157	
$F(H\beta)$ ^b		2.65	
EW(abs) Å		0.91	

^aIn Å.^bIn units of 10^{-14} ergs s⁻¹ cm⁻².

TABLE 4
IONIC AND TOTAL HEAVY ELEMENT AND HELIUM ABUNDANCES

PROPERTY	GALAXY						
	HS 2359+1659	UM 238	HS 0029+1748	HS 0111+2115	HS 0122+0743	HS 0128+2832	HS 0134+3415
T_e (O III) (K)	11870 \pm 160	12490 \pm 150	12820 \pm 150	11060 \pm 650	17740 \pm 230	12560 \pm 110	16390 \pm 180
T_e (O II) (K)	12080 \pm 150	12440 \pm 140	12620 \pm 140	11590 \pm 610	14930 \pm 180	12480 \pm 100	14380 \pm 150
T_e (S III) (K)	11970 \pm 140	12460 \pm 130	12720 \pm 130	11320 \pm 540	16420 \pm 190	12520 \pm 90	15300 \pm 150
N_e (S II) (cm $^{-3}$)	10 \pm 10	270 \pm 60	80 \pm 40	10 \pm 10	70 \pm 50	110 \pm 30	200 \pm 60
O^+/H^+ ($\times 10^4$)	0.225 \pm 0.010	0.158 \pm 0.006	0.139 \pm 0.005	0.657 \pm 0.117	0.064 \pm 0.002	0.125 \pm 0.004	0.065 \pm 0.002
O^{++}/H^+ ($\times 10^4$)	1.285 \pm 0.055	1.304 \pm 0.048	0.953 \pm 0.034	1.132 \pm 0.207	0.330 \pm 0.011	1.244 \pm 0.033	0.650 \pm 0.019
O^{+++}/H^+ ($\times 10^6$)	1.411 \pm 0.247	...	0.887 \pm 0.169	...	0.331 \pm 0.046	...	0.462 \pm 0.148
O/H ($\times 10^4$)	1.524 \pm 0.056	1.462 \pm 0.049	1.101 \pm 0.035	1.789 \pm 0.238	0.397 \pm 0.011	1.370 \pm 0.033	0.720 \pm 0.019
$12 + \log(O/H)$	8.183 \pm 0.016	8.165 \pm 0.014	8.042 \pm 0.014	8.253 \pm 0.058	7.599 \pm 0.012	8.137 \pm 0.011	7.857 \pm 0.012
N^+/H^+ ($\times 10^6$)	0.792 \pm 0.026	0.856 \pm 0.026	0.576 \pm 0.018	2.411 \pm 0.277	0.172 \pm 0.007	0.769 \pm 0.016	0.221 \pm 0.009
ICF	6.778	9.243	7.934	2.721	6.247	0.940	0.989
$\log(N/O)$	-1.453 \pm 0.022	-1.267 \pm 0.020	-1.382 \pm 0.019	-1.436 \pm 0.076	-1.569 \pm 0.021	-1.212 \pm 0.014	-1.471 \pm 0.021
Ne^{++}/H^+ ($\times 10^5$)	2.349 \pm 0.114	1.977 \pm 0.083	1.679 \pm 0.069	2.481 \pm 0.514	0.557 \pm 0.019	1.713 \pm 0.052	1.209 \pm 0.038
ICF	1.186	1.121	1.155	1.581	1.202	1.101	1.108
$\log(Ne/O)$	-0.738 \pm 0.026	-0.819 \pm 0.023	-0.754 \pm 0.023	-0.659 \pm 0.107	-0.773 \pm 0.019	-0.861 \pm 0.017	-0.730 \pm 0.018
S^+/H^+ ($\times 10^6$)	0.308 \pm 0.008	0.288 \pm 0.008	0.239 \pm 0.006	0.661 \pm 0.067	0.113 \pm 0.003	0.224 \pm 0.004	0.143 \pm 0.004
S^{++}/H^+ ($\times 10^6$)	1.778 \pm 0.126	1.481 \pm 0.116	2.017 \pm 0.109	0.969 \pm 0.390	0.491 \pm 0.034	1.546 \pm 0.066	0.676 \pm 0.055
ICF	1.880	2.309	2.079	1.278	1.791	2.608	2.617
$\log(S/O)$	-1.590 \pm 0.031	-1.554 \pm 0.032	-1.370 \pm 0.025	-1.934 \pm 0.120	-1.564 \pm 0.028	-1.472 \pm 0.019	-1.526 \pm 0.031
Cl^{++}/H^+ ($\times 10^8$)	3.842 \pm 0.635	3.389 \pm 0.622	2.950 \pm 0.385	2.466 \pm 0.301	...
ICF	1.773	2.075	1.880	2.274	...
$\log(Cl/O)$	-3.350 \pm 0.073	-3.318 \pm 0.081	-3.298 \pm 0.058	-3.388 \pm 0.054	...
Ar^{++}/H^+ ($\times 10^7$)	4.717 \pm 0.171	4.029 \pm 0.144	3.905 \pm 0.111	4.655 \pm 0.534	0.828 \pm 0.038	4.153 \pm 0.093	1.827 \pm 0.068
Ar^{++}/H^+ ($\times 10^7$)	...	2.565 \pm 0.393	1.236 \pm 0.313	...	0.780 \pm 0.109	2.574 \pm 0.186	2.762 \pm 0.167
ICF	2.234	1.010	1.013	1.485	1.021	1.008	1.008
$\log(Ar/O)$	-2.160 \pm 0.022	-2.341 \pm 0.031	-2.325 \pm 0.031	-2.413 \pm 0.076	-2.383 \pm 0.033	-2.305 \pm 0.017	-2.192 \pm 0.021
Fe^{++}/H^+ ($\times 10^6$)	...	0.150 \pm 0.043	0.060 \pm 0.015	0.191 \pm 0.026	...
ICF	...	1.554	7.808	3.676	...
$\log(Fe/O)$...	-1.925 \pm 0.126	-1.928 \pm 0.109	-1.720 \pm 0.061	...
[O/Fe]	...	0.505 \pm 0.126	0.508 \pm 0.109	0.300 \pm 0.061	...
$y^+(\lambda 4471)$	0.0808 \pm 0.0045	0.0805 \pm 0.0038	0.0735 \pm 0.0036	0.0791 \pm 0.0155	0.0773 \pm 0.0034	0.0787 \pm 0.0022	0.0805 \pm 0.0035
$y^+(\lambda 5876)$	0.0835 \pm 0.0018	0.0883 \pm 0.0019	0.0821 \pm 0.0016	0.0872 \pm 0.0034	0.0840 \pm 0.0017	0.0889 \pm 0.0014	0.0813 \pm 0.0016
$y^+(\lambda 6678)$	0.0827 \pm 0.0042	0.0838 \pm 0.0041	0.0822 \pm 0.0032	0.0800 \pm 0.0100	0.0822 \pm 0.0031	0.0829 \pm 0.0021	0.0811 \pm 0.0037
$y^+(\text{mean})$	0.0830 \pm 0.0015	0.0864 \pm 0.0015	0.0810 \pm 0.0013	0.0861 \pm 0.0032	0.0826 \pm 0.0013	0.0852 \pm 0.0010	0.0812 \pm 0.0013
$y^+(\lambda 4686)$	0.0008 \pm 0.0001	0.0000 \pm 0.0000	0.0007 \pm 0.0001	0.0000 \pm 0.0000	0.0007 \pm 0.0001	0.0000 \pm 0.0000	0.0005 \pm 0.0002
y	0.0838 \pm 0.0015	0.0864 \pm 0.0015	0.0816 \pm 0.0013	0.0861 \pm 0.0032	0.0833 \pm 0.0013	0.0852 \pm 0.0010	0.0817 \pm 0.0013
Y	0.2503 \pm 0.0048	0.2561 \pm 0.0047	0.2456 \pm 0.0042	0.2552 \pm 0.0098	0.2497 \pm 0.0042	0.2534 \pm 0.0032	0.2459 \pm 0.0042

TABLE 4—Continued

PROPERTY	GALAXY						
	UM 133	UM 396	Mrk 1063	J 0519+0007	HS 0735+3512	HS 0811+4913	HS 0837+4717
T_e (O III) (K)	16700 ± 310	11360 ± 150	10240 ± 600	20740 ± 340	12030 ± 140	14450 ± 150	19510 ± 240
T_e (O II) (K)	14510 ± 260	11770 ± 150	11060 ± 570	15900 ± 240	12170 ± 130	13490 ± 130	15540 ± 180
T_e (S III) (K)	15560 ± 260	11560 ± 130	10650 ± 500	18920 ± 280	12100 ± 120	13690 ± 120	17900 ± 200
N_e (S II) (cm ⁻³)	10 ± 10	40 ± 40	90 ± 40	340 ± 210	80 ± 30	60 ± 40	340 ± 90
O^+/H^+ ($\times 10^4$)	0.173 ± 0.009	0.217 ± 0.010	0.574 ± 0.105	0.032 ± 0.001	0.364 ± 0.014	0.142 ± 0.005	0.050 ± 0.002
O^{++}/H^+ ($\times 10^4$)	0.317 ± 0.015	1.457 ± 0.063	0.950 ± 0.183	0.231 ± 0.009	1.117 ± 0.041	0.782 ± 0.023	0.338 ± 0.010
O^{++}/H^+ ($\times 10^6$)	0.924 ± 0.102	3.377 ± 0.377	...	0.745 ± 0.079	1.187 ± 0.266	0.408 ± 0.135	1.017 ± 0.070
O/H ($\times 10^4$)	0.498 ± 0.017	1.708 ± 0.064	1.524 ± 0.211	0.270 ± 0.009	1.493 ± 0.043	0.928 ± 0.024	0.398 ± 0.010
12 + log(O/H)	7.698 ± 0.015	8.233 ± 0.016	8.183 ± 0.060	7.432 ± 0.014	8.174 ± 0.013	7.968 ± 0.011	7.599 ± 0.011
N^+/H^+ ($\times 10^6$)	0.326 ± 0.014	1.001 ± 0.032	3.626 ± 0.418	0.112 ± 0.009	1.270 ± 0.034	0.505 ± 0.014	0.275 ± 0.009
ICF	2.886	7.878	2.656	8.433	4.099	6.531	7.981
log(N/O)	-1.724 ± 0.023	-1.336 ± 0.021	-1.199 ± 0.078	-1.458 ± 0.037	-1.457 ± 0.017	-1.450 ± 0.016	-1.258 ± 0.018
Ne^{++}/H^+ ($\times 10^5$)	0.728 ± 0.036	2.807 ± 0.138	2.012 ± 0.444	0.479 ± 0.018	2.519 ± 0.104	1.423 ± 0.047	0.692 ± 0.021
ICF	1.575	1.172	1.604	1.171	1.337	1.187	1.178
log(Ne/O)	-0.638 ± 0.026	-0.715 ± 0.027	-0.674 ± 0.113	-0.683 ± 0.022	-0.647 ± 0.022	-0.740 ± 0.018	-0.688 ± 0.017
S^+/H^+ ($\times 10^6$)	0.204 ± 0.006	0.314 ± 0.009	0.731 ± 0.075	0.037 ± 0.002	0.436 ± 0.010	0.205 ± 0.005	0.064 ± 0.002
S^{++}/H^+ ($\times 10^6$)	0.598 ± 0.051	1.635 ± 0.167	...	0.190 ± 0.025	1.698 ± 0.113	1.085 ± 0.070	0.280 ± 0.023
ICF	1.296	2.070	...	2.166	1.451	1.838	2.088
log(S/O)	-1.681 ± 0.032	-1.627 ± 0.041	...	-1.740 ± 0.050	-1.683 ± 0.026	-1.593 ± 0.026	-1.743 ± 0.031
Cl^{++}/H^+ ($\times 10^8$)	6.171 ± 1.923	...	3.925 ± 0.788	1.969 ± 0.358	0.704 ± 0.173
ICF	1.422	...	1.569	1.770	1.797
log(Cl/O)	-3.240 ± 0.148	...	-3.385 ± 0.088	-3.425 ± 0.080	-3.497 ± 0.107
Ar^{++}/H^+ ($\times 10^7$)	1.686 ± 0.080	5.243 ± 0.184	4.597 ± 0.515	0.486 ± 0.059	4.103 ± 0.136	2.762 ± 0.086	0.732 ± 0.036
Ar^{++}/H^+ ($\times 10^7$)	1.078 ± 0.127	...	1.529 ± 0.200	1.360 ± 0.095
ICF	1.508	2.420	1.476	1.012	1.730	1.020	1.013
log(Ar/O)	-2.292 ± 0.025	-2.129 ± 0.022	-2.351 ± 0.077	-2.232 ± 0.041	-2.323 ± 0.019	-2.327 ± 0.025	-2.273 ± 0.024
Fe^{++}/H^+ ($\times 10^6$)	0.121 ± 0.025	0.246 ± 0.054	0.781 ± 0.224	...	0.419 ± 0.063	0.064 ± 0.031	...
ICF	3.608	9.847	3.320	...	5.124	8.164	...
log(Fe/O)	-2.056 ± 0.092	-1.848 ± 0.096	-1.769 ± 0.138	...	-1.842 ± 0.066	-2.253 ± 0.214	...
[O/Fe]	0.637 ± 0.092	0.428 ± 0.096	0.349 ± 0.138	...	0.422 ± 0.066	0.832 ± 0.214	...
$y^+(\lambda 4471)$	0.0715 ± 0.0045	0.0794 ± 0.0039	0.0699 ± 0.0076	0.0788 ± 0.0046	0.0779 ± 0.0033	0.0802 ± 0.0035	0.0785 ± 0.0026
$y^+(\lambda 5876)$	0.0795 ± 0.0017	0.0840 ± 0.0016	0.0850 ± 0.0022	0.0781 ± 0.0017	0.0849 ± 0.0015	0.0817 ± 0.0015	0.0758 ± 0.0013
$y^+(\lambda 6678)$	0.0766 ± 0.0038	0.0830 ± 0.0046	0.0765 ± 0.0069	0.0791 ± 0.0048	0.0855 ± 0.0038	0.0790 ± 0.0032	0.0758 ± 0.0028
y^+ (mean)	0.0782 ± 0.0015	0.0833 ± 0.0014	0.0832 ± 0.0020	0.0783 ± 0.0015	0.0838 ± 0.0013	0.0810 ± 0.0013	0.0763 ± 0.0011
$y^{++}(\lambda 4686)$	0.0014 ± 0.0001	0.0017 ± 0.0001	0.0000 ± 0.0000	0.0023 ± 0.0002	0.0007 ± 0.0002	0.0004 ± 0.0001	0.0021 ± 0.0001
y	0.0796 ± 0.0015	0.0850 ± 0.0014	0.0832 ± 0.0020	0.0806 ± 0.0015	0.0845 ± 0.0013	0.0814 ± 0.0013	0.0784 ± 0.0011
Y	0.2413 ± 0.0046	0.2528 ± 0.0044	0.2490 ± 0.0062	0.2437 ± 0.0047	0.2519 ± 0.0041	0.2451 ± 0.0040	0.2386 ± 0.0034

TABLE 4—Continued

PROPERTY	GALAXY						
	HS 0924+3821	CGCG 007-025 (#1)	CGCG 007-025 (#2)	Mrk 1236	HS 1028+3843	Mrk 724	Mrk 35
T_e (O III) (K)	12550 ± 200	16470 ± 170	16560 ± 260	12220 ± 120	15820 ± 160	12960 ± 140	10190 ± 120
T_e (O II) (K)	12470 ± 190	14420 ± 140	14460 ± 210	12280 ± 110	14140 ± 140	12700 ± 130	11030 ± 110
T_e (S III) (K)	12510 ± 170	15370 ± 140	15440 ± 210	12250 ± 100	14830 ± 130	12830 ± 120	10610 ± 100
N_e (S II) (cm $^{-3}$)	30 ± 30	120 ± 40	10 ± 10	50 ± 30	450 ± 110	30 ± 30	180 ± 30
O^+/H^+ ($\times 10^4$)	0.291 ± 0.014	0.108 ± 0.003	0.151 ± 0.007	0.243 ± 0.008	0.059 ± 0.002	0.222 ± 0.008	0.634 ± 0.025
O^{++}/H^+ ($\times 10^4$)	0.887 ± 0.042	0.479 ± 0.013	0.390 ± 0.016	1.154 ± 0.035	0.712 ± 0.020	0.854 ± 0.028	1.342 ± 0.053
O^{++}/H^+ ($\times 10^6$)	...	0.880 ± 0.049	0.516 ± 0.087	0.565 ± 0.120	1.080 ± 0.105
O/H ($\times 10^4$)	1.178 ± 0.045	0.596 ± 0.014	0.547 ± 0.017	1.403 ± 0.036	0.781 ± 0.020	1.076 ± 0.029	1.977 ± 0.058
$12 + \log(O/\text{H})$	8.071 ± 0.016	7.775 ± 0.010	7.738 ± 0.013	8.147 ± 0.011	7.893 ± 0.011	8.032 ± 0.012	8.296 ± 0.013
N^+/H^+ ($\times 10^6$)	1.524 ± 0.053	0.258 ± 0.006	0.360 ± 0.014	1.134 ± 0.026	0.339 ± 0.010	0.610 ± 0.016	2.809 ± 0.071
ICF	4.052	5.510	3.611	5.775	3.247	4.850	3.116
$\log(N/\text{O})$	-1.281 ± 0.022	-1.622 ± 0.014	-1.624 ± 0.022	-1.331 ± 0.015	-1.241 ± 0.017	-1.561 ± 0.016	-1.354 ± 0.017
$N\text{e}^{++}/\text{H}^+$ ($\times 10^5$)	1.677 ± 0.089	0.972 ± 0.029	0.849 ± 0.037	2.261 ± 0.078	1.290 ± 0.039	1.850 ± 0.068	2.865 ± 0.131
ICF	1.328	1.244	1.401	1.215	1.098	1.260	1.473
$\log(Ne/\text{O})$	-0.724 ± 0.028	-0.692 ± 0.016	-0.662 ± 0.023	-0.708 ± 0.019	-0.742 ± 0.017	-0.664 ± 0.020	-0.671 ± 0.024
S^+/H^+ ($\times 10^6$)	0.449 ± 0.014	0.134 ± 0.003	0.200 ± 0.006	0.358 ± 0.007	0.077 ± 0.002	0.253 ± 0.006	0.509 ± 0.012
S^{++}/H^+ ($\times 10^6$)	1.309 ± 0.155	0.696 ± 0.026	0.538 ± 0.052	1.703 ± 0.079	0.612 ± 0.043	1.677 ± 0.079	2.116 ± 0.096
ICF	1.444	1.669	1.384	1.712	3.016	1.564	1.322
$\log(S/\text{O})$	-1.667 ± 0.042	-1.634 ± 0.017	-1.729 ± 0.034	-1.599 ± 0.020	-1.575 ± 0.029	-1.552 ± 0.021	-1.756 ± 0.021
$\text{Cl}^{++}/\text{H}^+$ ($\times 10^8$)	4.331 ± 0.671	1.353 ± 0.135	...	4.112 ± 0.397	...	2.498 ± 0.357	5.401 ± 0.371
ICF	1.576	1.660	...	1.706	...	1.640	1.483
$\log(\text{Cl}/\text{O})$	-3.237 ± 0.069	-3.424 ± 0.045	...	-3.301 ± 0.043	...	-3.419 ± 0.063	-3.392 ± 0.032
$\text{Ar}^{++}/\text{H}^+$ ($\times 10^7$)	...	1.602 ± 0.040	1.646 ± 0.072	4.053 ± 0.099	1.485 ± 0.062	4.364 ± 0.112	6.418 ± 0.164
$\text{Ar}^{++}/\text{H}^+$ ($\times 10^7$)	...	1.014 ± 0.074	0.804 ± 0.218	1.530 ± 0.213	2.737 ± 0.159
ICF	...	1.028	1.072	1.025	1.006	1.877	1.545
$\log(\text{Ar}/\text{O})$...	-2.345 ± 0.017	-2.318 ± 0.043	-2.389 ± 0.021	-2.265 ± 0.021	-2.118 ± 0.016	-2.299 ± 0.017
$\text{Fe}^{++}/\text{H}^+$ ($\times 10^6$)	0.332 ± 0.051	0.106 ± 0.012	...	0.234 ± 0.030	0.191 ± 0.028	0.196 ± 0.024	0.410 ± 0.025
ICF	5.065	6.887	...	7.219	6.559	6.062	3.895
$\log(\text{Fe}/\text{O})$	-1.845 ± 0.068	-1.911 ± 0.049	...	-1.920 ± 0.057	-1.393 ± 0.064	-1.958 ± 0.054	-2.092 ± 0.030
$[\text{O}/\text{Fe}]$	0.425 ± 0.068	0.491 ± 0.049	...	0.500 ± 0.057	-0.027 ± 0.064	0.538 ± 0.054	0.672 ± 0.030
$y^+(\lambda 4471)$	0.0738 ± 0.0042	0.0759 ± 0.0020	0.0758 ± 0.0042	0.0775 ± 0.0022	0.0801 ± 0.0024	0.0801 ± 0.0028	0.0835 ± 0.0019
$y^+(\lambda 5876)$	0.0846 ± 0.0018	0.0788 ± 0.0013	0.0820 ± 0.0019	0.0882 ± 0.0015	0.0798 ± 0.0014	0.0818 ± 0.0014	0.0845 ± 0.0013
$y^+(\lambda 6678)$	0.0817 ± 0.0049	0.0802 ± 0.0018	0.0816 ± 0.0042	0.0841 ± 0.0022	0.0813 ± 0.0031	0.0832 ± 0.0026	0.0875 ± 0.0017
$y^+(\text{mean})$	0.0828 ± 0.0016	0.0786 ± 0.0009	0.0811 ± 0.0016	0.0847 ± 0.0011	0.0800 ± 0.0011	0.0818 ± 0.0011	0.0851 ± 0.0009
$y^{++}(\lambda 4686)$	0.0000 ± 0.0000	0.0012 ± 0.0001	0.0008 ± 0.0001	0.0003 ± 0.0001	0.0012 ± 0.0001	0.0000 ± 0.0000	0.0000 ± 0.0000
y	0.0828 ± 0.0016	0.0798 ± 0.0009	0.0819 ± 0.0016	0.0850 ± 0.0011	0.0813 ± 0.0011	0.0818 ± 0.0011	0.0851 ± 0.0009
Y	0.2482 ± 0.0049	0.2417 ± 0.0029	0.2464 ± 0.0049	0.2531 ± 0.0033	0.2449 ± 0.0035	0.2459 ± 0.0036	0.2529 ± 0.0028

TABLE 4—Continued

PROPERTY	GALAXY						
	UM 422	UM 439	POX 36	Mrk 1315	HS 1213+3636A	HS 1214+3801	Mrk 1329
T_e (O III) (K)	12960 ± 130	14060 ± 140	12560 ± 290	11030 ± 80	10770 ± 270	13360 ± 120	10780 ± 90
T_e (O II) (K)	12700 ± 120	13290 ± 120	12480 ± 270	11560 ± 80	11400 ± 250	12920 ± 110	11410 ± 80
T_e (S III) (K)	12830 ± 110	13370 ± 110	12520 ± 240	11300 ± 70	11090 ± 220	13140 ± 100	11090 ± 70
N_e (S II) (cm $^{-3}$)	20 ± 30	170 ± 50	60 ± 30	20 ± 20	40 ± 30	30 ± 30	20 ± 20
O^+/H^+ ($\times 10^4$)	0.152 ± 0.005	0.136 ± 0.004	0.438 ± 0.030	0.224 ± 0.006	0.681 ± 0.053	0.196 ± 0.006	0.270 ± 0.008
O^{++}/H^+ ($\times 10^4$)	1.131 ± 0.035	1.031 ± 0.029	0.693 ± 0.047	1.550 ± 0.040	0.880 ± 0.070	0.848 ± 0.024	1.517 ± 0.043
O^{+++}/H^+ ($\times 10^6$)	0.725 ± 0.177
O/H ($\times 10^4$)	1.291 ± 0.036	1.167 ± 0.029	1.131 ± 0.056	1.774 ± 0.041	1.561 ± 0.087	1.044 ± 0.024	1.787 ± 0.044
12 + log(O/H)	8.111 ± 0.012	8.067 ± 0.011	8.053 ± 0.022	8.249 ± 0.010	8.193 ± 0.024	8.019 ± 0.010	8.252 ± 0.011
N^+/H^+ ($\times 10^6$)	0.402 ± 0.013	0.410 ± 0.012	1.143 ± 0.053	0.727 ± 0.014	2.308 ± 0.115	0.581 ± 0.013	0.905 ± 0.019
ICF	8.482	8.555	2.584	7.917	2.293	5.327	6.611
log(N/O)	-1.578 ± 0.018	-1.522 ± 0.017	-1.583 ± 0.029	-1.489 ± 0.013	-1.470 ± 0.032	-1.528 ± 0.014	-1.475 ± 0.014
Ne^{++}/H^+ ($\times 10^5$)	2.213 ± 0.078	1.992 ± 0.063	1.632 ± 0.123	3.260 ± 0.099	1.723 ± 0.155	1.505 ± 0.047	2.944 ± 0.097
ICF	1.141	1.132	1.631	1.145	1.774	1.231	1.178
log(Ne/O)	-0.709 ± 0.019	-0.714 ± 0.018	-0.628 ± 0.039	-0.677 ± 0.017	-0.708 ± 0.046	-0.751 ± 0.017	-0.712 ± 0.018
S^+/H^+ ($\times 10^6$)	0.178 ± 0.004	0.175 ± 0.004	0.455 ± 0.018	0.201 ± 0.004	0.515 ± 0.023	0.215 ± 0.004	0.243 ± 0.005
S^{++}/H^+ ($\times 10^6$)	1.263 ± 0.085	1.086 ± 0.066	1.061 ± 0.117	2.181 ± 0.072	2.409 ± 0.247	1.432 ± 0.055	2.422 ± 0.082
ICF	2.175	2.188	1.264	2.076	1.235	1.639	1.852
log(S/O)	-1.615 ± 0.028	-1.627 ± 0.025	-1.771 ± 0.040	-1.555 ± 0.016	-1.636 ± 0.044	-1.587 ± 0.018	-1.559 ± 0.017
Cl^{++}/H^+ ($\times 10^8$)	2.581 ± 0.451	1.710 ± 0.438	4.664 ± 0.668	3.774 ± 0.241	3.945 ± 0.658	2.394 ± 0.241	3.182 ± 0.221
ICF	1.948	1.998	1.413	1.928	1.394	1.679	1.795
log(Cl/O)	-3.409 ± 0.077	-3.533 ± 0.112	-3.234 ± 0.066	-3.387 ± 0.029	-3.453 ± 0.076	-3.415 ± 0.045	-3.495 ± 0.032
Ar^{++}/H^+ ($\times 10^7$)	3.480 ± 0.106	3.188 ± 0.087	3.977 ± 0.173	6.245 ± 0.132	4.656 ± 0.225	3.437 ± 0.079	5.336 ± 0.118
Ar^{+++}/H^+ ($\times 10^7$)	1.724 ± 0.316	2.120 ± 0.218	...	1.530 ± 0.139	1.447 ± 0.638	1.175 ± 0.139	1.213 ± 0.144
ICF	1.012	1.012	1.468	1.013	1.215	1.030	1.019
log(Ar/O)	-2.389 ± 0.030	-2.337 ± 0.022	-2.287 ± 0.029	-2.352 ± 0.015	-2.323 ± 0.054	-2.342 ± 0.018	-2.428 ± 0.016
Fe^{++}/H^+ ($\times 10^6$)	...	0.107 ± 0.035	0.211 ± 0.050	0.092 ± 0.018	0.112 ± 0.018
ICF	...	0.693	3.230	9.896	8.263
log(Fe/O)	...	-2.009 ± 0.144	-2.220 ± 0.106	-2.292 ± 0.086	-2.287 ± 0.073
[O/Fe]	...	0.589 ± 0.144	0.800 ± 0.106	0.872 ± 0.086	0.867 ± 0.073
$y^+(\lambda 4471)$	0.0751 ± 0.0031	0.0810 ± 0.0034	0.0714 ± 0.0052	0.0834 ± 0.0017	0.0784 ± 0.0035	0.0799 ± 0.0022	0.0829 ± 0.0017
$y^+(\lambda 5876)$	0.0831 ± 0.0016	0.0812 ± 0.0015	0.0826 ± 0.0017	0.0845 ± 0.0013	0.0869 ± 0.0016	0.0814 ± 0.0013	0.0895 ± 0.0014
$y^+(\lambda 6678)$	0.0830 ± 0.0031	0.0808 ± 0.0029	0.0806 ± 0.0042	0.0861 ± 0.0018	0.0817 ± 0.0037	0.0798 ± 0.0019	0.0853 ± 0.0018
y^+ (mean)	0.0818 ± 0.0013	0.0811 ± 0.0012	0.0814 ± 0.0015	0.0846 ± 0.0009	0.0849 ± 0.0014	0.0807 ± 0.0010	0.0864 ± 0.0009
$y^{++}(\lambda 4686)$	0.0005 ± 0.0001	0.0000 ± 0.0000	0.0000 ± 0.0000	0.0000 ± 0.0000	0.0000 ± 0.0000	0.0000 ± 0.0000	0.0000 ± 0.0000
y	0.0822 ± 0.0013	0.0811 ± 0.0012	0.0814 ± 0.0015	0.0846 ± 0.0009	0.0849 ± 0.0014	0.0807 ± 0.0010	0.0864 ± 0.0009
Y	0.2469 ± 0.0040	0.2444 ± 0.0039	0.2450 ± 0.0048	0.2520 ± 0.0028	0.2526 ± 0.0042	0.2435 ± 0.0031	0.2560 ± 0.0028

TABLE 4—Continued

PROPERTY	GALAXY				
	HS 1311+3628	Mrk 450 (#1)	Mrk 450 (#2)	Mrk 67	HS 2236+1344
T_e (O III) (K)	11410 ± 130	11690 ± 130	12500 ± 290	13190 ± 230	21120 ± 290
T_e (O II) (K)	11800 ± 120	11970 ± 120	12450 ± 260	12830 ± 210	15990 ± 200
T_e (S III) (K)	11610 ± 110	11830 ± 100	12470 ± 240	13010 ± 190	19230 ± 240
N_e (S II) (cm $^{-3}$)	100 ± 30	130 ± 30	10 ± 10	10 ± 10	110 ± 100
O^+/H^+ ($\times 10^4$)	0.349 ± 0.013	0.326 ± 0.012	0.273 ± 0.019	0.259 ± 0.014	0.044 ± 0.002
O^{++}/H^+ ($\times 10^4$)	1.176 ± 0.043	1.091 ± 0.037	0.921 ± 0.062	0.857 ± 0.044	0.248 ± 0.008
O^{+++}/H^+ ($\times 10^6$)	...	0.448 ± 0.109	0.355 ± 0.046
O/H ($\times 10^4$)	1.525 ± 0.045	1.422 ± 0.039	1.195 ± 0.064	1.116 ± 0.046	0.296 ± 0.008
12 + log(O/H)	8.183 ± 0.013	8.153 ± 0.012	8.077 ± 0.023	8.048 ± 0.018	7.472 ± 0.012
N^+/H^+ ($\times 10^6$)	1.417 ± 0.038	1.330 ± 0.033	1.111 ± 0.056	0.697 ± 0.029	0.110 ± 0.006
ICF	4.372	4.358	4.370	4.308	6.694
log(N/O)	-1.391 ± 0.017	-1.390 ± 0.016	-1.391 ± 0.032	-1.570 ± 0.025	-1.604 ± 0.026
Ne^{++}/H^+ ($\times 10^5$)	2.309 ± 0.098	2.138 ± 0.084	1.881 ± 0.142	1.779 ± 0.100	0.400 ± 0.013
ICF	1.297	1.303	1.297	1.302	1.192
log(Ne/O)	-0.707 ± 0.023	-0.708 ± 0.021	-0.690 ± 0.040	-0.683 ± 0.030	-0.793 ± 0.019
S^+/H^+ ($\times 10^6$)	0.413 ± 0.010	0.405 ± 0.009	0.428 ± 0.018	0.333 ± 0.011	0.054 ± 0.002
S^{++}/H^+ ($\times 10^6$)	2.419 ± 0.142	2.240 ± 0.107	1.811 ± 0.237	1.440 ± 0.145	0.223 ± 0.022
ICF	1.491	1.489	1.490	1.481	1.866
log(S/O)	-1.558 ± 0.025	-1.558 ± 0.021	-1.554 ± 0.052	-1.628 ± 0.040	-1.758 ± 0.037
Cl^{++}/H^+ ($\times 10^8$)	4.813 ± 0.563	4.296 ± 0.389
ICF	1.602	1.596
log(Cl/O)	-3.296 ± 0.052	-3.317 ± 0.041
Ar^{++}/H^+ ($\times 10^7$)	5.613 ± 0.163	5.412 ± 0.137	4.446 ± 0.252	3.658 ± 0.141	0.570 ± 0.041
Ar^{+++/H^+} ($\times 10^7$)	...	1.254 ± 0.255	1.648 ± 0.095
ICF	1.783	1.047	1.783	1.771	1.019
log(Ar/O)	-2.183 ± 0.018	-2.309 ± 0.022	-2.178 ± 0.034	-2.236 ± 0.024	-2.118 ± 0.024
Fe^{++}/H^+ ($\times 10^6$)	...	0.190 ± 0.030
ICF	...	5.448
log(Fe/O)	...	-2.138 ± 0.069
[O/Fe]	...	0.718 ± 0.069
$y^+(\lambda 4471)$	0.0785 ± 0.0029	0.0781 ± 0.0023	0.0753 ± 0.0068	0.0757 ± 0.0049	0.0755 ± 0.0034
$y^+(\lambda 5876)$	0.0864 ± 0.0016	0.0855 ± 0.0014	0.0848 ± 0.0025	0.0851 ± 0.0021	0.0795 ± 0.0015
$y^+(\lambda 6678)$	0.0831 ± 0.0029	0.0845 ± 0.0024	0.0834 ± 0.0085	0.0805 ± 0.0049	0.0794 ± 0.0036
y^+ (mean)	0.0843 ± 0.0013	0.0836 ± 0.0011	0.0837 ± 0.0023	0.0833 ± 0.0018	0.0789 ± 0.0013
$y^{++}(\lambda 4686)$	0.0000 ± 0.0000	0.0003 ± 0.0001	0.0000 ± 0.0000	0.0000 ± 0.0000	0.0010 ± 0.0001
y	0.0843 ± 0.0013	0.0839 ± 0.0011	0.0837 ± 0.0023	0.0833 ± 0.0018	0.0799 ± 0.0013
Y	0.2514 ± 0.0039	0.2506 ± 0.0034	0.2502 ± 0.0070	0.2494 ± 0.0055	0.2421 ± 0.0040

Table 5. Sample Used for Primordial Helium Abundance Determination

Object	O/H $\times 10^4$	N/H $\times 10^6$	Y	References
I Zw 18 SE	1.53 \pm 0.06	4.06 \pm 0.51	0.2414 \pm 0.0063	2
I Zw 18 SE	1.55 \pm 0.10	4.06 \pm 0.51	0.2389 \pm 0.0057	3
SBS 0335-052E	1.99 \pm 0.08	5.23 \pm 0.81	0.2515 \pm 0.0052	4
SBS 0335-052E	1.99 \pm 0.05	5.23 \pm 0.81	0.2466 \pm 0.0029	2
SBS 0335-052E	2.02 \pm 0.05	5.23 \pm 0.81	0.2475 \pm 0.0027	5
J 0519+0007	2.70 \pm 0.09	9.42 \pm 0.74	0.2437 \pm 0.0047	1
SBS 0940+544	2.71 \pm 0.11	6.61 \pm 0.40	0.2455 \pm 0.0066	6
SBS 0940+544	2.74 \pm 0.12	6.92 \pm 0.71	0.2431 \pm 0.0070	7
HS 2236+1344	2.96 \pm 0.08	7.37 \pm 0.39	0.2421 \pm 0.0040	1
SBS 0940+544	3.14 \pm 0.08	7.05 \pm 0.28	0.2468 \pm 0.0034	7
SBS 1159+545	3.14 \pm 0.10	8.20 \pm 0.37	0.2409 \pm 0.0043	6
Tol 1214-277	3.45 \pm 0.10	7.90 \pm 0.50	0.2432 \pm 0.0038	8
UGC 4483	3.45 \pm 0.09	7.73 \pm 0.24	0.2439 \pm 0.0037	6
Tol 65	3.48 \pm 0.10	7.92 \pm 0.37	0.2495 \pm 0.0043	8
SBS 1415+437 (#1)	3.88 \pm 0.09	8.50 \pm 0.25	0.2451 \pm 0.0032	6
HS 0122+0743	3.97 \pm 0.11	10.72 \pm 0.42	0.2497 \pm 0.0042	1
SBS 1415+437 (#1)	3.97 \pm 0.10	11.41 \pm 0.36	0.2451 \pm 0.0038	9
HS 0837+4717	3.98 \pm 0.10	21.97 \pm 0.69	0.2386 \pm 0.0034	1
SBS 1415+437 (#1)	4.10 \pm 0.07	11.29 \pm 1.20	0.2460 \pm 0.0030	10
SBS 1415+437 (#2)	4.12 \pm 0.28	12.64 \pm 2.00	0.2430 \pm 0.0100	10
HS 1442+4250	4.31 \pm 0.19	15.63 \pm 1.17	0.2432 \pm 0.0075	11
SBS 1211+540	4.36 \pm 0.11	9.79 \pm 0.36	0.2510 \pm 0.0038	6
VII Zw 403	4.93 \pm 0.19	14.63 \pm 0.62	0.2415 \pm 0.0052	6
UM 133	4.98 \pm 0.17	9.41 \pm 0.39	0.2413 \pm 0.0046	1
SBS 1249+493	5.38 \pm 0.18	13.65 \pm 0.60	0.2452 \pm 0.0055	6
CGCG 007-025 (#2)	5.47 \pm 0.17	13.00 \pm 0.50	0.2464 \pm 0.0049	1
SBS 1331+493	5.60 \pm 0.16	15.85 \pm 0.60	0.2507 \pm 0.0047	6
SBS 1128+573	5.67 \pm 0.45	17.54 \pm 2.67	0.2425 \pm 0.0169	6
SBS 1420+544	5.70 \pm 0.16	15.81 \pm 0.71	0.2447 \pm 0.0038	6
SBS 1205+557	5.75 \pm 0.43	18.12 \pm 1.57	0.2437 \pm 0.0128	6
Mrk 209	5.94 \pm 0.14	19.33 \pm 0.44	0.2472 \pm 0.0027	6
CGCG 007-025 (#1)	5.96 \pm 0.14	14.24 \pm 0.33	0.2417 \pm 0.0029	1
UM 461	6.09 \pm 0.41	19.31 \pm 2.80	0.2466 \pm 0.0115	4
SBS 1030+583	6.29 \pm 0.20	15.75 \pm 0.69	0.2444 \pm 0.0051	6
Mrk 71 (#2)	6.62 \pm 0.30	17.96 \pm 1.04	0.2383 \pm 0.0071	6
Mrk 600	6.70 \pm 0.24	14.42 \pm 0.57	0.2397 \pm 0.0057	4
Mrk 36	6.70 \pm 0.35	21.68 \pm 1.46	0.2395 \pm 0.0089	4
Mrk 71 (#1)	7.12 \pm 0.16	21.67 \pm 0.46	0.2503 \pm 0.0025	6

Table 5—Continued

Object	O/H $\times 10^4$	N/H $\times 10^6$	Y	References
HS 0134+3415	7.20 \pm 0.19	24.31 \pm 0.96	0.2459 \pm 0.0042	1
SBS 0917+527	7.35 \pm 0.29	17.69 \pm 0.82	0.2483 \pm 0.0067	6
SBS 1152+579	7.61 \pm 0.18	31.43 \pm 0.74	0.2516 \pm 0.0030	6
SBS 1533+574A	7.65 \pm 0.60	28.35 \pm 2.19	0.2422 \pm 0.0100	6
HS 1028+3843	7.81 \pm 0.20	44.86 \pm 1.32	0.2449 \pm 0.0035	1
SBS 0926+606	8.27 \pm 0.30	28.14 \pm 1.07	0.2466 \pm 0.0057	6
SBS 1437+370	8.43 \pm 0.21	26.18 \pm 0.68	0.2517 \pm 0.0036	6
UM 420	8.56 \pm 1.00	71.44 \pm 7.91	0.2607 \pm 0.0172	4
SBS 1222+614	9.04 \pm 0.26	22.26 \pm 0.78	0.2430 \pm 0.0046	6
UM 462 SW	9.06 \pm 0.30	27.80 \pm 0.99	0.2445 \pm 0.0049	4
HS 0811+4913	9.28 \pm 0.24	32.95 \pm 0.92	0.2451 \pm 0.0040	1
SBS 1054+365	9.37 \pm 0.39	30.92 \pm 1.50	0.2524 \pm 0.0067	6
UM 448	9.89 \pm 0.92	95.92 \pm 8.27	0.2513 \pm 0.0076	4
Mrk 1271	9.89 \pm 0.32	41.17 \pm 1.63	0.2375 \pm 0.0060	4
Mrk 59	9.90 \pm 0.21	29.85 \pm 0.61	0.2416 \pm 0.0027	6
SBS 0946+558	9.93 \pm 0.23	28.54 \pm 0.68	0.2516 \pm 0.0034	6
SBS 0741+535	10.23 \pm 0.97	29.68 \pm 2.79	0.2465 \pm 0.0131	6
HS 1214+3801	10.44 \pm 0.24	30.96 \pm 0.70	0.2435 \pm 0.0031	1
Mrk 724	10.76 \pm 0.29	29.58 \pm 0.77	0.2459 \pm 0.0036	1
HS 0029+1748	11.01 \pm 0.35	45.68 \pm 1.40	0.2456 \pm 0.0042	1
NGC 1741	11.12 \pm 1.42	99.73 \pm 11.48	0.2573 \pm 0.0078	4
Mrk 67	11.16 \pm 0.46	30.03 \pm 1.26	0.2494 \pm 0.0055	1
SBS 1135+581	11.26 \pm 0.25	47.68 \pm 0.99	0.2439 \pm 0.0028	6
POX 36	11.31 \pm 0.56	29.54 \pm 1.37	0.2450 \pm 0.0048	1
Mrk 5	11.39 \pm 1.04	48.96 \pm 4.15	0.2487 \pm 0.0094	4
Mrk 930	11.53 \pm 0.80	46.71 \pm 2.96	0.2502 \pm 0.0079	4
SBS 0948+532	11.63 \pm 0.30	51.03 \pm 1.30	0.2480 \pm 0.0037	6
UM 439	11.67 \pm 0.29	35.11 \pm 1.01	0.2444 \pm 0.0039	1
HS 0924+3821	11.78 \pm 0.45	61.74 \pm 2.16	0.2482 \pm 0.0049	1
Mrk 450 (#2)	11.95 \pm 0.64	48.55 \pm 2.43	0.2502 \pm 0.0070	1
SBS 1319+579A	12.32 \pm 0.35	42.17 \pm 1.23	0.2522 \pm 0.0043	6
Mrk 750	12.90 \pm 0.64	46.05 \pm 2.17	0.2436 \pm 0.0063	4
UM 422	12.91 \pm 0.36	34.09 \pm 1.07	0.2469 \pm 0.0040	1
SBS 1533+574B	13.13 \pm 0.67	37.78 \pm 1.78	0.2466 \pm 0.0062	6
SBS 1319+579C	13.13 \pm 1.06	52.09 \pm 3.76	0.2432 \pm 0.0069	6
Mrk 162	13.55 \pm 1.10	54.68 \pm 4.13	0.2493 \pm 0.0084	4
HS 0128+2832	13.70 \pm 0.33	84.10 \pm 1.75	0.2534 \pm 0.0032	1
Mrk 1236	14.03 \pm 0.36	65.48 \pm 1.48	0.2531 \pm 0.0033	1

Table 5—Continued

Object	O/H $\times 10^4$	N/H $\times 10^6$	Y	References
Mrk 450 (#1)	14.22 ± 0.39	57.95 ± 1.42	0.2506 ± 0.0034	1
UM 238	14.62 ± 0.49	79.10 ± 2.43	0.2561 ± 0.0047	1
HS 0735+3512	14.94 ± 0.43	52.09 ± 1.39	0.2519 ± 0.0041	1
Mrk 1063	15.24 ± 2.11	96.31 ± 11.10	0.2490 ± 0.0062	1
HS 2359+1659	15.24 ± 0.56	53.69 ± 1.78	0.2503 ± 0.0048	1
HS 1311+3628	15.25 ± 0.45	61.96 ± 1.64	0.2514 ± 0.0039	1
HS 1213+3636A	15.61 ± 0.87	52.93 ± 2.64	0.2526 ± 0.0042	1
UM 396	17.08 ± 0.64	78.86 ± 2.54	0.2528 ± 0.0044	1
Mrk 1315	17.74 ± 0.41	57.57 ± 1.14	0.2520 ± 0.0028	1
Mrk 1329	17.87 ± 0.44	59.81 ± 1.23	0.2560 ± 0.0028	1
HS 0111+2115	17.89 ± 2.38	65.62 ± 7.52	0.2552 ± 0.0098	1
Mrk 35	19.77 ± 0.58	87.53 ± 2.22	0.2529 ± 0.0028	1
UM 311	20.34 ± 2.07	111.90 ± 8.62	0.2533 ± 0.0063	4

References. — (1) this paper; (2) Izotov et al. (1999); (3) Izotov & Thuan (1998a); (4) IT98; (5) Izotov et al. (2001b); (6) ITL97; (7) Guseva et al. (2001); (8) Izotov et al. (2001a); (9) Thuan et al. (1999); (10) Guseva et al. (2003b); (11) Guseva et al. (2003a).

Table 6. Maximum Likelihood Linear Regressions

Method	Number of H II Regions	Oxygen		Nitrogen	
		Regression	σ	Regression	σ
3 He I lines ^{a,b}	45	$0.2451 \pm 0.0018 + 21 \pm 21(\text{O}/\text{H})$	0.0048	$0.2452 \pm 0.0012 + 603 \pm 372(\text{N}/\text{H})$	0.0044
3 He I lines ^b	89	$0.2429 \pm 0.0009 + 51 \pm 9(\text{O}/\text{H})$	0.0040	$0.2439 \pm 0.0008 + 1063 \pm 183(\text{N}/\text{H})$	0.0037
5 He I lines ^{c,d}	7	$0.2421 \pm 0.0021 + 68 \pm 22(\text{O}/\text{H})$	0.0035	$0.2446 \pm 0.0016 + 1084 \pm 442(\text{N}/\text{H})$	0.0040
5 He I lines ^{c,e}	7	$0.2444 \pm 0.0020 + 61 \pm 21(\text{O}/\text{H})$	0.0040	$0.2466 \pm 0.0016 + 954 \pm 411(\text{N}/\text{H})$	0.0044

^aData are from IT98.

^bOnly collisional and fluorescent enhancements are taken into account. We have adopted $T_e(\text{He II}) = T_e(\text{O III})$ and $ICF(\text{He}) = 1$.

^cCollisional and fluorescent enhancements of the He I lines, collisional excitation of hydrogen lines, underlying He I stellar absorption and differences between $T_e(\text{He II})$ and $T_e(\text{O III})$ are taken into account. $ICF(\text{He})$ is set to 1.

^dCalculated with $EW_a(\text{H8} + \text{He I 3889}) = 3.0\text{\AA}$, $EW_a(\text{He I 4471}) = 0.4\text{\AA}$, $EW_a(\text{He I 5876}) = 0.3$ $EW_a(\text{He I 4471})$, $EW_a(\text{He I 6678}) = EW_a(\text{He I 7065}) = 0.1$ $EW_a(\text{He I 4471})$.

^eCalculated with $EW_a(\text{H8} + \text{He I 3889}) = 3.0\text{\AA}$, $EW_a(\text{He I 4471}) = 0.5\text{\AA}$, $EW_a(\text{He I 5876}) = 0.3$ $EW_a(\text{He I 4471})$, $EW_a(\text{He I 6678}) = EW_a(\text{He I 7065}) = 0.1$ $EW_a(\text{He I 4471})$.

Table 7. Best model parameters for the restricted sample

Parameter	I Zw 18	SBS 0335–052	Mrk 209	Mrk 71	NGC 346	Mrk 450	UM 311
$EW_a(\lambda 3889) = 3.0\text{\AA}$, $EW_a(\lambda 4471) = 0.4\text{\AA}$, $EW_a(\lambda 5876) = 0.17\text{\AA}$, $EW_a(\lambda 6678) = 0.05\text{\AA}$, $EW_a(\lambda 7065) = 0.05\text{\AA}$							
χ^2	1.2	4.6	0.56	3.4×10^{-3}	4.1	0.89	3.4×10^{-5}
$\Delta I(\text{H}\alpha)/I(\text{H}\alpha)$	0.0495	0.0005	0.0005	0.0375	0.0380	0.0005	0.0210
$T_e(\text{He II})$	17150	18270	15970	14130	13000	11580	9439
$T_e(\text{He II})/T_e(\text{O III})$	0.902	0.902	0.990	0.902	1.000	0.992	0.970
$N_e(\text{He II})$	10	235	52	193	64	450	79
$\tau(\lambda 3889)$	0.81	4.31	0.21	1.71	0.01	2.16	3.56
$EW_a/EW_e(\lambda 3889)^a$	0.238	0.185	0.125	0.085	0.094	0.095	0.121
$EW_a/EW_e(\lambda 4471)^a$	0.108	0.078	0.063	0.039	0.049	0.049	0.046
$EW_a/EW_e(\lambda 5876)^a$	0.008	0.005	0.005	0.003	0.004	0.004	0.003
$EW_a/EW_e(\lambda 6678)^a$	0.006	0.004	0.004	0.002	0.003	0.003	0.002
$EW_a/EW_e(\lambda 7065)^a$	0.006	0.002	0.004	0.002	0.004	0.003	0.003
$y^+(\lambda 3889)$	0.0743 ± 0.0060	0.0746 ± 0.0030	0.0829 ± 0.0028	0.0825 ± 0.0029	0.0898 ± 0.0036	0.0831 ± 0.0042	0.0868 ± 0.0067
$y^+(\lambda 4471)$	0.0829 ± 0.0061	0.0740 ± 0.0016	0.0814 ± 0.0016	0.0826 ± 0.0014	0.0819 ± 0.0020	0.0801 ± 0.0024	0.0868 ± 0.0057
$y^+(\lambda 5876)$	0.0800 ± 0.0024	0.0780 ± 0.0012	0.0824 ± 0.0013	0.0826 ± 0.0013	0.0842 ± 0.0016	0.0818 ± 0.0014	0.0868 ± 0.0025
$y^+(\lambda 6678)$	0.0804 ± 0.0056	0.0774 ± 0.0016	0.0831 ± 0.0017	0.0826 ± 0.0015	0.0852 ± 0.0018	0.0830 ± 0.0024	0.0868 ± 0.0049
$y^+(\lambda 7065)$	0.0779 ± 0.0051	0.0762 ± 0.0014	0.0825 ± 0.0018	0.0826 ± 0.0015	0.0844 ± 0.0022	0.0821 ± 0.0027	0.0868 ± 0.0053
$y^+(\text{mean})$	0.0795 ± 0.0018	0.0765 ± 0.0007	0.0824 ± 0.0008	0.0826 ± 0.0007	0.0844 ± 0.0009	0.0818 ± 0.0010	0.0868 ± 0.0019
$y^{++}(\lambda 4686)$	0.0008 ± 0.0002	0.0024 ± 0.0001	0.0011 ± 0.0001	0.0008 ± 0.0001	0.0002 ± 0.0000	0.0003 ± 0.0001	...
$y(\text{mean})$	0.0803 ± 0.0018	0.0789 ± 0.0007	0.0834 ± 0.0008	0.0834 ± 0.0007	0.0846 ± 0.0009	0.0821 ± 0.0010	0.0868 ± 0.0019
$Y(\text{mean})$	0.2430 ± 0.0057	0.2399 ± 0.0022	0.2500 ± 0.0023	0.2499 ± 0.0021	0.2523 ± 0.0028	0.2465 ± 0.0030	0.2566 ± 0.0057
$12 + \log(\text{O/H})^c$	7.28	7.39	7.78	7.97	8.01	8.16	8.36
$EW_a(\lambda 3889) = 3.0\text{\AA}$, $EW_a(\lambda 4471) = 0.5\text{\AA}$, $EW_a(\lambda 5876) = 0.17\text{\AA}$, $EW_a(\lambda 6678) = 0.05\text{\AA}$, $EW_a(\lambda 7065) = 0.05\text{\AA}$							
χ^2	1.7	2.7	0.052	0.034	3.0	0.46	4.5×10^{-6}
$\Delta I(\text{H}\alpha)/I(\text{H}\alpha)$	0.0495	0.0005	0.0005	0.0475	0.0440	0.0005	0.0390
$T_e(\text{He II})$	17150	18270	16140	14110	12990	11630	9112
$T_e(\text{He II})/T_e(\text{O III})$	0.902	0.902	1.000	0.902	1.000	0.996	0.938
$N_e(\text{He II})$	10	214	16	157	64	450	151
$\tau(\lambda 3889)$	0.81	4.36	0.31	1.86	0.01	2.11	3.71
$EW_a/EW_e(\lambda 3889)^a$	0.238	0.185	0.125	0.085	0.094	0.095	0.121
$EW_a/EW_e(\lambda 4471)^a$	0.130	0.094	0.075	0.047	0.059	0.059	0.055
$EW_a/EW_e(\lambda 5876)^a$	0.008	0.005	0.005	0.003	0.004	0.004	0.003
$EW_a/EW_e(\lambda 6678)^a$	0.006	0.004	0.004	0.002	0.003	0.003	0.002
$EW_a/EW_e(\lambda 7065)^a$	0.006	0.002	0.004	0.002	0.004	0.003	0.003
$y^+(\lambda 3889)$	0.0742 ± 0.0060	0.0754 ± 0.0030	0.0839 ± 0.0029	0.0834 ± 0.0029	0.0896 ± 0.0036	0.0827 ± 0.0041	0.0879 ± 0.0068
$y^+(\lambda 4471)$	0.0848 ± 0.0063	0.0757 ± 0.0017	0.0833 ± 0.0017	0.0838 ± 0.0015	0.0828 ± 0.0020	0.0810 ± 0.0024	0.0879 ± 0.0058
$y^+(\lambda 5876)$	0.0801 ± 0.0024	0.0787 ± 0.0013	0.0835 ± 0.0013	0.0839 ± 0.0013	0.0847 ± 0.0016	0.0818 ± 0.0014	0.0879 ± 0.0026
$y^+(\lambda 6678)$	0.0805 ± 0.0056	0.0777 ± 0.0016	0.0837 ± 0.0017	0.0837 ± 0.0015	0.0858 ± 0.0019	0.0831 ± 0.0024	0.0879 ± 0.0050
$y^+(\lambda 7065)$	0.0781 ± 0.0051	0.0768 ± 0.0014	0.0836 ± 0.0018	0.0837 ± 0.0015	0.0851 ± 0.0022	0.0823 ± 0.0027	0.0879 ± 0.0054
$y^+(\text{mean})$	0.0798 ± 0.0018	0.0773 ± 0.0007	0.0835 ± 0.0008	0.0838 ± 0.0007	0.0850 ± 0.0009	0.0820 ± 0.0010	0.0879 ± 0.0019
$y^{++}(\lambda 4686)$	0.0008 ± 0.0002	0.0024 ± 0.0001	0.0011 ± 0.0001	0.0008 ± 0.0001	0.0002 ± 0.0000	0.0003 ± 0.0001	...
$y(\text{mean})$	0.0806 ± 0.0018	0.0797 ± 0.0007	0.0846 ± 0.0008	0.0846 ± 0.0007	0.0852 ± 0.0009	0.0823 ± 0.0010	0.0879 ± 0.0019
$Y(\text{mean})$	0.2437 ± 0.0057	0.2417 ± 0.0022	0.2525 ± 0.0024	0.2536 ± 0.0022	0.2469 ± 0.0030	0.2590 ± 0.0058	
$12 + \log(\text{O/H})^c$	7.28	7.39	7.77	7.98	8.01	8.16	8.41

^aRatio of the absorption-to-emission line equivalent widths.

^bCorrection of Y for systematic effects.

^cCalculated with $T_e(\text{He II})$.

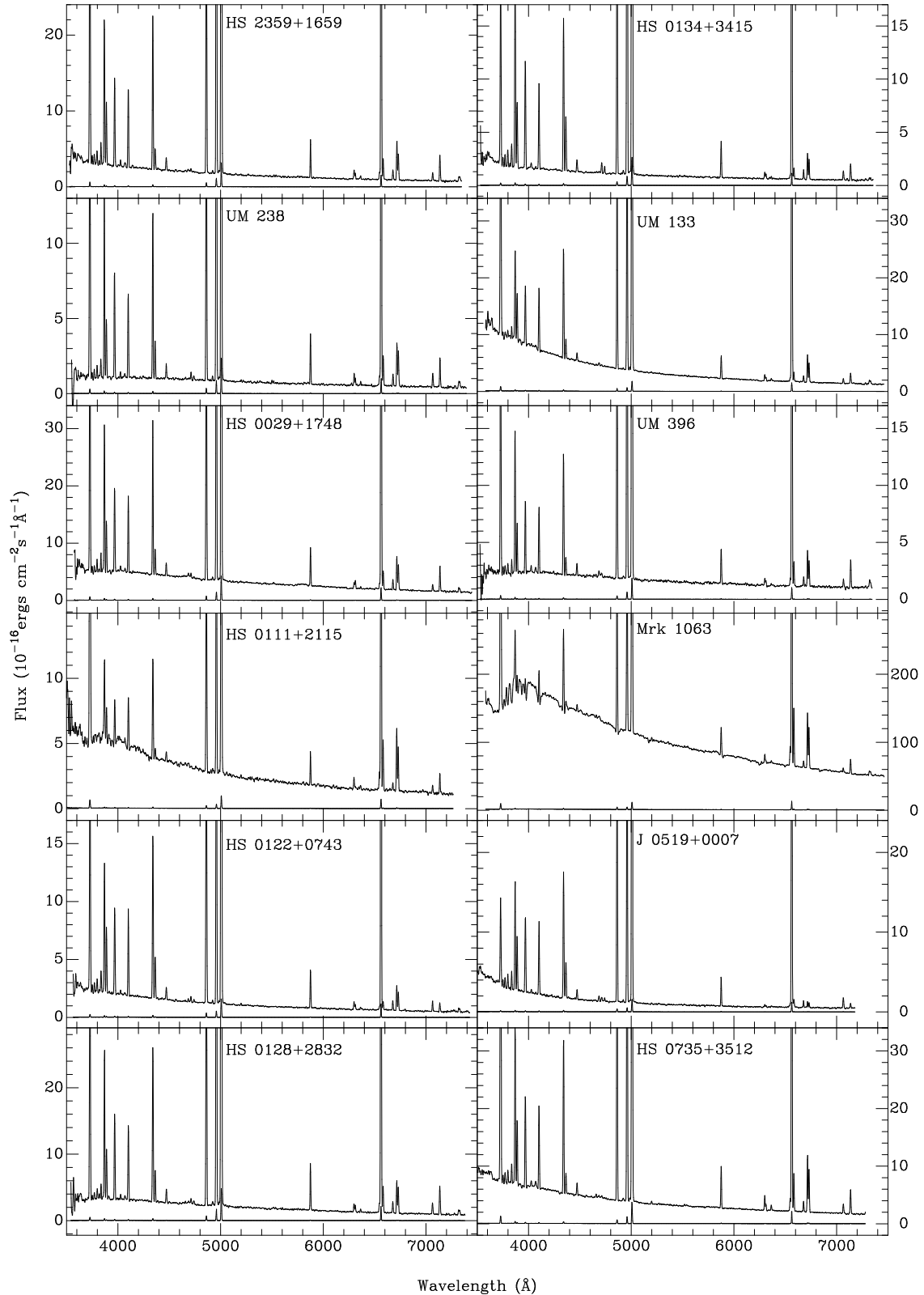


Fig. 1.— Mayall 4-m telescope spectra of 33 H II regions in 31 blue compact galaxies.

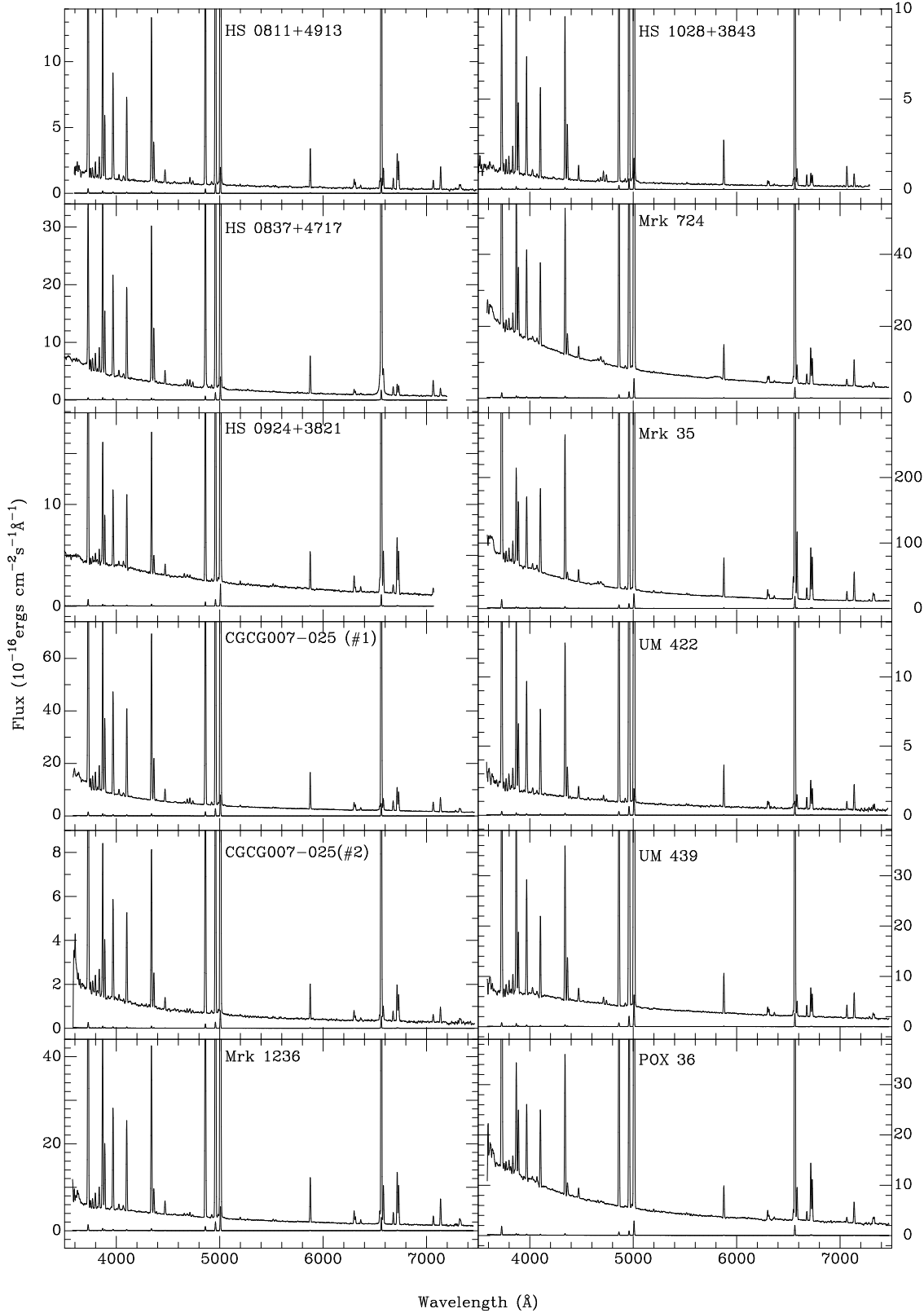


Fig. 1.— Continued.

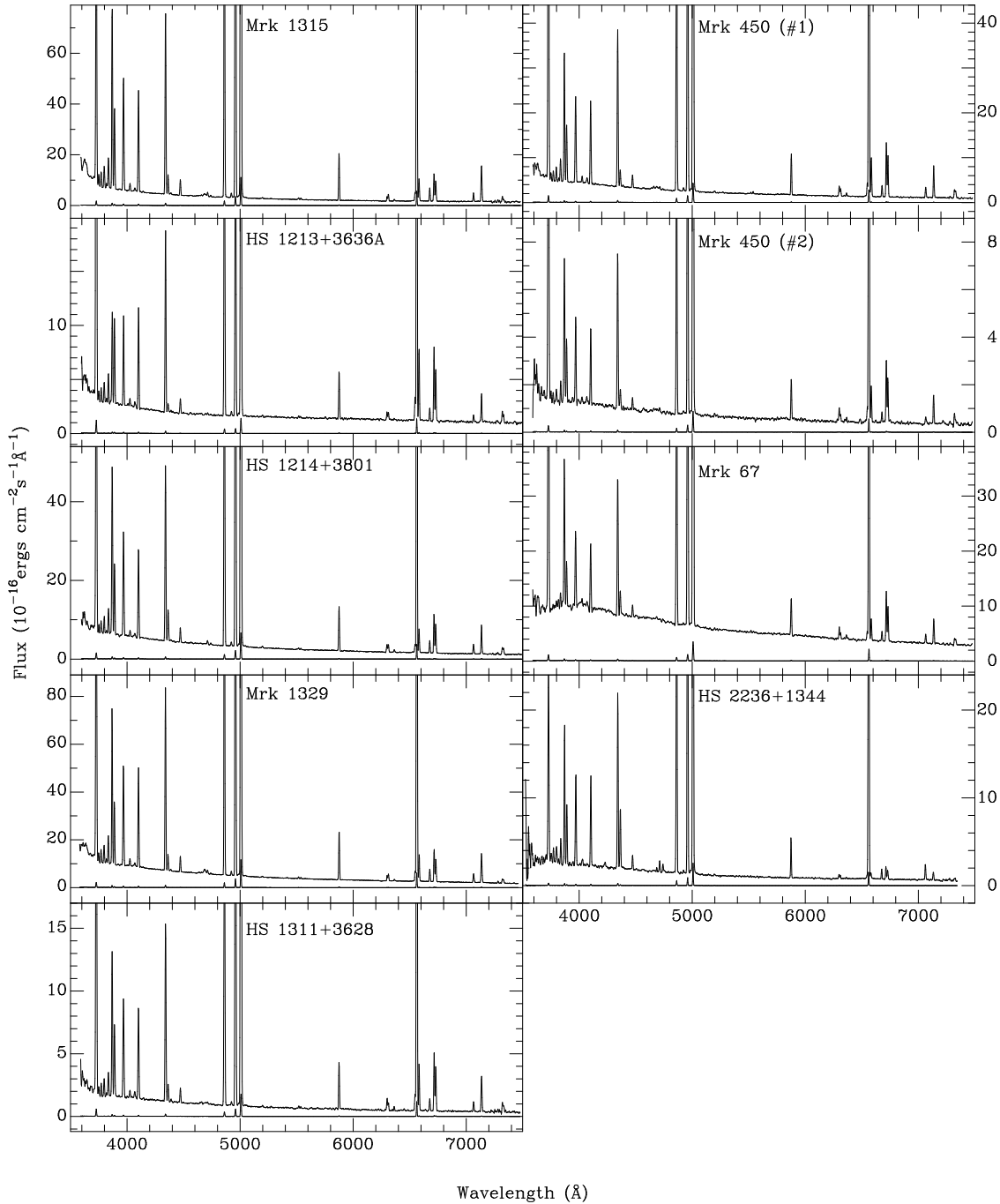


Fig. 1.— Continued.

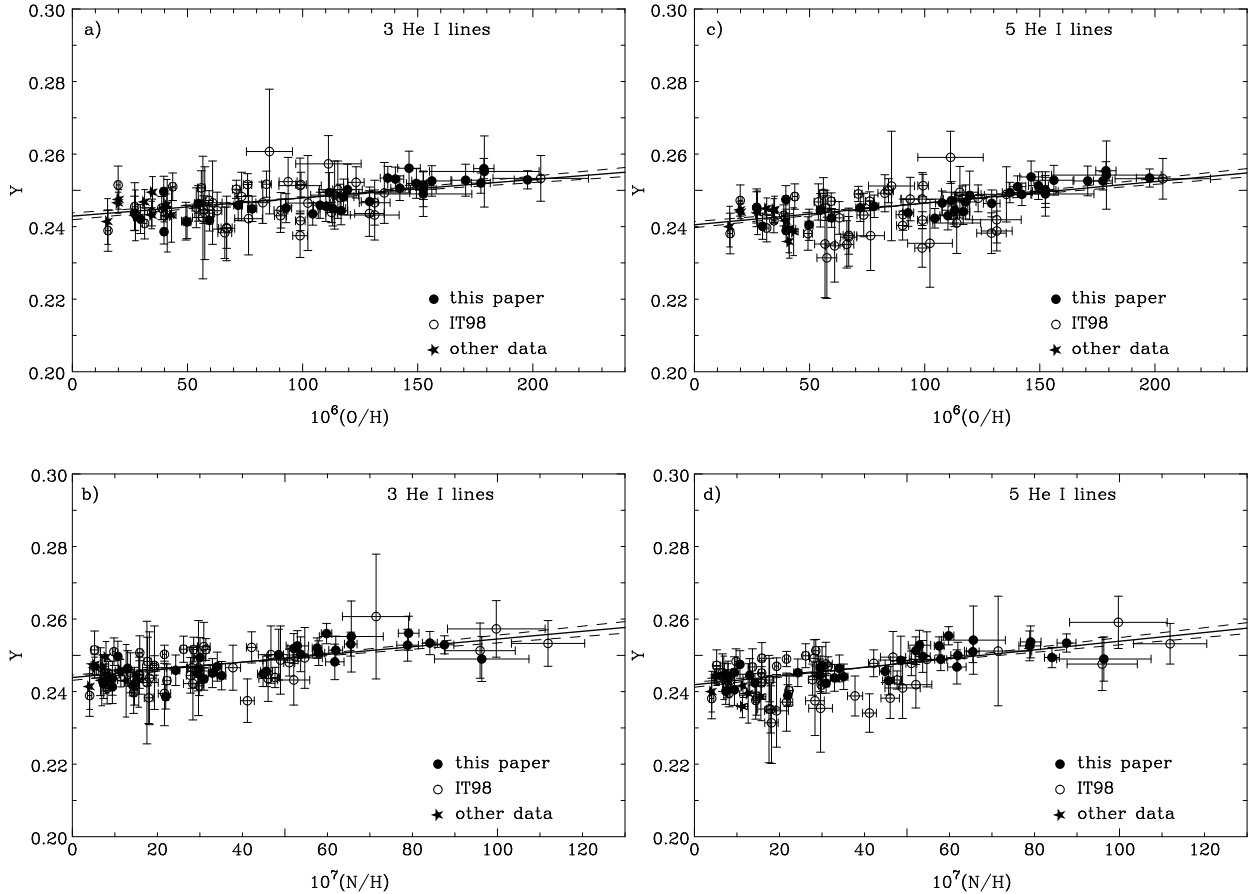


Fig. 2.— Linear regressions of the helium mass fraction Y vs. oxygen and nitrogen abundances for a total of 82 H II regions in 76 blue compact galaxies. In panels a) and b), Y was derived using the 3 $\lambda 4471$, $\lambda 5876$ and $\lambda 6678$ He I lines, and in panels c) and d), Y was derived using the 5 $\lambda 3889$, $\lambda 4471$, $\lambda 5876$, $\lambda 6678$ and $\lambda 7065$ He I lines.

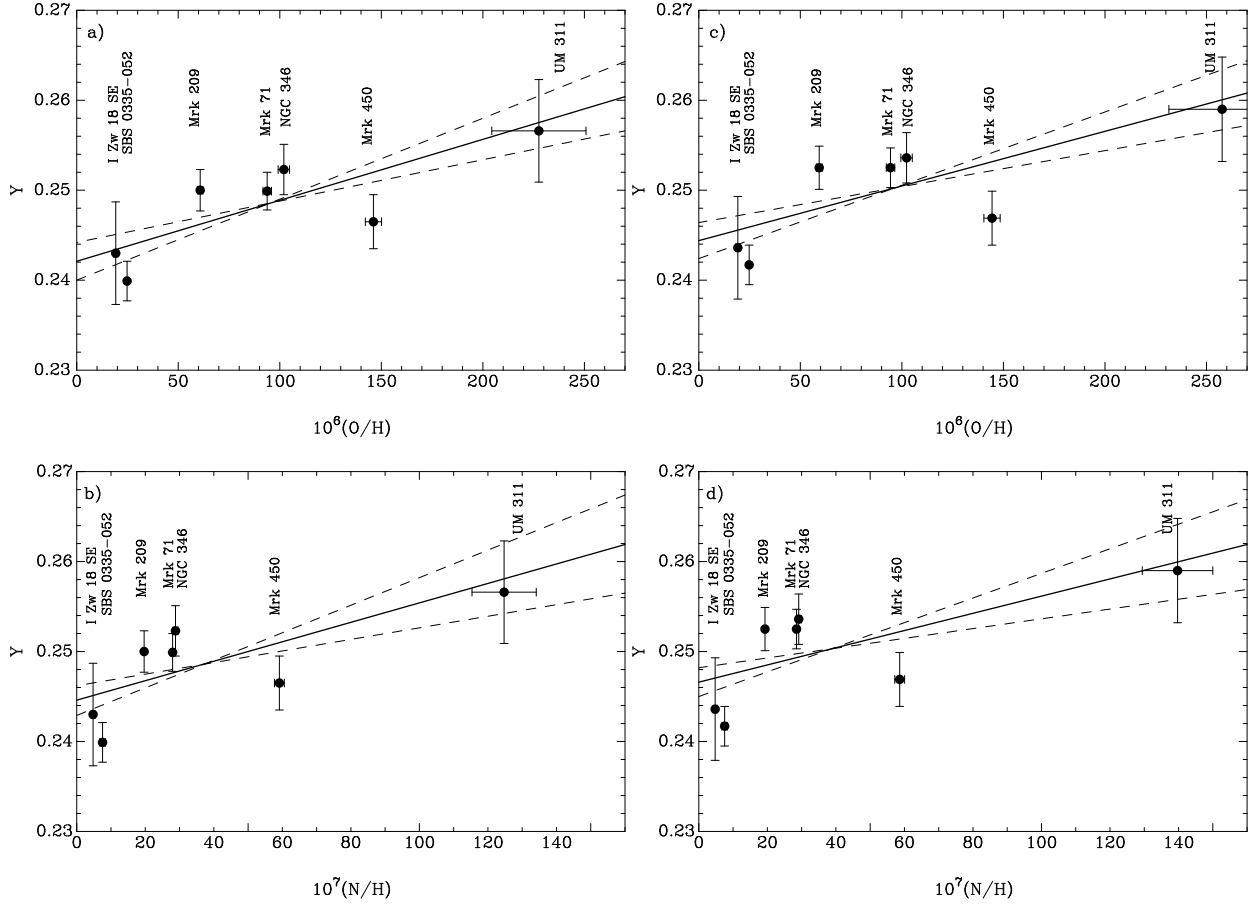


Fig. 3.— $Y - \text{O/H}$ (a,c) and $Y - \text{N/H}$ (b,d) linear regressions (solid lines) for seven H II regions. Their helium mass fraction Y has been corrected for known systematic effects by a χ^2 minimization procedure (see §6). The filled circles represent the solution with the lowest χ^2 . Oxygen and nitrogen abundances for all points are calculated by setting the electron temperatures in the O III zone equal to $T_e(\text{He II})$, the latter being derived from χ^2 minimization. The equivalent widths of the absorption lines adopted in (a) and (b) are $\text{EW}_a(\lambda 3889) = 3.0\text{\AA}$, $\text{EW}_a(\lambda 4471) = 0.4\text{\AA}$, $\text{EW}_a(\lambda 5876) = 0.17\text{\AA}$, $\text{EW}_a(\lambda 6678) = \text{EW}_a(\lambda 7065) = 0.05\text{\AA}$. The corresponding values in (c) and (d) are $\text{EW}_a(\lambda 3889) = 3.0\text{\AA}$, $\text{EW}_a(\lambda 4471) = 0.5\text{\AA}$, $\text{EW}_a(\lambda 5876) = 0.17\text{\AA}$, $\text{EW}_a(\lambda 6678) = \text{EW}_a(\lambda 7065) = 0.05\text{\AA}$.